

10-14-1998

## STOCHASTIC METHODS FOR EVALUATING THE POTENTIAL FOR WETLAND REHYDRATION IN COVERED-KARST TERRANES

Christian David Langevin  
*University of South Florida*

Follow this and additional works at: <https://digitalcommons.usf.edu/etd>



Part of the [Geology Commons](#)

---

### Scholar Commons Citation

Langevin, Christian David, "STOCHASTIC METHODS FOR EVALUATING THE POTENTIAL FOR WETLAND REHYDRATION IN COVERED-KARST TERRANES" (1998). *USF Tampa Graduate Theses and Dissertations*. <https://digitalcommons.usf.edu/etd/8708>

This Dissertation is brought to you for free and open access by the USF Graduate Theses and Dissertations at Digital Commons @ University of South Florida. It has been accepted for inclusion in USF Tampa Graduate Theses and Dissertations by an authorized administrator of Digital Commons @ University of South Florida. For more information, please contact [digitalcommons@usf.edu](mailto:digitalcommons@usf.edu).

Graduate School  
University of South Florida  
Tampa, Florida

CERTIFICATE OF APPROVAL

---

Ph.D. Dissertation

---

This is to certify that the Ph.D. Dissertation of

CHRISTIAN DAVID LANGEVIN

with a major in Geology has been approved by  
the Examining Committee on October 14, 1998  
as satisfactory for the dissertation requirement  
for the Doctor of Philosophy degree

Examining Committee:

---

Major Professor: Mark Stewart, Ph.D.

---

Member: Mark Ross, Ph.D.

---

Member: Jeff Ryan, Ph.D.

---

Member: Carl Steefel, Ph.D.

---

Member: H. Leonard Vacher, Ph.D.



STOCHASTIC METHODS FOR EVALUATING THE POTENTIAL  
FOR WETLAND REHYDRATION IN COVERED-KARST TERRANES

by

CHRISTIAN DAVID LANGEVIN

A dissertation submitted in partial fulfillment  
of the requirements for the degree of  
Doctor of Philosophy  
Department of Geology  
University of South Florida

December 1998

Major Professor: Mark Stewart, Ph.D.

## **DEDICATION**

In memory of Barbara Theresa Langevin (1963 – 1998).

## TABLE OF CONTENTS

LIST OF TABLES	iii
LIST OF FIGURES	iv
ABSTRACT	vii
PREFACE	x
CHAPTER 1. INTRODUCTION	1
CHAPTER 2. ESTIMATING GROUNDWATER FLOW VELOCITIES IN A LEAKY AQUIFER SYSTEM IN WEST-CENTRAL FLORIDA	5
Introduction	5
Description of Study Area	7
Methods and Results	9
Installation of Monitoring Wells	9
Sediment Sampling and Grain-Size Analysis	12
Groundwater Pumping Test	15
Flooding Test	17
Surficial Aquifer Tracer Test	23
Floridan Aquifer Tracer Test	30
Groundwater Elevations and Vertical Head Differences	33
Surficial Aquifer	33
Floridan Aquifer	37
Vertical Head Differences	40
Estimation of Groundwater Flow Velocities	44
Horizontal Flow in the Surficial Aquifer	44
Vertical Flow in the Surficial Aquifer	48
Horizontal Flow in the Floridan Aquifer	49
Discussion	52
Reliability of Estimated Groundwater Flow Velocities	52
Feasibility of Rehydration	55
Significance of Karst Conduits	57
Conclusions	58
CHAPTER 3. INCORPORATING LARGE-SCALE, VERTICAL FRACTURES IN GROUNDWATER FLOW MODELS	60
Introduction	60
Method for Conducting Monte-Carlo Analysis with a Grid-Based Discrete-Fracture Model	62
Fracture Statistics	63
Equivalent Porous Media Site Model	64
Bulk Transmissivity versus Block Transmissivity	64
Monte-Carlo Analysis with Discrete-Fracture Model of Site	65
Implementation	66
Application to North Lakes Wetland Project	67
Background	67
Fracture Statistics	67

Development of Equivalent Porous Media Model	73
Effects of Fractures on Bulk Transmissivity	74
Monte-Carlo Analysis with North Lakes Model	77
Discussion	80
Benefits and Limitations	80
North Lakes Application	83
Importance of Adjusting for Bulk Transmissivity	84
Future Applications	87
Summary	88
 CHAPTER 4. THE PROBABILITY OF RESTORING WATER LEVELS IN A DAMAGED WETLAND	 89
Introduction	89
Description of Study Site	90
Background Theory	100
Random Variables	100
Stochastic Analysis	103
Water Balance Equation and Development of Input Parameters	104
Approach	104
Rainfall	105
Reclaimed Water Application Rate	107
ET Estimation	107
Surface Water Flow	110
Groundwater Flow	110
Change in Storage	111
Numerical Formulation	113
Outline of Model Runs	113
Results	115
Scenario 1. Natural Conditions without Addition of Reclaimed Water	115
Scenario 2. Rehydration with Reclaimed Water	115
Discussion	119
Potential for Wetland Restoration	119
Probability of Worst Case	120
Model Improvements	123
Conclusions	124
 CHAPTER 5. CONCLUSIONS AND SIGNIFICANCE	 126
 REFERENCES	 129
 VITA	 End Page

## **LIST OF TABLES**

Table 1. Geology and hydrogeology of west-central Florida.	10
Table 2. Values of average horizontal and vertical hydraulic conductivity for the surficial aquifer.	14
Table 3. Estimates of transmissivity, hydraulic conductivity, storativity, and leakance from results of the groundwater pumping test.	19
Table 4. Summary of the results from the surficial aquifer tracer test.	28
Table 5. Summary of the total head differences between the surficial and Floridan aquifers.	47
Table 6. Summary of groundwater flow velocities.	54
Table 7. Leakance values estimated from the North Lakes aquifer performance test (from Langevin et al., 1998).	97
Table 8. Summary of rainfall statistics for the St. Leo weather monitoring station.	109

## LIST OF FIGURES

Figure 1. Location of the North Lakes wetland and the Section 21 wellfield.	6
Figure 2. North Lakes Park and surrounding area.	8
Figure 3. Locations of surficial and Floridan aquifer monitoring wells.	11
Figure 4. (a) Median grain size versus depth for the five sampling locations. (b) Estimated hydraulic conductivity versus depth.	13
Figure 5. Drawdown versus time for Floridan aquifer monitoring wells.	16
Figure 6. Drawdown versus time for selected monitoring wells in the surficial aquifer.	18
Figure 7. Cumulative volume of water added to the wetland versus time.	21
Figure 8. Adjusted fluid conductivity versus time for SW-2.	24
Figure 9. Locations for the surficial aquifer tracer tests.	25
Figure 10. Breakthrough curves for the four sampling ports where the bromide tracer was detected.	27
Figure 11. Observed and predicted bromide concentrations for G Shallow.	29
Figure 12. Observed and predicted bromide concentrations for G Intermediate.	31
Figure 13. Fluid conductivity versus time as recorded during the Floridan aquifer tracer test.	32
Figure 14. Water level hydrographs for monitoring wells in the surficial aquifer.	34
Figure 15. Water table surface for (a) July 10, 1997, and (b) March 13, 1998.	38
Figure 16. Water-level hydrographs for monitoring wells in the Floridan aquifer.	39
Figure 17. Azimuth of groundwater flow direction in the Floridan aquifer.	41
Figure 18. Maximum hydraulic gradient versus time for Areas A and B.	42
Figure 19. Total head difference between the shallow surficial aquifer monitoring wells and the Floridan aquifer monitoring wells.	43
Figure 20. Vertical head difference versus time for the surficial aquifer.	45
Figure 21. Vertical head difference versus time for the uppermost 17 m of the Floridan aquifer.	46
Figure 22. Vertical flow velocity versus time for the surficial aquifer.	50

Figure 23. Vertical flow velocity versus time for the surficial aquifer.	51
Figure 24. Estimated values of maximum groundwater flow velocity versus time for the Floridan aquifer.	53
Figure 25. Location of the North Lakes wetland and Section 21 wellfield.	68
Figure 26. Photolineaments at the Cross Bar Ranch Wellfield.	70
Figure 27. Frequency histogram for fracture length of the photolineaments mapped by Williams (1985).	71
Figure 28. Frequency histogram for photolineament orientation as mapped by Williams (1985).	72
Figure 29. Path of particle simulated with the equivalent porous media model.	75
Figure 30. Relationship between bulk transmissivity and block transmissivity.	76
Figure 31. Transmissivity “ellipse” calculated from Monte-Carlo analysis with rotated model domain.	78
Figure 32. Results from one simulation with randomly generated fractures.	79
Figure 33. Travel paths for the first 100 Monte-Carlo simulations.	81
Figure 34. Plot of cumulative probability versus advective travel time.	82
Figure 35. Results from the first 100 Monte-Carlo simulations where the block transmissivity has not been adjusted to reproduce the appropriate value for bulk transmissivity.	85
Figure 36. Cumulative pdf for the case where block transmissivity has not been adjusted to reproduce the appropriate value for bulk transmissivity.	86
Figure 37. Location of the North Lakes wetland and Section 21 wellfield.	91
Figure 38. North Lakes Park and surrounding area.	93
Figure 39. Locations of the five sites with nested wells.	94
Figure 40. Geologic section of the North Lakes wetland.	96
Figure 41. Differences in head between the surficial and Floridan aquifers.	98
Figure 42. Annual rainfall totals measured at the St. Leo monitoring station.	99
Figure 43. a) Probability density function for a normal distribution. b) Cumulative probability density function for the normal distribution.	102
Figure 44. Monthly statistics from historical rainfall data at the St. Leo weather monitoring station.	106
Figure 45. Cumulative probability graph of rainfall for the month of January.	108
Figure 46. Histogram of time-series dh values for four of the five nested wells at the North Lakes wetland.	112

Figure 47. Flow chart for running Monte Carlo analysis with the water balance equation.	114
Figure 48. Results from the stochastic simulation of head versus time for the calibration run that produces an acceptable median water level.	116
Figure 49. Stochastic simulation of head versus time.	117
Figure 50. Cumulative probability plots for five stochastic simulations.	118
Figure 51. Probability that the six-year, median water level will be above the threshold elevation (15.07 m) plotted against the reclaimed water application rates (RW).	121
Figure 52. Simulated PDF of the six-year, median water level.	122



STOCHASTIC METHODS FOR EVALUATING THE POTENTIAL  
FOR WETLAND REHYDRATION IN COVERED-KARST TERRANES

by

CHRISTIAN DAVID LANGEVIN

An Abstract

Of a dissertation submitted in partial fulfillment  
of the requirements for the degree of  
Doctor of Philosophy  
Department of Geology  
University of South Florida

December 1998

Major Professor: Mark Stewart, Ph.D.

Augmentation with reclaimed water is one method for rehydrating wetlands damaged by water-level declines. Augmentation with reclaimed water has been proposed for rehydrating a wetland in the covered-karst terrane of west-central Florida. There is concern because reclaimed water may contain harmful agents that could flow from the wetland 1.4 km to a municipal wellfield that withdraws 30,000 m<sup>3</sup>/day. Estimates of groundwater flow velocities were calculated from the results of detailed field studies at the wetland. Results indicate that groundwater flows downward in the surficial aquifer at rates of 0.1 to 0.2 m/day and horizontally in the Floridan aquifer at rates of 0.02 to 0.5 m/day. Sinkholes do not appear to be preferential pathways for downward groundwater flow at the site because the confining layer is thin to absent, and low-permeability soil layers may restrict flow within the sinkholes.

A method was developed for incorporating large-scale, vertical fracture zones into two-dimensional, finite-difference models of groundwater flow (MODFLOW) and particle tracking (PATH3D). Fracture zones are included in the numerical model by increasing transmissivity values in selected cells. The selection of cells is based on existing patterns of fracture zones, which can be inferred from maps of photolineaments. To quantify the uncertainties in knowing the exact location, orientation, and hydraulic properties of the fracture zones, these parameters are treated stochastically through Monte Carlo simulation. Stochastic results from an example simulation of groundwater flow and advective transport between the North Lakes wetland and Section 21 wellfield indicate a 50 and 10 percent chance that travel times will be less than 9 and 2 years, respectively.

The probability of rehydrating a wetland with an additional source of water can be estimated by combining a form of the water balance equation with Monte Carlo analysis. Parameters that contain large uncertainties, such as future values of rainfall, ET, and groundwater flow, are treated stochastically, while the additional source of water is treated deterministically. Stochastic simulation results in an ensemble of water-level time series that contain all statistically reasonable predictions. Statistics performed on the

ensemble indicate that worst-case predictions are highly improbable, and that a recharge rate of 5700 m<sup>3</sup>/day will maintain the target water level in the example wetland used to illustrate the method.

Abstract Approved: \_\_\_\_\_

Major Professor: Mark Stewart, Ph.D.  
Professor and Chair, Department of Geology

Date Approved: \_\_\_\_\_

## **PREFACE**

As an undergraduate student at the University of Wisconsin, I began my studies as a business major.

During my first semester, I stumbled upon "Introduction to Geology" and ended up taking the course. That semester I learned a great deal about geology, particularly because the teaching assistant, Kent Syverson, was very energetic. The next academic year, when pre-business courses weren't capturing my interests, I decided to switch gear and focus on geology. This was something Kent had suggested the year before. For that initial encouragement, I thank my Geology 101 Teaching Assistant, Kent Syverson (who is now Dr. Syverson).

Towards the end of my Bachelor's degree, I began searching for a graduate program to continue with my interests in hydrogeology, mathematics, and computer programming. The hydrogeology professor at UW, Dr. Mary Anderson, highly recommended one her former students, Dr. Mark Stewart, at the University of South Florida. Most of what I have learned at USF during the past 7 years is the result of interaction with Drs. Mark Stewart, Len Vacher, and Tom Juster. Tom always made himself available and provided many useful suggestions and solutions. Len taught me how to solve complex hydrogeological problems using mathematics and statistics. He also demonstrated the satisfaction in tackling a new problem and solving it from start to finish. Much of what I have learned from Mark cannot be taught in the classroom. He has shown many ways to decipher scientific results and recognize their significance. I want to thank these three people for having meaningful impacts on my graduate education.

I would also like to extend my gratitude to the other members of my committee, Jeff Ryan, Carl Steefel, and Mark Ross. Through my friendship and weightlifting experiences with Jeff, I have learned a great deal about many things, including the fractionation properties of boron, and to a lesser extent, beryllium. Carl provided much needed assistance for computer- and programming-related problems. Interaction with Mark Ross has taught me to look at the water balance as a whole, rather than just the hydrogeological component. I also want to thank Mark for introducing me to dolphin fishing in the Florida Keys.

At the beginning of my Ph. D. studies, Dr. Stewart and I were very fortunate in that we received funding from the Southwest Florida Water Management District to conduct an extensive study of the North Lakes wetland. The purpose of this study was to determine the feasibility of using reclaimed water to rehydrate the damaged wetland. Much of the field work at North Lakes was hot and tedious and could not have been completed without the help from many USF students, faculty and staff. I would like to thank Noreen Purcell, Tony Countryman, Patrick Barnard, Holly Barnette, James Broska, Meghan Elliot, Lucy Gerle, Henri Liauw-A-Pau, Keith Morrison, Dilo Senanyake, Ken Trout, Tom Griggs, David Ufnar, Sandy Blansett, and everyone else who spent time in the swamp. Dr. Sarah Kruse helped with geophysical equipment whenever we needed it. My roommate at the time, Dave Latham, tolerated lengthy conversations about the North Lakes project. Patrick Tara provided weekly assistance with field equipment and computer problems. I would like to thank Nancy Mole for dealing with the bureaucracy of graduating, and I would particularly like to thank Mary Haney for bailing me out of numerous jams during my 7+ years at USF.

The North Lakes study could not have been performed without the funding and support from the Southwest Florida Water Management District. Gregg Jones provided equipment and manpower whenever we requested. Kathleen Coates and Ron Basso carefully reviewed technical reports. Most importantly, Don Thompson provided technical assistance, equipment, and supplies. Don took a personal interest in the North Lakes project. Most of our successes at the site are directly related to his involvement.

I would also like to thank the members of Mark Stewart's Hydrogeology Laboratory. Without the help from Juana Montane, Carl Albury, Jason LaRoche, and Barclay Shoemaker, this dissertation and the North Lakes study would not have been possible. Juana provided a great deal of enthusiasm when work in the swamp got us down. Conversations with Carl provided the basis for much of the technical matter in this dissertation and the North Lake reports. Jason helped from the beginning of the North Lakes study and provided valuable information on the stratigraphy at the site. Through use of his exceptionally large biceps, Barclay significantly increased our manpower in the field. I would also like to thank Barclay for faithfully collecting water-level data at the site. Most of all, I would like to thank these four people for their friendship and support during the past few years.

Finally, I would like to thank my mother and father, brothers, and sister for encouraging me during my rather lengthy college experience. Their love of life is best expressed by the Langevin saying: “We’re not here for a long time—we’re here for a good time”.

## **CHAPTER 1. INTRODUCTION**

Since the mid-1800's, the deliberate destruction of wetlands was routinely performed in the United States to increase the available land for agriculture and development (Mitch and Gosselink, 1993). Over the past few decades, however, the push for environmental preservation has slowed the intentional destruction of wetlands. Today, the destruction of wetlands often occurs indirectly from reduced stream flows and lowered water tables. These reductions in the water available for wetlands result from the increased use of surface water and groundwater for potable supplies and irrigation.

Groundwater withdrawals at municipal wellfields are a major cause of lowered water-table elevations and reduced baseflow to streams. When groundwater is pumped from deep aquifers, the water table can lower significantly if low-permeability materials do not restrict flow between the water-table aquifer and the pumped aquifer. In covered-karst terranes, for example, sinkholes breach low-permeability units and provide preferential pathways for groundwater flow into deeper aquifers. Stewart and Parker (1990) estimate that in west-central Florida, 90 percent of the flow from the clastic surficial aquifer into the underlying carbonate aquifer occurs through sinkholes. These preferential pathways are significant near wellfields because they drain the surficial aquifer and reduce the groundwater available for wetland use. Declines in water-table elevation spread away from pumping wells until the rate of "salvaged" evapotranspiration is equal to the groundwater pumping rate (Stewart, 1998).

Augmentation with highly treated wastewater, or reclaimed water, is one method for increasing the water table in wetlands affected by groundwater pumping. The method is appealing because it supports the concept of resource sustainability. Water withdrawn from the aquifer is used, treated, and then returned to the system. Using reclaimed water in this manner falls into the category of "indirect potable reuse", as defined by the National Research Council (NRC, 1994). There is concern with indirect potable reuse because reclaimed water contains low levels of harmful chemicals and pathogenic viruses. By augmenting with reclaimed water, there is potential for introducing these harmful agents into potable groundwater

supplies. The viability for indirect potable reuse relies on an aquifer's ability to filter and degrade contaminants.

The feasibility of rehydrating wetlands with reclaimed water depends on the answers to two important questions: (1) how long will it take reclaimed water to be withdrawn by a municipal well? and (2) can water levels in a wetland be maintained with available quantities of reclaimed water? To answer these questions, one must predict the effects of rehydration prior to the application of reclaimed water. The purpose of this dissertation is to develop methods for predicting the response of groundwater flow velocities and water-table elevations to the application of an additional source of water. The field example used to illustrate the methods refers to the recharge water as reclaimed water. The methods are based on physical principles of flow and advective transport but do not directly address water quality. Dispersive transport of contaminants within the reclaimed water is beyond the scope of this dissertation. The results from this study, however, are important for describing the parameters that control contaminant transport, such as the residence time of groundwater in different geologic materials.

For feasibility studies of rehydration, it is important to quantify uncertainties in predictions because of the health risks associated with indirect potable reuse, and because rehydration systems are costly to implement. Two methods are used to make predictions. The deterministic method assumes that the data used to make the prediction do not contain uncertainty. For many studies, particularly those of subsurface groundwater flow, this limitation is restrictive because most of the data contain some level of uncertainty. With the stochastic approach, the uncertainties in predictions can be quantified. Both deterministic and stochastic methods are used in this dissertation to evaluate the feasibility of wetland rehydration, but emphasis is placed on the stochastic approach.

This dissertation contains the results of three related studies. The subject of Chapter 2 is a field study conducted to determine the feasibility of using reclaimed water to rehydrate a wetland in a covered-karst terrane. Chapter 3 presents the results of a stochastic analysis of the significance of large-scale heterogeneities (vertical fracture zones) on groundwater flow paths and velocities. Chapter 4 presents a stochastic method for determining if an available amount of recharge water can successfully rehydrate a wetland. While all three chapters are related through the North Lakes wetland and the west-central Florida



location, each is written as a stand-alone manuscript, so that each can be published without requiring direct reference to the other chapters. This requires some repetition in each chapter, but greatly facilitates preparing the chapters for publication.

Chapter 2 presents the results from a detailed field study at the North Lakes wetland. The North Lakes wetland is located in the covered-karst terrane of west-central Florida. Historic data suggest that the wetland has been damaged by groundwater withdrawals from the Section 21 wellfield, 1.4 km to the west. The purpose of Chapter 2 is to show how the field data collected at the site can be used to answer feasibility questions that relate to groundwater flow velocities and travel times. In addition, the hydraulic significance of sinkholes is determined for the site. Data from Chapter 2 are also used in Chapters 3 and 4 to illustrate the stochastic methods developed in this dissertation.

In Chapter 3, predictions of groundwater travel times are explored by developing a method to incorporate large-scale, vertical fracture zones into numerical models of groundwater flow and particle tracking. Because the properties of these fracture zones are often unknown, the method treats them as stochastic parameters. The method generates a random set of fracture zones, incorporates the highly transmissive zones into a numerical model, and runs the model to determine groundwater flow directions and velocities. This procedure is performed many times with many different sets of fracture zones. The results from this type of Monte Carlo analysis are useful for estimating the uncertainty in groundwater travel times. To illustrate the procedure, the method is used to quantify uncertainties in groundwater travel times between the North Lakes wetland and Section 21 wellfield. To apply the method to the study area, a number of simplifying assumptions were made about the properties of fracture zones.

To determine if a specified augmentation rate will maintain target water levels in a wetland, Chapter 4 combines stochastic analysis with a form of the water balance equation. The method results in many statistically reasonable time series of water levels. The purpose for developing this method is to quantify the probability that an allocated augmentation rate will achieve adequate rehydration. The use of this method can reduce the risk of implementing of a costly rehydration system that cannot maintain target water levels.

The methods developed in this dissertation combine site-specific data with deterministic and stochastic methods. The result is a powerful approach to evaluating the potential for wetland rehydration with reclaimed water. While the methods are illustrated with the North Lakes example, they are applicable to other settings and problems. For example, the prediction of groundwater flow velocities and the uncertainties in the predictions is important for the wide range of hydrogeological problems that relate to contaminant transport.

## **CHAPTER 2. ESTIMATING GROUNDWATER FLOW VELOCITIES IN A LEAKY AQUIFER SYSTEM IN WEST-CENTRAL FLORIDA**

### **Introduction**

Where aquifers that supply potable water for municipal wellfields are hydraulically connected to shallow unconfined aquifers and surface water bodies, municipal withdrawals can adversely affect wetland and lake levels. In west-central Florida, significant withdrawals of groundwater from the Floridan aquifer have lowered the water table in the shallow surficial aquifer and have reduced surface water flows. As a result, wetlands located near pumping centers can no longer support wetland vegetation and are being invaded by upland species. To mitigate the environmental damage sustained by numerous wetlands, the Southwest Florida Water Management District (SWFWMD) is investigating the possibility of using reclaimed water to restore selected wetlands. The concern with this approach is that reclaimed water added to a wetland could travel rapidly to a municipal supply well. Groundwater flow rates and travel times are dependent on many site-specific factors. Selection of appropriate wetlands, therefore, should be evaluated case by case.

The North Lakes wetland, in Hillsborough County, Florida, has been selected as a potential site for rehydration with reclaimed water. During the past few decades, water levels within the wetland have declined to levels that cannot support wetland vegetation. Consequently, cypress trees are dying, and much of the wetland is being invaded by upland vegetation. One of the reasons the North Lakes wetland was selected as a potential site for rehydration is that two storage tanks for reclaimed water are located next to the wetland. The cost of implementing a rehydration program, therefore, would be minimal. The main concern with rehydration is that the residence time of reclaimed water in the aquifer system will not be long enough for sufficient renovation. Located approximately 1.4 km from the wetland, the Section 21 wellfield is permitted to withdraw groundwater at an average annual rate of 40,000 m<sup>3</sup>/day (10 million gallons per day; Figure 1). This wellfield is operated by the City of St. Petersburg and supplies potable water to the

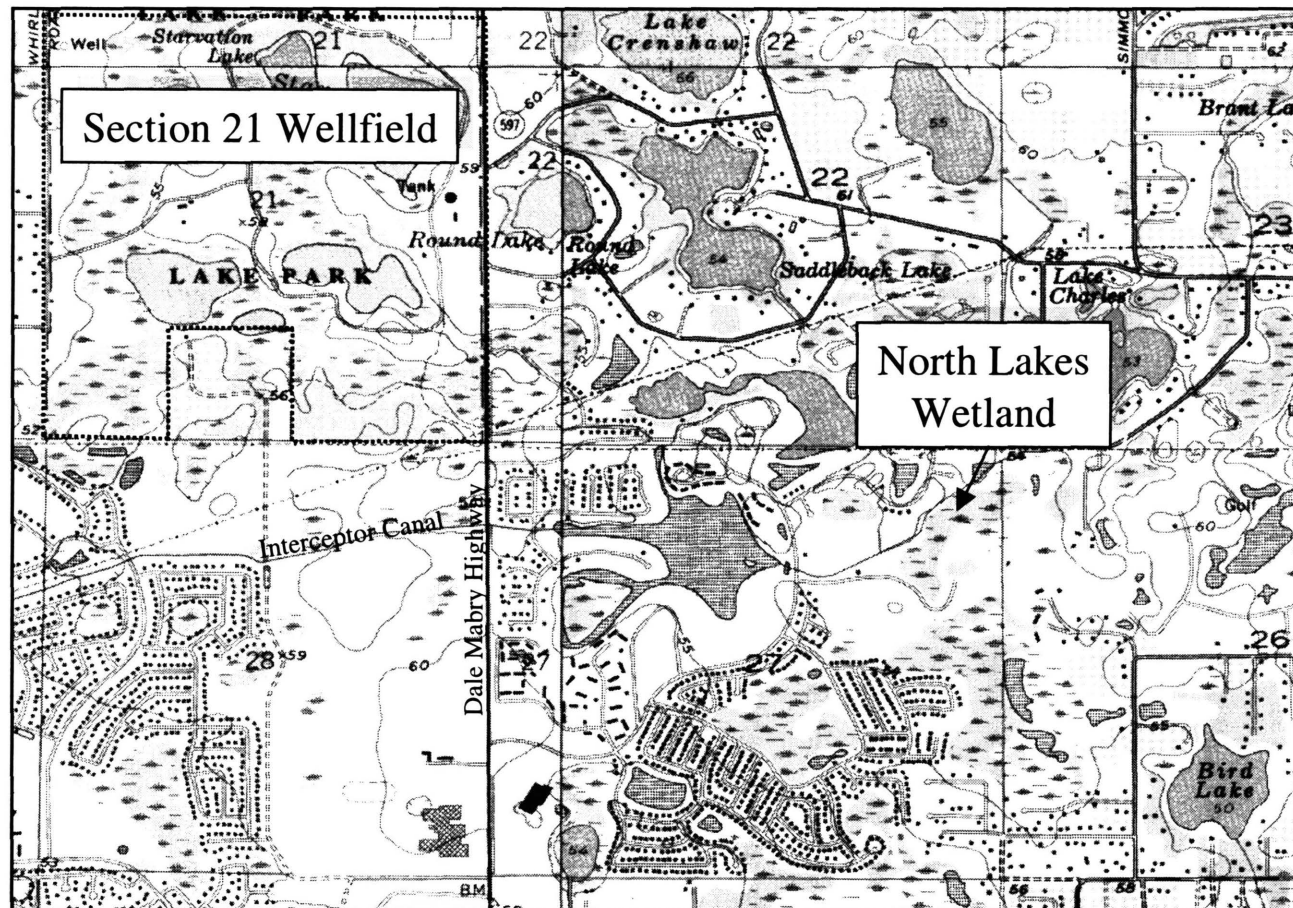


Figure 1. Location of the North Lakes wetland and the Section 21 wellfield.

residents of Hillsborough County. Environmental managers at the SWFWMD have determined that reclaimed water added to the wetland must reside in the aquifer system for at least two years before being withdrawn by a supply well. This residence time was considered to be conservative as viral inactivation rates are on the order of months. The purpose of this study is to estimate the groundwater flow velocities at the North Lakes wetland. From these velocities, the residence time of reclaimed water in the aquifer system will be calculated.

The Geology Department at the University of South Florida was subcontracted by SWFWMD to conduct a detailed field study of the North Lakes wetland. The purpose of the field study was to collect the data required for estimating groundwater flow paths and travel times. In addition, the data collected during the field study will be used in a separate study to estimate how much reclaimed water will be required to restore the original hydrologic conditions at the wetland. During the field investigation, a variety of methods were used to develop a hydrogeological model for the site, including monitoring well installation, groundwater pumping tests, tracer tests, and temporal monitoring of water levels. A detailed description of the field study is presented in a report to SWFWMD by Langevin et al. (1998). The purpose of this chapter is to describe the groundwater flow patterns at the North Lakes wetland by reporting the results from the field study and presenting estimates of groundwater flow velocity and residence time. Special emphasis is placed on those methods that proved most useful for estimating groundwater flow velocities.

### **Description of Study Area**

The North Lakes wetland is located in the North Lakes County Park (Figure 2). The wetland is approximately 65,000 m<sup>2</sup> in area. The northern boundary of the wetland is marked by the Interceptor Canal, which was constructed in the 1960's to prevent residential areas from flooding. In an effort to restore the wetland, a weir was constructed in the Interceptor Canal near the tennis courts (Figure 2; Florida Land Design and Engineering 1987). The purpose of the weir was to dam surface water flowing from the northeast and flood the wetland. To prevent the park from flooding, a meter-high berm was constructed around the wetland. Thus far, the plan to restore the original wetland hydrology has failed because surface

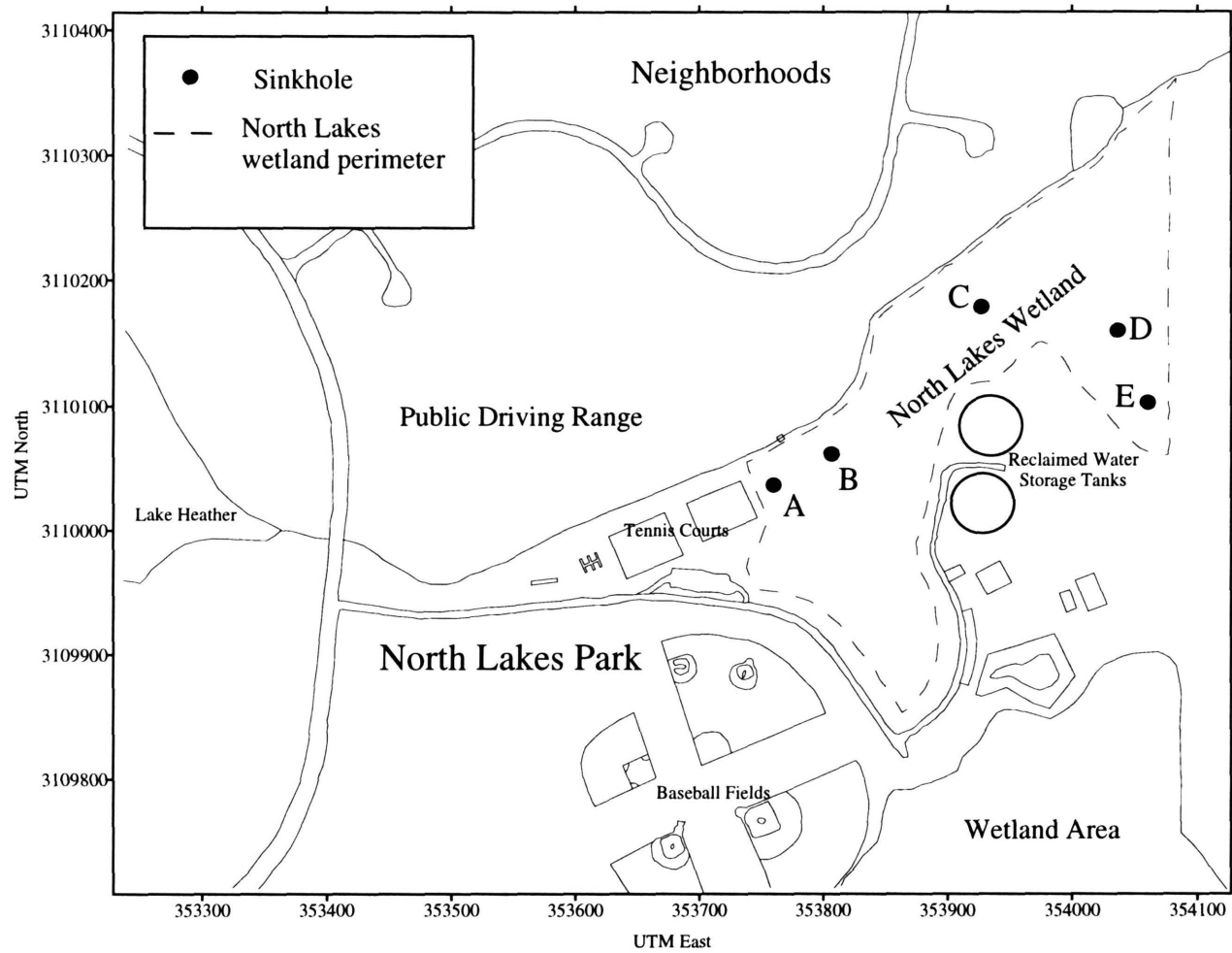


**Figure 2. North Lakes Park and surrounding area. Sinkholes that can be seen at land surface are labeled A through E.**

water flows from the northeast have nearly ceased. The only time the wetland floods is during years with above-normal rainfall conditions.

The geology and hydrogeology of the North Lakes wetland corresponds with the geology and hydrogeology of west-central Florida as defined by Miller (1986). Miller (1986) summarizes the geology and hydrogeology of the area with four principal units (Table 1). The uppermost unit is the surficial aquifer. It consists of sands, silts and clays. Separating the surficial aquifer from the Upper Floridan aquifer (referred to here as the “Floridan aquifer”) is the Upper Confining unit, a discontinuous clayey sand to sandy clay. Results from the field study suggest that at North Lakes the Upper Confining unit is thin, and in most places is probably absent (Langevin and Stewart 1997; Langevin et al. 1998). The Floridan aquifer lies below the Upper Confining unit (or surficial aquifer when the Upper Confining unit is absent) and consists of limestones and dolostones of Tertiary age. In west-central Florida, municipal wellfields withdraw groundwater from the Floridan aquifer. The base of the Upper Floridan aquifer is called the Middle Confining unit, a low-porosity dolostone with intergranular anhydrite (Miller, 1986).

Five sinkholes were located within the boundaries of the wetland (Figure 2). The sinkholes are 1 to 2 m in depth and, based on the steep slopes of the sinkhole walls, appear to be relatively young. The formation of Sinkhole B began after the start of the North Lakes field study in 1996. Stewart and Parker (1990) examined the hydraulic significance of sinkholes at a site approximately 15 km from North Lakes. Results from their study suggest that 90 percent of the recharge to the Floridan aquifer occurs through sinkholes. Many of the field tests conducted at North Lakes were designed to test the hypothesis that sinkholes have a large effect on vertical flow velocities.

## **Methods and Results**

### ***Installation of Monitoring Wells***

Using different well installation methods, 39 monitoring wells were installed at North Lakes County Park (Figure 3). Nine wells were installed in the Floridan aquifer with mud-rotary techniques. For six of the monitoring wells in the Floridan aquifer (FMW-1, and FMW-3 through FMW-7), 4-inch-diameter PVC

Table 1. Geology and hydrogeology of west-central Florida.

System	Age B.P. (m.y.)	Series	Stratigraphic Unit	General Lithology	Hydrogeologic Unit
Quaternary	0 2	Holocene and Pleistocene	Surficial sand, terrace sand, phosphorite	Predominantly fine sand; interbedded clay, marl, shell, limestone, phosphorite	surficial aquifer
Tertiary	7	Miocene	Hawthorn Group	Clayey sand and limestone; silty, phosphatic	upper semi- confining unit
	26		Tampa Member	Limestone, sandy, fossil- iferous; sand and clay in lower part in some areas	Upper Floridan aquifer
	37	Oligocene	Suwannee Limestone	Limestone, sandy lime- stone, fossiliferous	
	53	Eocene	Ocala Limestone	Limestone, chalky, foram- iniferal, dolomitic near bottom	
			Avon Park Formation	Limestone and hard brown dolomite; intergranular evaporite in lower part in some areas	
			Oldsmar Formation	Dolomite and limestone with intergranular gypsum in most areas	Middle confining unit and Lower Floridan aquifer undifferentiated
	65	Paleocene	Cedar Keys Formation	Dolomite and limestone with intergranular gypsum and bedded anhydrite	Sub-Floridan confining unit



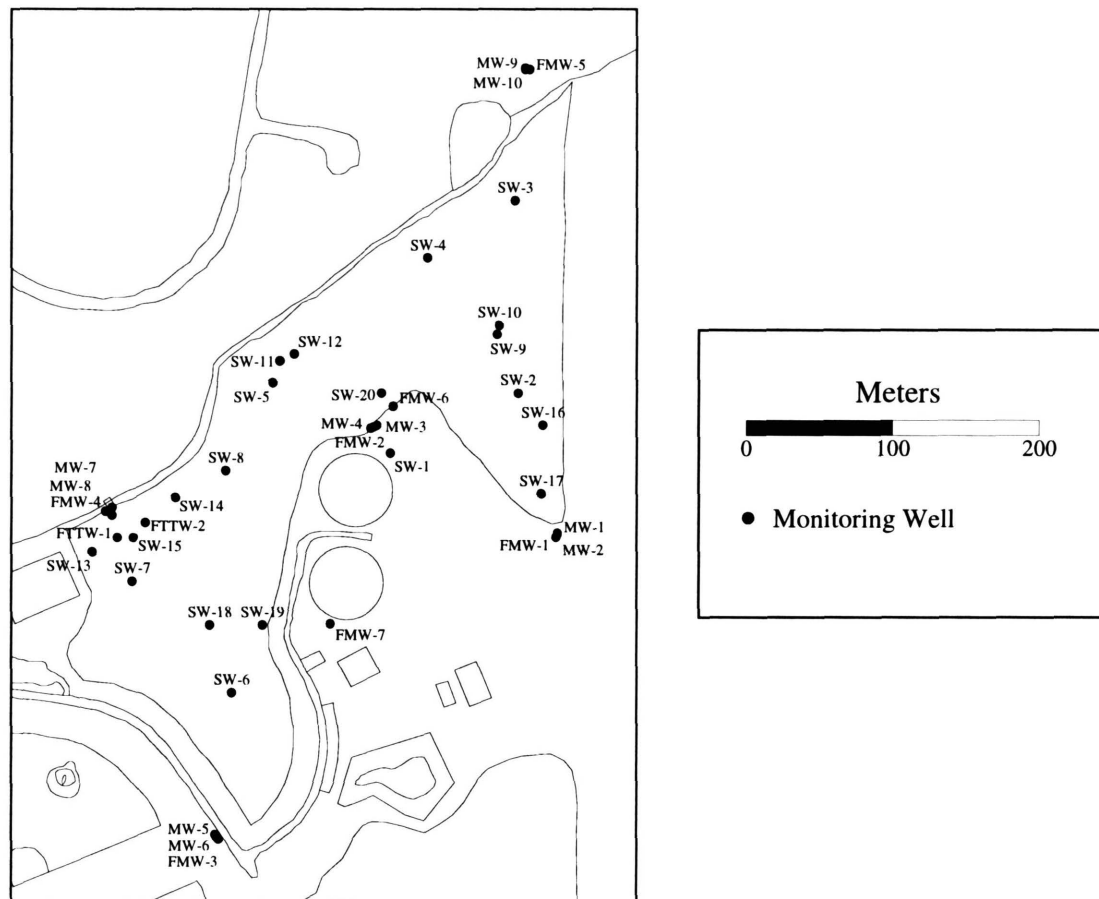


**Figure 3. Locations of surficial and Floridan aquifer monitoring wells. Well "nests" are found at FMW-1 through FMW-5.**

casing was set to a depth of approximately 30 m below land surface. Beneath the PVC casing a 3-m length of borehole was left open to the aquifer. FMW-2 is the deepest well at North Lakes and has an open-hole interval of 50 m, starting at a depth of 30 m below land surface. The PVC casing at FMW-2 is 12 inches in diameter. FMW-2 was used as the supply well for the groundwater pumping test. FTTW-1 and FTTW-2 have open-hole intervals from 10 to 13 m below land surface. These wells also have 4-inch-diameter PVC casing set above the open-hole interval. FTTW-1 and FTTW-2 were used for the tracer test in the Floridan aquifer and were installed 7.6 m apart from one another.

Monitoring wells in the surficial aquifer were installed with a hollow-stem auger, solid-stem auger, or hand auger. Monitoring wells installed with the hollow-stem auger (MW wells; Figure 3) have coarse-grained sand packs around the well screens. The monitoring wells installed with the solid-stem auger or hand auger (SW wells; Figure 3) do not have sand packs around their well screens.

#### ***Sediment Sampling and Grain-Size Analysis***

During the installation of FMW-1 through FMW-5, samples of the unconsolidated surficial deposits were collected from land surface to top of rock with a split spoon. These samples, collected at 0.6-m intervals, were stored in core boxes for further analysis. In the laboratory, the split-spoon core was separated into discrete sedimentary layers. The separation was based on visual inspection with a hand lens. It is assumed that each discrete layer is homogeneous with respect to grain-size parameters, and homogeneous and isotropic with respect to hydraulic parameters. From each of the sedimentary layers, at least one sample was removed for grain-size analysis. The methods used for grain-size analysis conform strictly to the guidelines stipulated by the American Society for Testing and Materials (ASTM 1990). A detailed description of the grain-size analysis, results, and conclusions is in process (LaRoche, in preparation).

For each of the five sites, the median grain size ( $d_{50}$ ) is plotted versus depth (Figure 4a). The results of the grain-size analysis were translated to values of hydraulic conductivity using the empirical relationship of Zamarin (in Vukovic and Soro, 1992). A plot of hydraulic conductivity versus depth, for each of the five sites, suggests that the surficial aquifer may be differentiable into discrete units (Figure 4b). For this study, however, the surficial aquifer is treated as a single hydrostratigraphic unit. Single values for hydraulic

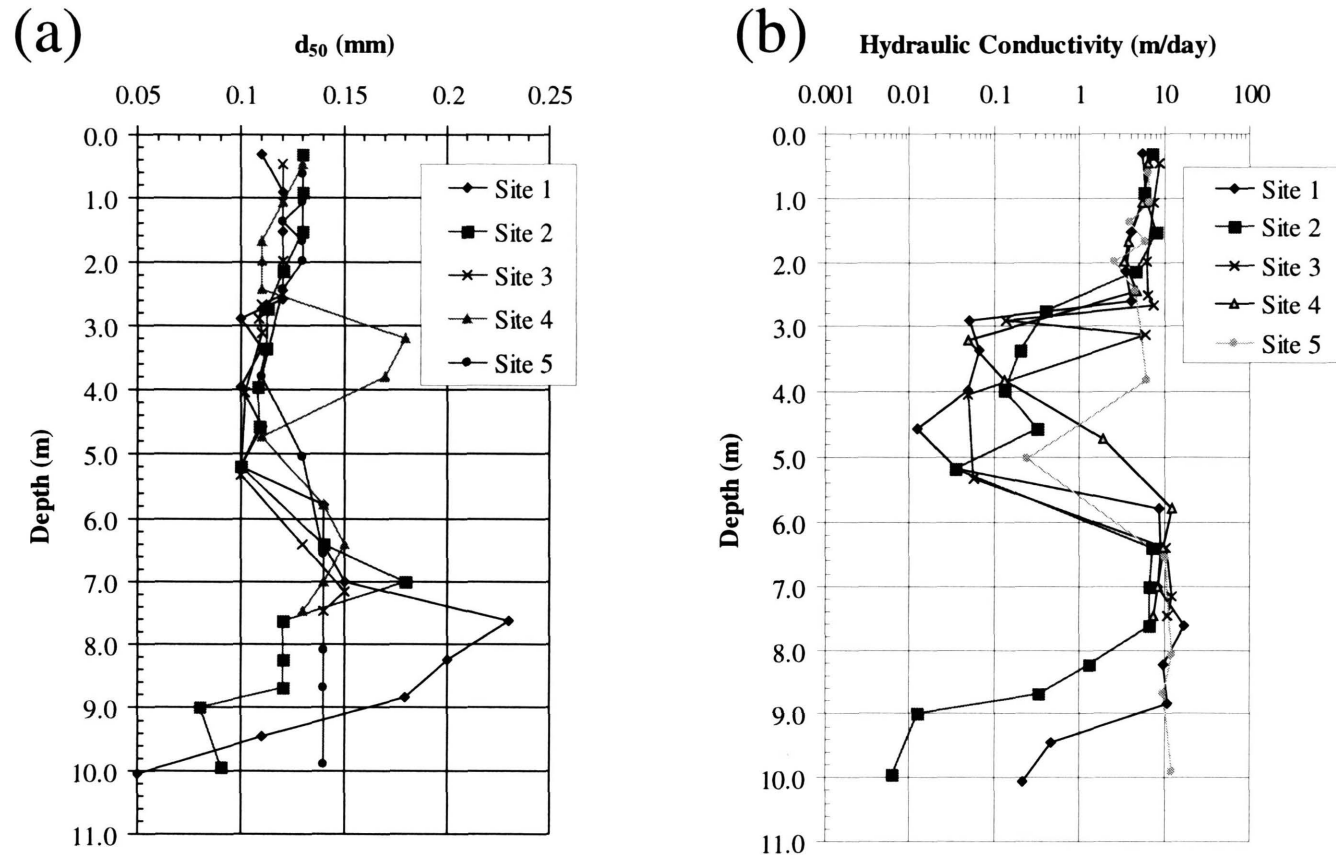


**Figure 4. (a) Median grain size versus depth for the five sampling locations. (b) Estimated hydraulic conductivity versus depth. The estimated values of hydraulic conductivity were calculated from the results of the grain-size analysis using the empirical relationship of Zammarin (as referenced in Vukovic and Soro, 1992).**

**Table 2. Values of average horizontal and vertical hydraulic conductivity for the surficial aquifer.  
Hydraulic conductivity values were calculated using a relationship with grain size  
(Zamarin, as referenced in Vukovic and Soro, 1992)**

Site	$K_x$ (m/day)	$K_z$ (m/day)	$K_x/K_z$
Site 1	5.1	0.2	26
Site 2	3.3	0.31	11
Site 3	5.2	0.19	27
Site 4	4.9	0.20	24
Site 5	8.2	0.12	67

conductivity in the horizontal ( $K_x$ ) and vertical ( $K_z$ ) directions were calculated for the surficial aquifer from the data in Figure 4b. Values of  $K_x$  were calculated by taking the arithmetic average of the hydraulic conductivity values for each layer, weighted on each layer's thickness. Values of  $K_z$  were calculated by taking the harmonic mean of the hydraulic conductivity for each layer, also weighted by each layer's thickness. The hydraulic conductivity in the horizontal direction ranges from 3.3 to 8.2 m/day (Table 2). The hydraulic conductivity in the vertical direction ranges from 0.12 to 0.31 m/day (Table 2).

Values of porosity were also estimated from the results of grain-size analysis. The empirical relationship developed by Isotomina (in Vukovic and Soro, 1992) suggests that the porosity at North Lakes is nearly constant with a value of approximately 0.4. Results from grain-size analysis indicate that the surficial aquifer is composed primarily of fine-grained sand with some silt and clay. The porosity value estimated from the grain-size data lies near the middle of the range presented by Domenico and Schwartz (1990) for a fine-grained sand (0.26 to 0.53).

### ***Groundwater Pumping Test***

A groundwater pumping test was conducted at North Lakes to measure the response of the surficial and Floridan aquifers to a pumping stress. The groundwater pumping test was conducted during the week of March 17, 1997. Water was withdrawn from the large-diameter well (FMW-2) at a nearly constant rate of 5150 m<sup>3</sup>/day (1000 gallons per minute). The discharge water from FMW-2 was transmitted approximately 370 m to the Interceptor Canal on the west side of the weir. The Interceptor Canal was lined with impermeable plastic sheeting prior to the pumping test to prevent the discharge water from reentering the aquifer and interfering with the test. Most of the monitoring wells at the site were equipped with pressure transducers connected to a data logger. The data logger was used to record water levels on a logarithmic time interval. For those wells that were not equipped with a pressure transducer, water levels were measured frequently with a water-level indicator.

Monitoring wells in the Floridan aquifer react quickly to the initiation of pumping at FMW-2 (Figure 5). Drawdowns at the end of the test range from 0.93 to 2.58 m. As expected, the largest drawdown is at FMW-6, the well closest to the pumping well. The drawdown data for the pumping well, FMW-2, is not

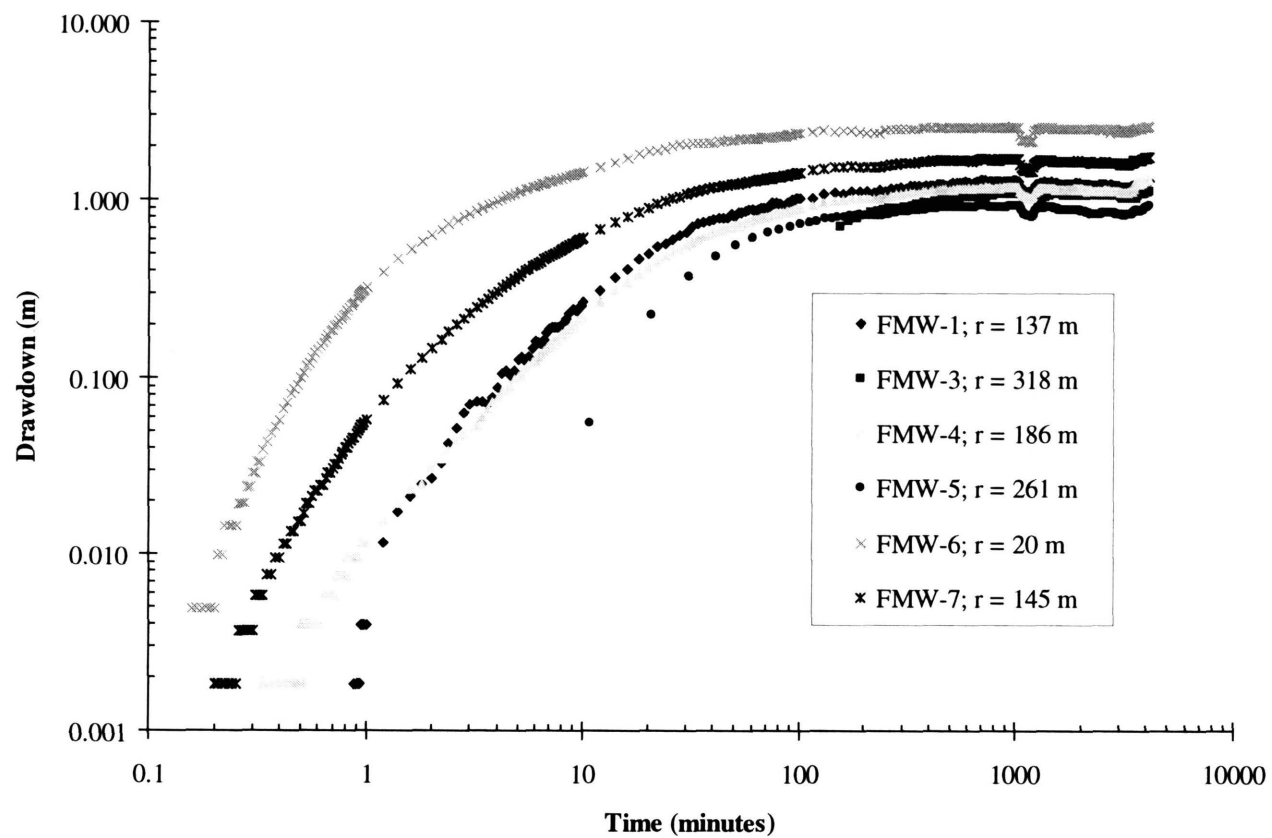


**Figure 5. Drawdown versus time for Floridan aquifer monitoring wells. Drawdown was measured during the groundwater pumping test conducted in March of 1997.**

included because the large pumping rate induced a significant head loss within the well. The data for FMW-2, therefore, is not considered representative of the drawdown in the aquifer.

Water levels in the monitoring wells of the surficial aquifer were also influenced by the pumping of FMW-2. Drawdown curves for selected monitoring wells in the surficial aquifer are presented in Figure 6. The graphs in Figure 6 are separated by location within the wetland. The first graph, Figure 6a, contains drawdown data for the wells at sinkhole D. At sinkhole D, SW-10 is located within the sinkhole, and SW-9 is located just outside of the sinkhole. The drawdown in the sinkhole (SW-10) is approximately 20 cm less than the drawdown outside the sinkhole in SW-9. A similar response is shown in Figure 6b. Drawdown in the sinkhole well, SW-11, is less than the drawdown in the well outside of the sinkhole, SW-12. Three monitoring wells in the surficial aquifer are located near sinkhole E. At these three wells, drawdowns are higher outside of the sinkhole (SW-2 and SW-17) than in the sinkhole (SW-16; Figure 6c). On the other hand, monitoring wells at sinkholes A and B exhibit a different drawdown response from the other sinkholes. Drawdown in the sinkholes (SW-13 and SW-14; Figure 6d) is greater than the drawdown in a well located between the two sinkholes (SW-15).

The Hantush method (1960) was used with data recorded during the groundwater pumping test to estimate values for confining unit leakance, Floridan aquifer storativity, and Floridan aquifer transmissivity. The Hantush method is based on the conceptual model of a two-aquifer system separated by a semi-confining layer. Results from the Hantush analysis are presented in Table 3. Transmissivity of the Floridan aquifer ranges from 243 to 1080 m<sup>2</sup>/day. To calculate hydraulic conductivity, the estimated value of transmissivity is divided by the open-hole interval of the pumping well (50 m). Values of hydraulic conductivity range from 5 to 22 m/day. Storativity values of the Floridan aquifer range from  $2 \times 10^{-4}$  to  $3 \times 10^{-3}$ . Leakance values range from  $1 \times 10^{-3}$  to  $4 \times 10^{-2}$  day<sup>-1</sup>.

### ***Flooding Test***

To mimic the hydraulic conditions that would exist if the wetland was flooded with reclaimed water, the southeast portion of the wetland was flooded with potable water. The southeast portion of the wetland was selected because this area is a topographic low and it contains two sinkholes. The goal of the flooding was

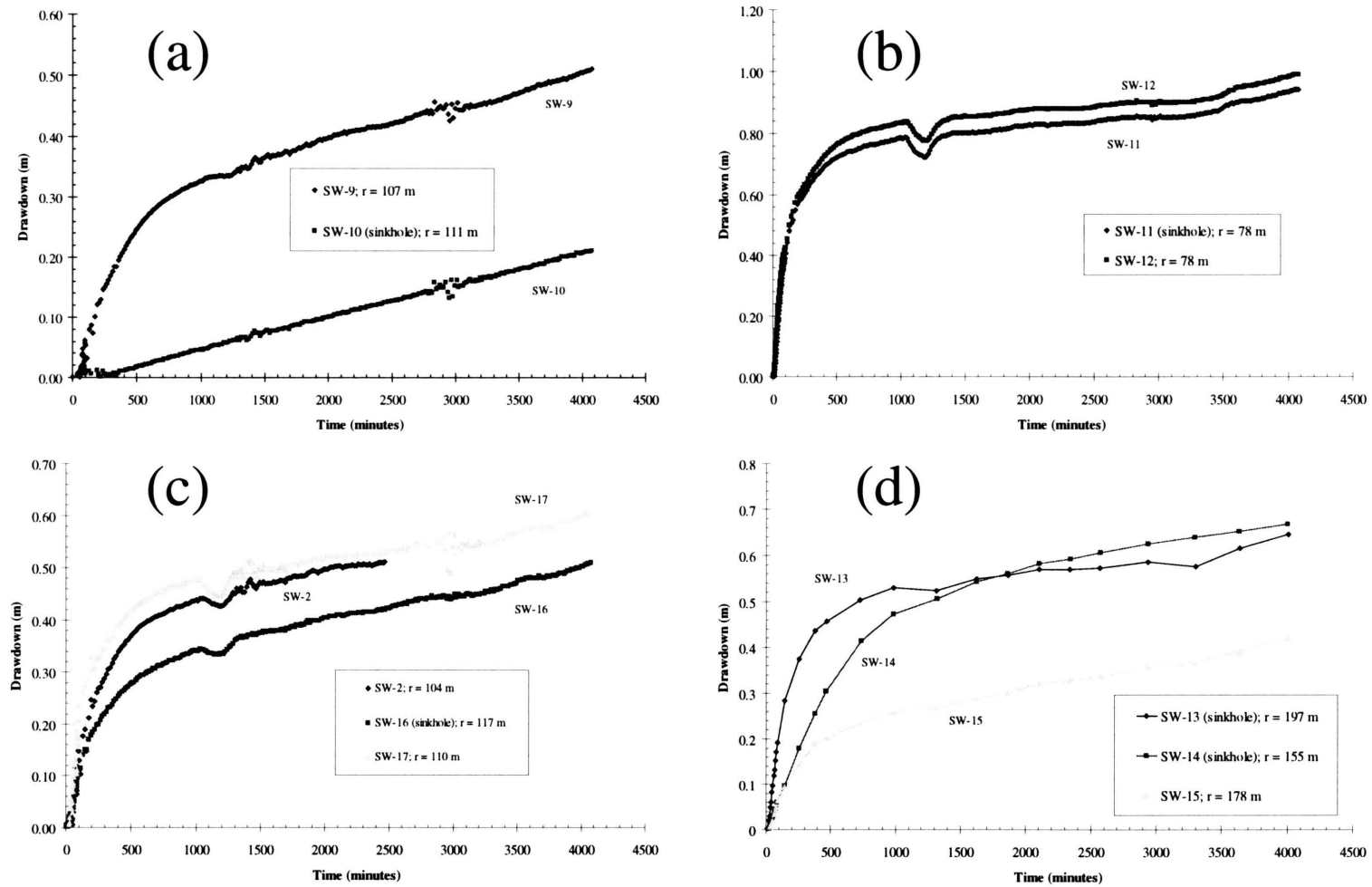


**Figure 6. Drawdown versus time for selected monitoring wells in the surficial aquifer. Drawdown was measured during the groundwater pumping test conducted in March of 1997. (a) wells in and around Sinkhole D. (b) wells in and around Sinkhole C. (c) wells in and around Sinkhole E. (d) wells in and around sinkholes A and B.**



**Table 3. Estimates of transmissivity, hydraulic conductivity, storativity, and leakance from results of the groundwater pumping test. Values were determined with the Hantush curve-matching method for leaky aquifers.**

Well	Transmissivity (m <sup>2</sup> /day)	Hydraulic Conductivity (m/day)	Storativity	Leakance (day <sup>-1</sup> )
FMW-1	1080	22	$6 \times 10^{-4}$	$4 \times 10^{-3}$
FMW-3	344	7	$5 \times 10^{-4}$	$3 \times 10^{-3}$
FMW-4	1080	22	$4 \times 10^{-4}$	$3 \times 10^{-3}$
FMW-5	243	5	$2 \times 10^{-4}$	$9 \times 10^{-3}$
FMW-6	687	14	$3 \times 10^{-3}$	$4 \times 10^{-2}$
FMW-7	1080	22	$2 \times 10^{-4}$	$1 \times 10^{-3}$
Average	752	15	$8 \times 10^{-4}$	$1 \times 10^{-2}$

to maintain the stage in the wetland between 15.39 and 15.54 m. In order to flood the wetland with potable water, a discharge conveyance was constructed from the fire hydrant near the park recreation center to the southeastern portion of the wetland. The conveyance consisted of 270 m of lay-flat hose and PVC pipe. At the end of the discharge pipe, 24 m of septic diffuser pipe was used to evenly distribute the water over the flooded area.

During the test, the discharge rate was adjusted frequently to keep the stage between the desired elevations. An in-line flow meter was used to monitor the discharge volumes. The straight line on the plot of cumulative volume of water added to the wetland versus time suggests that steady state was achieved after approximately 3 days (Figure 6). The slope of the straight line on Figure 7 indicates that the discharge rate required to maintain steady state was approximately 175 m<sup>3</sup>/day.

By making use of the water balance equation, some quantitative approximations can be made about the water budget during the time that the flooding rate was constant (steady state). The water balance equation for this system is:

$$Q_{in} = E_{fs} + T + G_h + G_v$$

where,

$Q_{in}$  = steady state application rate of potable water to the wetland (m<sup>3</sup>/day);

$E_{fs}$  = free surface evaporation rate from the flooded portion of the wetland (m<sup>3</sup>/day);

$T$  = water lost to plant transpiration (m<sup>3</sup>/day);

$G_h$  = horizontal, or lateral groundwater flow rate (m<sup>3</sup>/day);

$G_v$  = downward, or vertical groundwater flow rate (m<sup>3</sup>/day).

As stated previously, the application rate to the wetland ( $Q_{in}$ ) was 175 m<sup>3</sup>/day. The approximate area of the flooded zone was 4340 m<sup>2</sup>. During the course of the test, the water level in a nearby evaporation pan dropped approximately 10.2 cm over 17.8 days, or 0.57 cm/day. By assuming that the pan evaporation rate is the same as the evaporation rate from standing water in the wetland, the evaporative flow rate for the

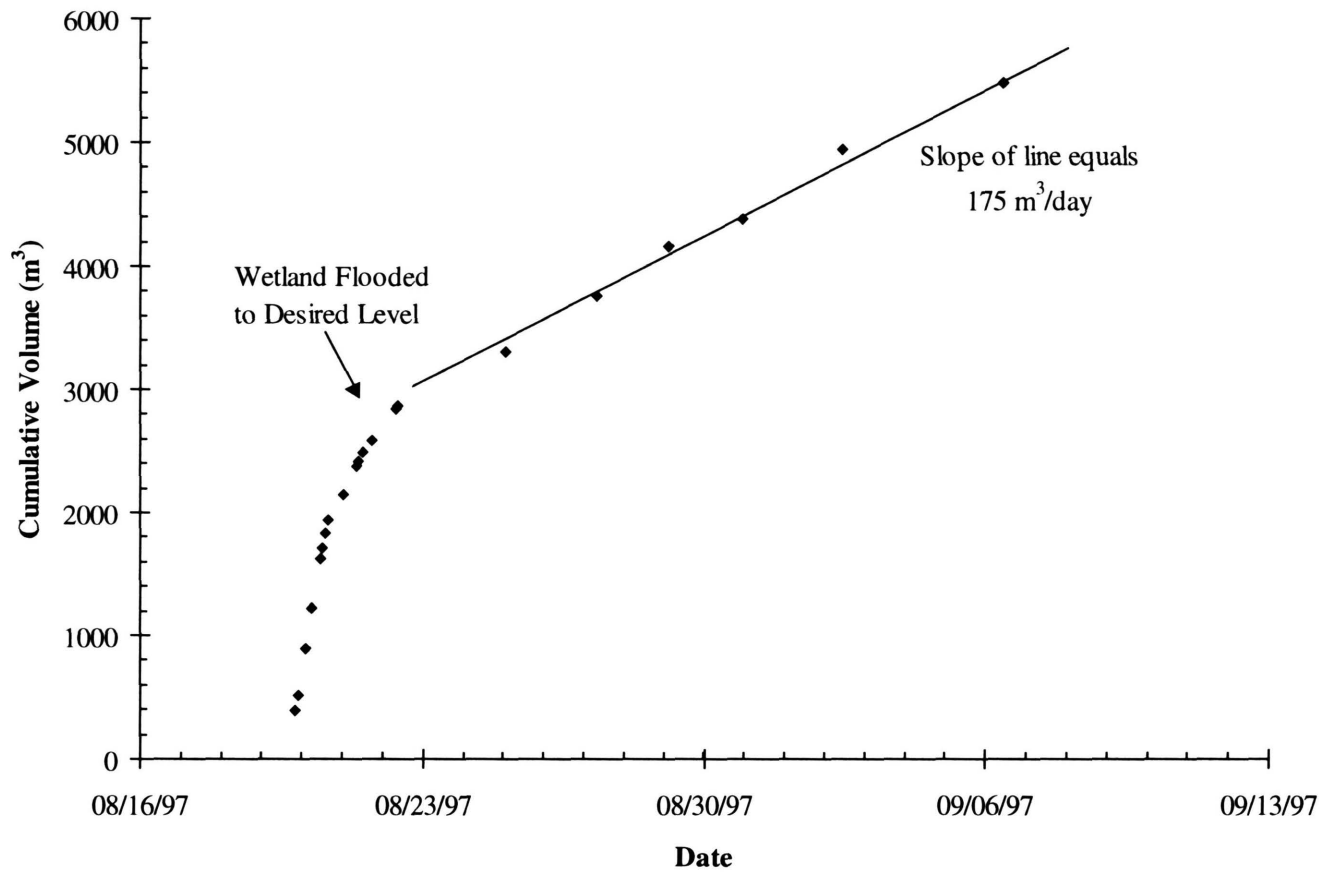


**Figure 7. Cumulative volume of water added to the wetland versus time. The slope of the regression line fit to the data points represents the volumetric flow rate required to maintain the desired stage in the wetland.**

entire flooded region ( $E_{fs}$ ) is calculated to be 25 m<sup>3</sup>/day. This means that approximately 14 percent of the water added to the wetland was lost to evaporation. Transpiration, horizontal groundwater flow, and vertical groundwater flow accounts for the remaining 86 percent of the water added to the wetland. Estimates of transpiration rates and horizontal flow rates are difficult to make, but they are likely much less than the vertical groundwater flow rate. By assuming, then, that transpiration ( $T$ ) and horizontal groundwater flow ( $G_h$ ) are zero, an average vertical groundwater flow rate ( $G_v$ ) is estimated to be 150 m<sup>3</sup>/day. The implied downward groundwater flow velocity is found by dividing this number ( $G_v$ ) by the flooded area, 4340 m<sup>2</sup> and porosity, 0.4. The result is 0.09 m/day or 9 cm/day. This estimate of the groundwater flow rate would be too large if the effects of transpiration and horizontal groundwater flow are significant.

An estimate for leakance ( $L$ ) independent of that of Table 3 can be made from the results of the flooding test. From Darcy's Law, the leakance ( $L$ ) is:

$$L = \frac{Q}{A \cdot dh}$$

The head difference between the surficial aquifer and the Floridan aquifer during the flooding test was approximately 2.3 m. As stated previously, the estimated groundwater flux was 150 m<sup>3</sup>/day over the flooded area of 4340 m<sup>2</sup>. Using these values, leakance for the flooded area is  $1.5 \times 10^{-2} \text{ day}^{-1}$ . Leakance is defined as the hydraulic conductivity of the semi-confining layer divided by the thickness of the layer. The semi-confining layer at North Lakes is thin to absent, which suggests that the resistance to vertical flow must come solely from the surficial aquifer itself. If the average thickness of the surficial aquifer is 10 m, then the average value of vertical hydraulic conductivity is approximately 0.15 m/day.

During the flooding test, the fluid conductivity in SW-2 was monitored with a conductivity probe and recorded with a data logger. After approximately 15 days of flooding, the conductivity of the fluid in SW-2 began to decrease. The decrease in fluid conductivity is attributed to the front of potable water passing the well screen at SW-2. The plot of conductivity versus time for SW-2 is assumed to represent a breakthrough curve for a one-dimensional front. The analytical solution for the transport of a continuous-source plume in

a one-dimensional flow field is reported by Fetter (1993). For this application, the constant source is the potable water, and the relative fluid conductivity is used as a proxy for concentration.

The analytical solution matches well with the conductivity data measured in the field (Figure 8). To fit the analytical solution to the field data, the values of velocity and longitudinal dispersivity were adjusted until the analytical curve matched the observed breakthrough curve. The groundwater flow velocity required to match the data is 0.11 m/day, a very consistent value with that estimated from the water balance method. The value of longitudinal dispersivity that was required to match the curve is 0.1 m.

### ***Surficial Aquifer Tracer Test***

During the time the wetland was flooded with potable water, tracer tests were conducted in the surficial aquifer to measure groundwater flow velocities. One tracer test was conducted in Sinkhole E (Figure 2). The other tracer test was conducted in the area between the Sinkholes D and E (Figure 9). After steady state was achieved for the flooding test, concentrated bromide solutions were injected just below land surface in TIP-1 and TIP-2 (Figure 9). Groundwater samples were then collected frequently from multi-level sampling tubes to monitor for the presence of the tracers.

The tracer fluid used for the tests was a highly concentrated bromide solution with a  $\text{Br}^-$  concentration of 353,000 mg/L. Half of this tracer fluid (1.9 liters) was injected in TIP-1 and the other half was injected at TIP-2. A peristaltic pump was used to inject the fluid into the tracer introduction points. Bromide concentrations were measured in the field with an Orion, Bromide-Specific Ion Probe and meter. In addition to measurements of bromide concentration that were made in the field, approximately 150 samples were collected during the course of the tracer tests. The field meter was used to determine which samples to collect. Blanks and duplicates were also collected to ensure quality control. These samples were analyzed for bromide by the analytical laboratory at SWFWMD with an ion chromatograph. Compared with the field meter and probe, the ion chromatograph produced results that were more accurate.

Of the 30 multi-level sampling ports (3 vertically distributed ports at each sampler location), three became clogged prior to the test and did not produce water. Sampling ports that show an increase in bromide

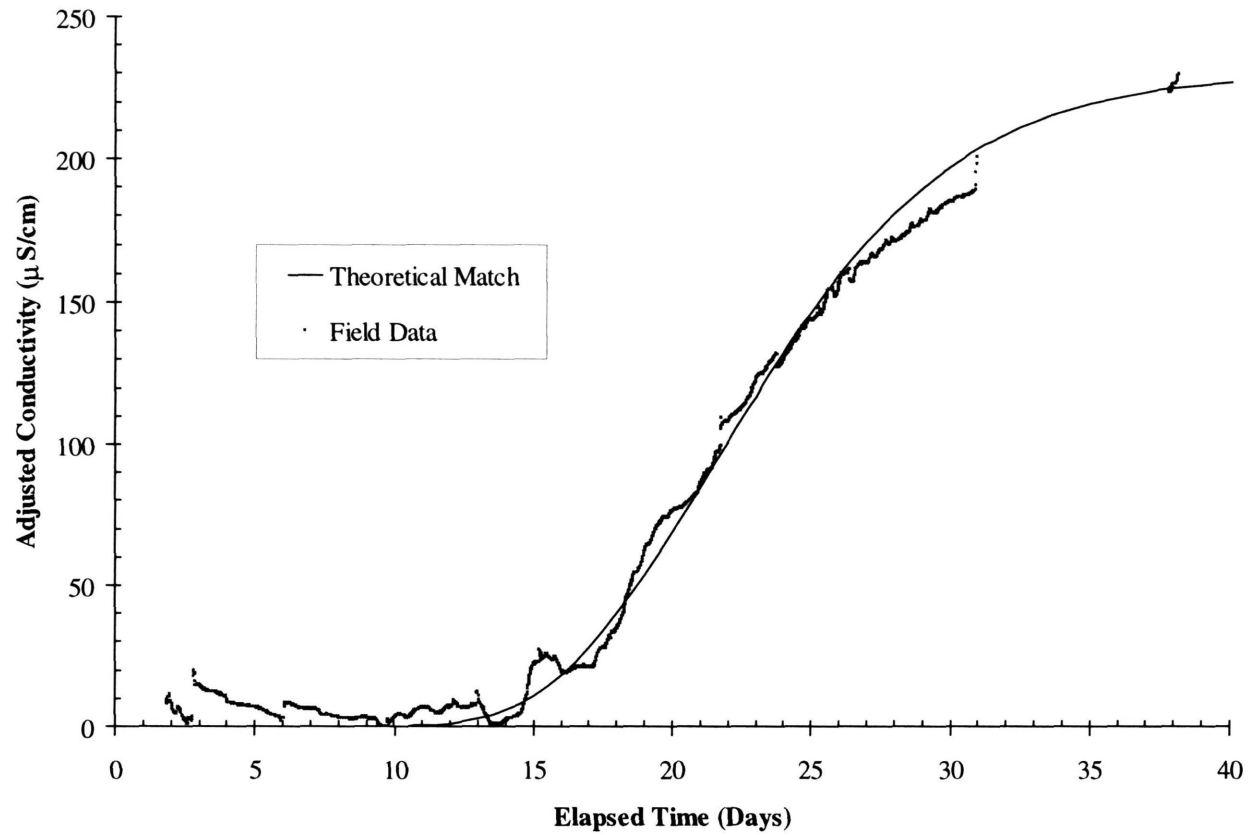


**Figure 8. Adjusted fluid conductivity versus time for SW-2. Change in fluid conductivity represents the breakthrough curve of the potable water front passing by the well screen. The solid line represents the match produced by an analytical equation.**

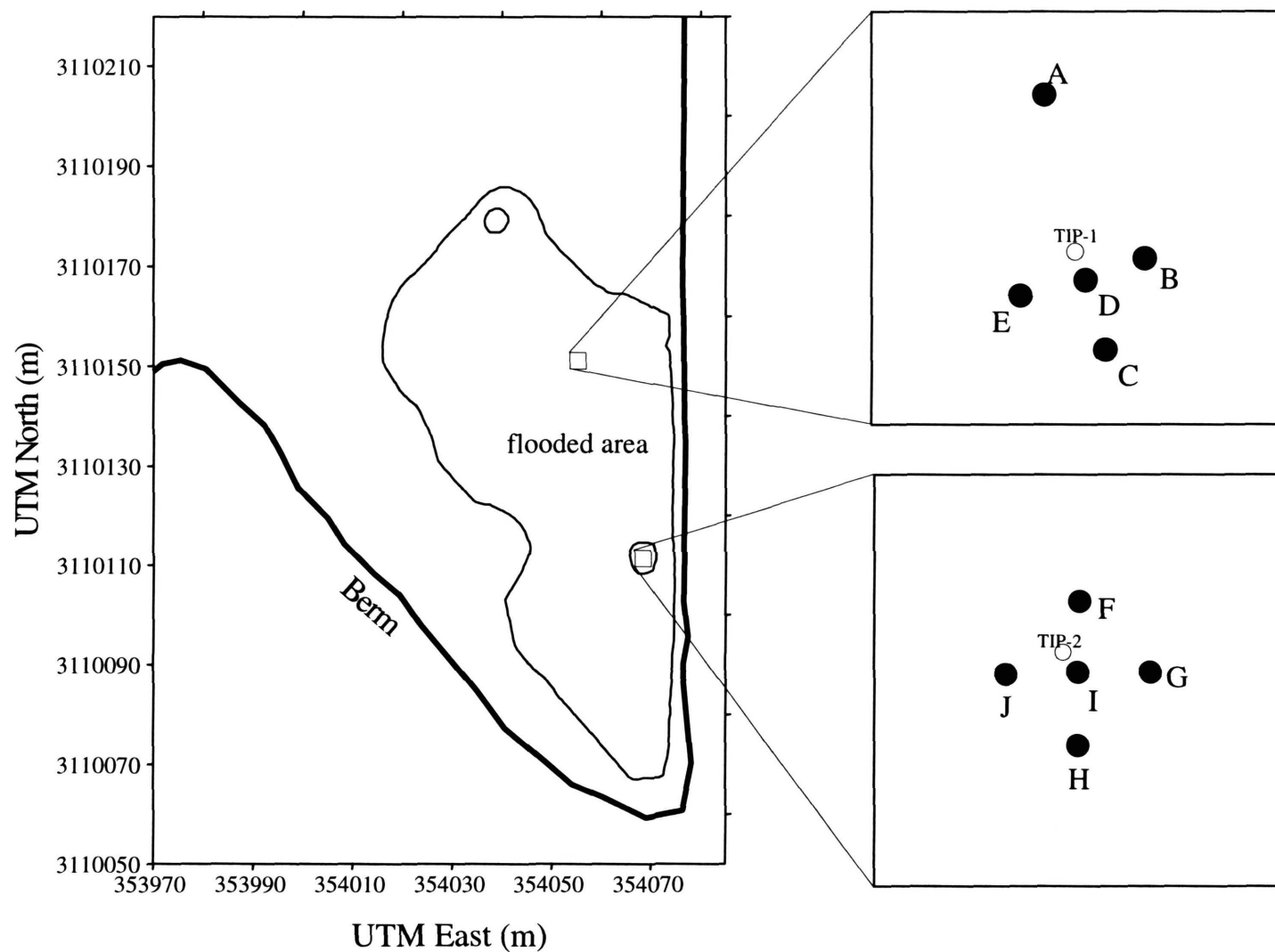


**Figure 9. Locations for the surficial aquifer tracer tests. Sampling points A through C are located outside of the sinkholes. Sampling points F through J are located in sinkhole E. TIP 1 and 2 are the introduction points for the bromide tracer.**

concentration are D Shallow, F Shallow, G Shallow, and G Intermediate (Figure 10 and Table 4). D Shallow is located at SATT-1. The other three are sampling ports within the sinkhole at SATT-2.

A curve-matching technique was used to estimate groundwater flow velocities for G Shallow and G Intermediate. Data from the G multi-level sampler was selected for curve matching because measured bromide concentrations at these ports were the highest. In addition to an estimate of groundwater flow velocity, the curve-matching technique provides estimates of longitudinal and transverse dispersivity. The method works by matching a predicted breakthrough curve, calculated with an analytical solution, to the observed data. The analytical solution is based on the transport of a three-dimensional, discontinuous, point-source groundwater plume flowing in a one-dimensional flow field (Domenico and Schwartz, 1990). Values of groundwater flow velocity, longitudinal dispersivity, and transverse dispersivities are adjusted in a spreadsheet until the predicted curve matches the observed data. Four variables can be adjusted in the analytical equation: groundwater flow velocity, longitudinal dispersivity, transverse dispersivity in the y direction, and transverse dispersivity in the z direction. The x direction of the analytical solution is oriented downward, in the same direction as groundwater flow. Advective flow in the horizontal direction is assumed negligible because standing water in the wetland is a horizontal plane. It is possible that horizontal flow components exist if, for example, there are heterogeneities in the surficial aquifer. Without a detailed description of these heterogeneities, however, it is assumed that all groundwater flow is vertical.

The number of variables used in the analytical equation to match the field data were reduced from four to two by setting the transverse dispersivities equal to 1/10 the longitudinal dispersivity. The multiplier of 1/10 is commonly found in the literature as the ratio of transverse dispersivity to longitudinal dispersivity (Anderson, 1979). The analytical solution best matches the field data when velocity is 0.18 m/day and the longitudinal dispersivity is 0.35 m (Figure 11). Both of the transverse dispersivities are 0.035 m. These parameter estimates appear to be a unique solution to the analytical transport equation. Reasonable curve matches could not be made with other values for the parameters. In addition, an iterative solver was used to match the analytical curve to the field data by minimizing the sum of the squares of the residuals. The iterative solver reproduced, nearly identically, the solution presented.



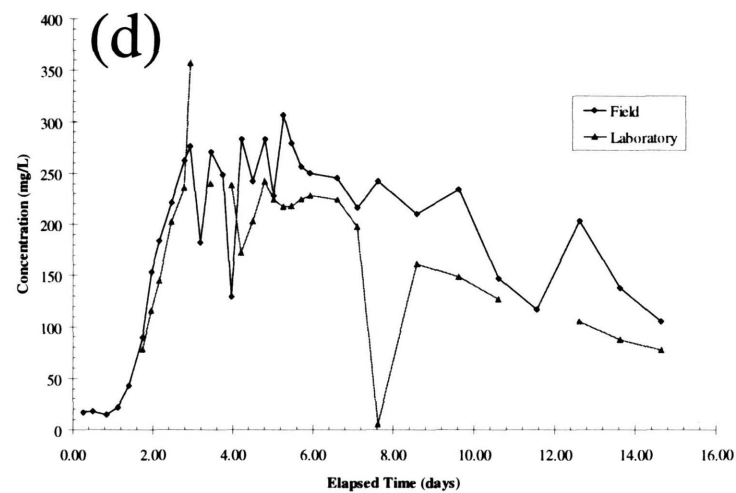
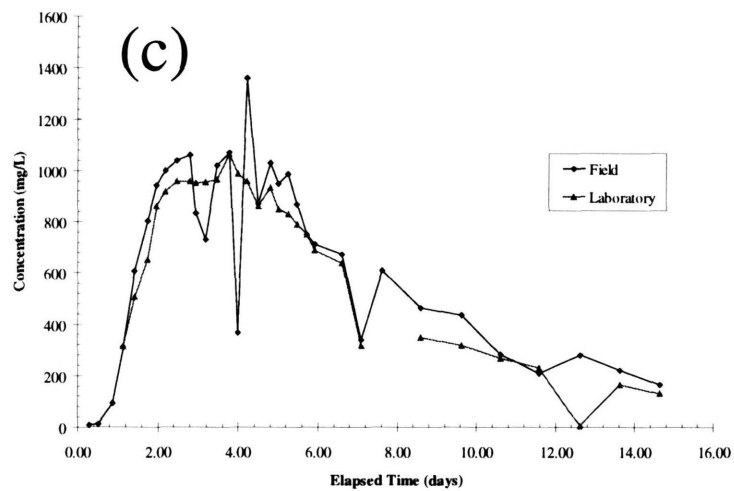
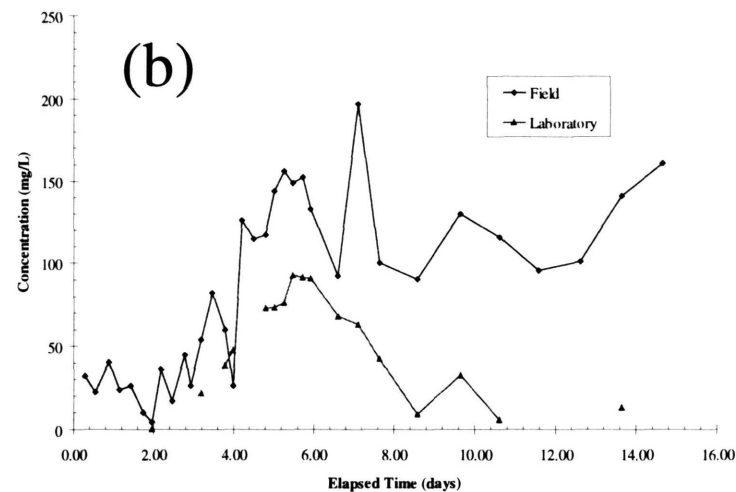
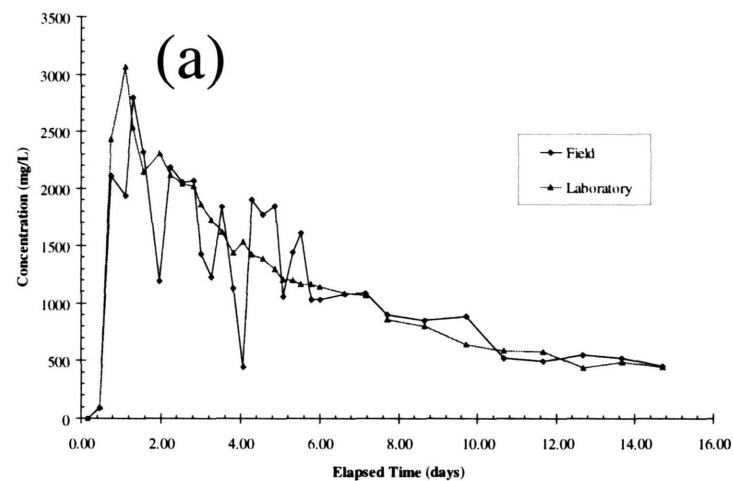


**Figure 10. Breakthrough curves for the four sampling ports where the bromide tracer was detected. (a) D Shallow. (b) F Shallow. (c) G Shallow. (d) G Intermediate. Concentrations for the field data were measured with a portable bromide probe. Concentrations for the laboratory data were measured with an ion chromatograph.**

**Table 4. Summary of the results from the surficial aquifer tracer test.**

<b>Sampling Point</b>	<b>Vertical Distance From Injection Point (m)</b>	<b>Peak Concentration (mg/L)</b>	<b>Time to Peak (days)</b>
D Shallow	1.4	3065	1.11
F Shallow	1.2	92.8	5.46
G Shallow	1.2	1066	3.77
G Intermediate	2.2	240	4.2

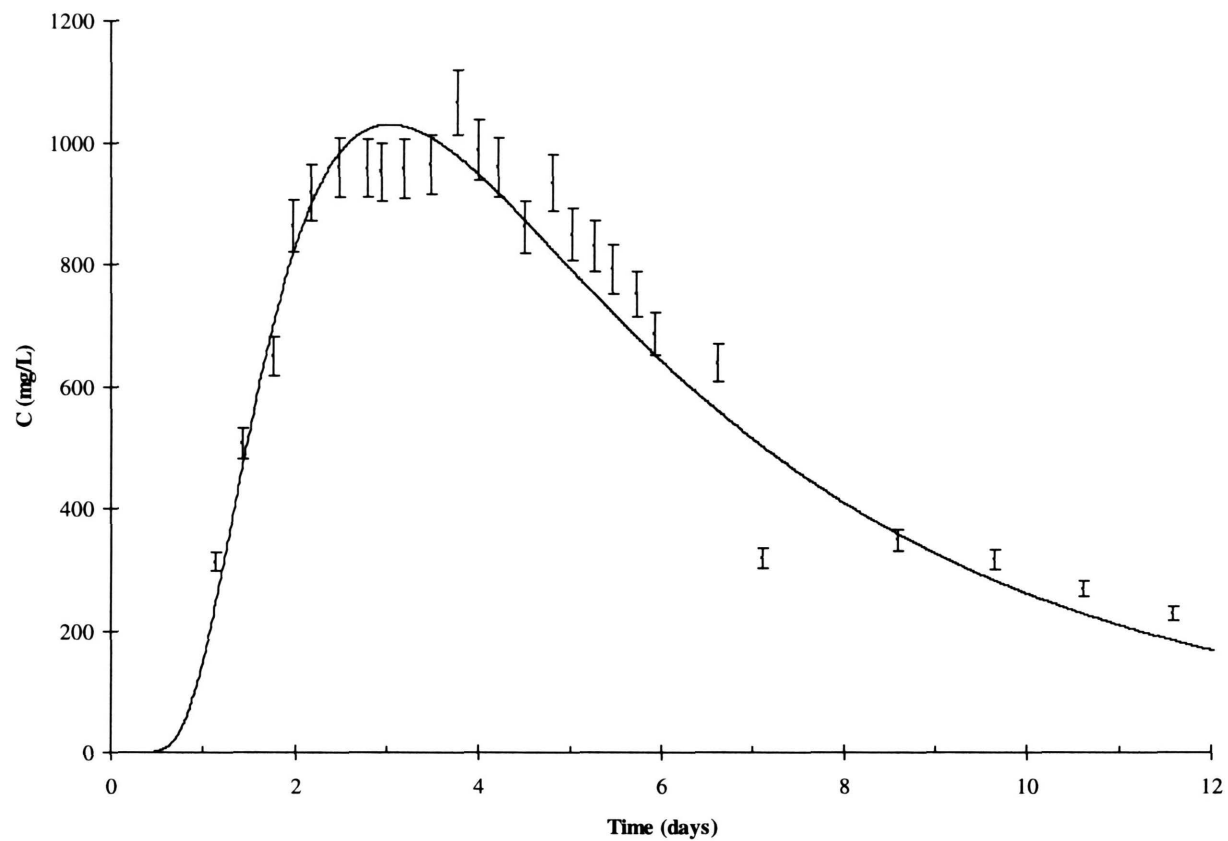


**Figure 11. Observed and predicted bromide concentrations for G Shallow. The solid line represents the predicted breakthrough curve for a three-dimensional groundwater plume. The analytical equation used to generate the solid line assumes advective and dispersive transport.**

For G Shallow, it was not possible to match the observed data by setting the transverse dispersivities equal to 1/10 the longitudinal dispersivity. Instead, three variables were allowed to vary in order to match the bromide concentrations from G Intermediate. These variables were velocity, longitudinal dispersivity, and transverse dispersivity (transverse dispersivity in the y direction is set equal to the transverse dispersivity in the z direction). For this data set, the analytical solution best matches the field data when velocity is 0.18 m/day, longitudinal dispersivity is 0.9 m, and the transverse dispersivities are 0.045 m (Figure 12).

### ***Floridan Aquifer Tracer Test***

To better understand the properties of the Floridan aquifer at the North Lakes, a forced-gradient tracer test was conducted on August 4, 1997. The objective of the test was to estimate the value of effective porosity in the Floridan aquifer. The tracer test was conducted by pumping groundwater from FTTW-1 and injecting a highly conductive tracer fluid in FTTW-2. The tracer fluid consisted of approximately 90 kg of sodium chloride dissolved into 150 L of water. The fluid conductivity of the tracer solution was approximately 360,000  $\mu\text{S}/\text{cm}$ . Before introducing the tracer, a steady-state flow system was achieved by pumping water from FTTW-1 with a submersible pump. FTTW-1 was pumped at rate of 350  $\text{m}^3/\text{day}$  (65 gpm). After steady state was achieved, the conductive tracer fluid was injected under pressure into FTTW-2 with a centrifugal pump. Discharge water from FTTW-1 was then monitored for the presence of the tracer with fluid conductivity meters.

Background conductivity, measured prior to the introduction of the tracer fluid, averaged 300  $\mu\text{S}/\text{cm}$ . Approximately 15 minutes after the injection of the conductive fluid, the first signs of the tracer appear as shown by the increase in fluid conductivity (Figure 13). After 40 minutes into the test, fluid conductivity reaches a maximum value of 1315  $\mu\text{S}/\text{cm}$ . The conductivity of the discharge water then decreases to background levels.

Robinson (1990) estimates the effective porosity of an aquifer unit with the volumetric displacement method. This method is based on the relationship between effective porosity and the time required to remove a cylindrical volume of water in the aquifer between the injection well and the pumped well at the specified discharge rate. The equation for the volumetric displacement method is:

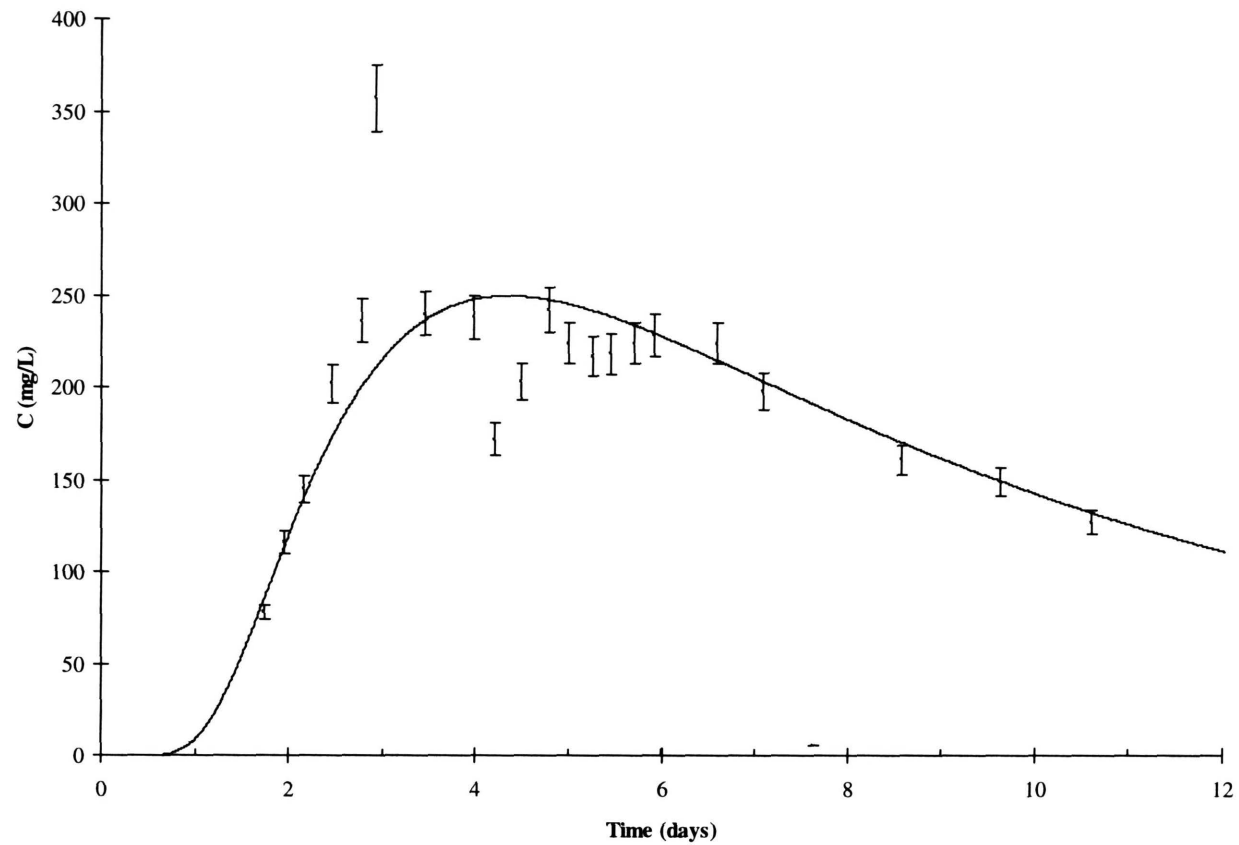


**Figure 12. Observed and predicted bromide concentrations for G Intermediate. The solid line represents the predicted breakthrough curve for a three-dimensional groundwater plume. The analytical equation used to generate the solid line assumes advective and dispersive transport.**

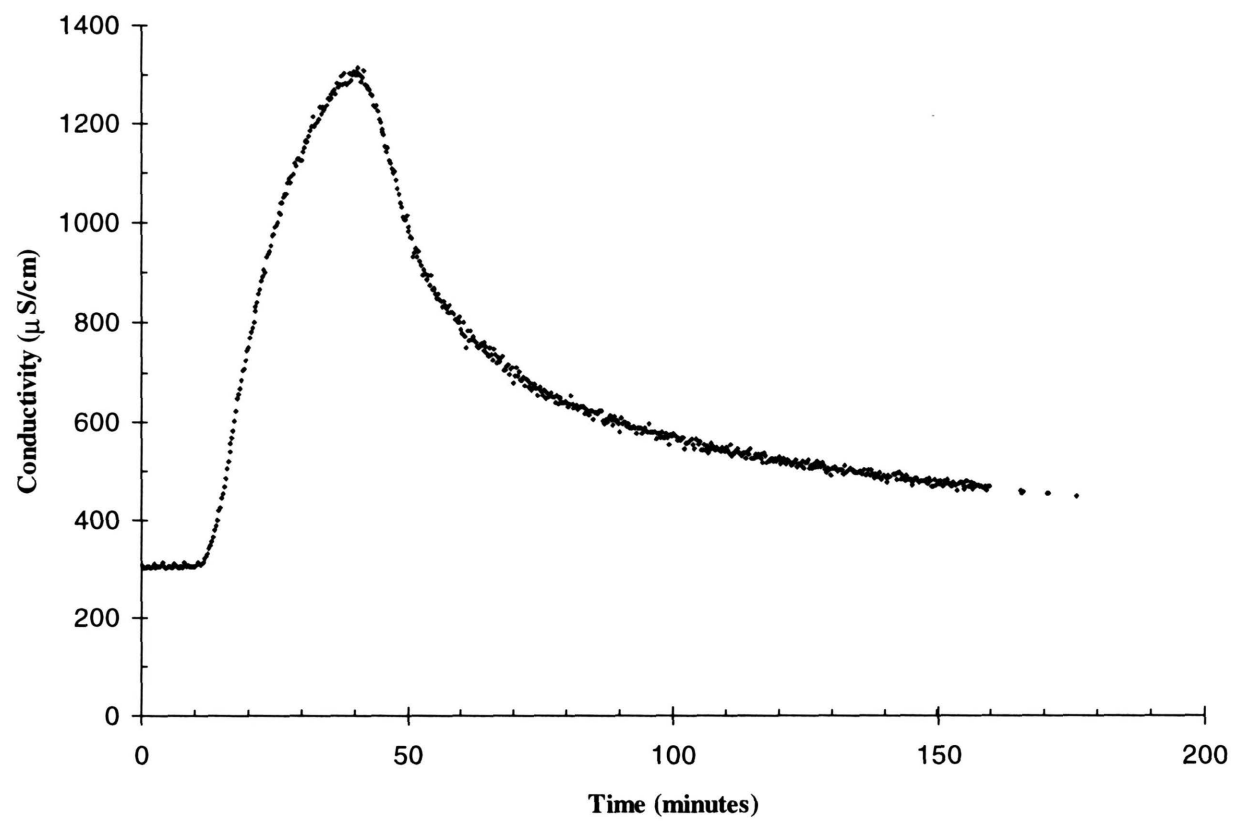


Figure 13. Fluid conductivity versus time as recorded during the Floridan aquifer tracer test.

$$n_e = \frac{Qt}{\pi r^2 h}$$

where,

$n_e$  = effective porosity;

$t$  = time to reach the tracer concentration peak, or the time required to replace the cylindrical volume of water between the pumped well and the injection well (minutes);

$Q$  = discharge rate (m<sup>3</sup>/min);

$r$  = radius from the pumped well to the injection well(m);

$h$  = thickness of the injected zone (m).

Using this method, the effective porosity is estimated to be approximately 2 percent. This estimate is based on a time to peak concentration of 40 minutes, a discharge rate of 0.25 m<sup>3</sup>/min, a radius (or distance between the two wells) of 7.6 m, and an injected thickness of 3 m.

### ***Groundwater Elevations and Vertical Head Differences***

The measurement of water levels at North Lake wells began in August of 1996 and continued through April of 1998. Measurements of depth to water in each well were made with a water-level indicator and recorded manually in a field notebook. Using a spreadsheet and the elevations of the tops of the well casings, these depths were then converted to elevations in meters above sea level.

### ***Surficial Aquifer***

Water-level hydrographs for the 30 monitoring wells of the surficial aquifer illustrate the fluctuations of the water table during the period of record (Figure 14). From August of 1996 to June of 1997, water levels decline continuously. Beginning in September of 1997, water levels begin to rise, and in September of

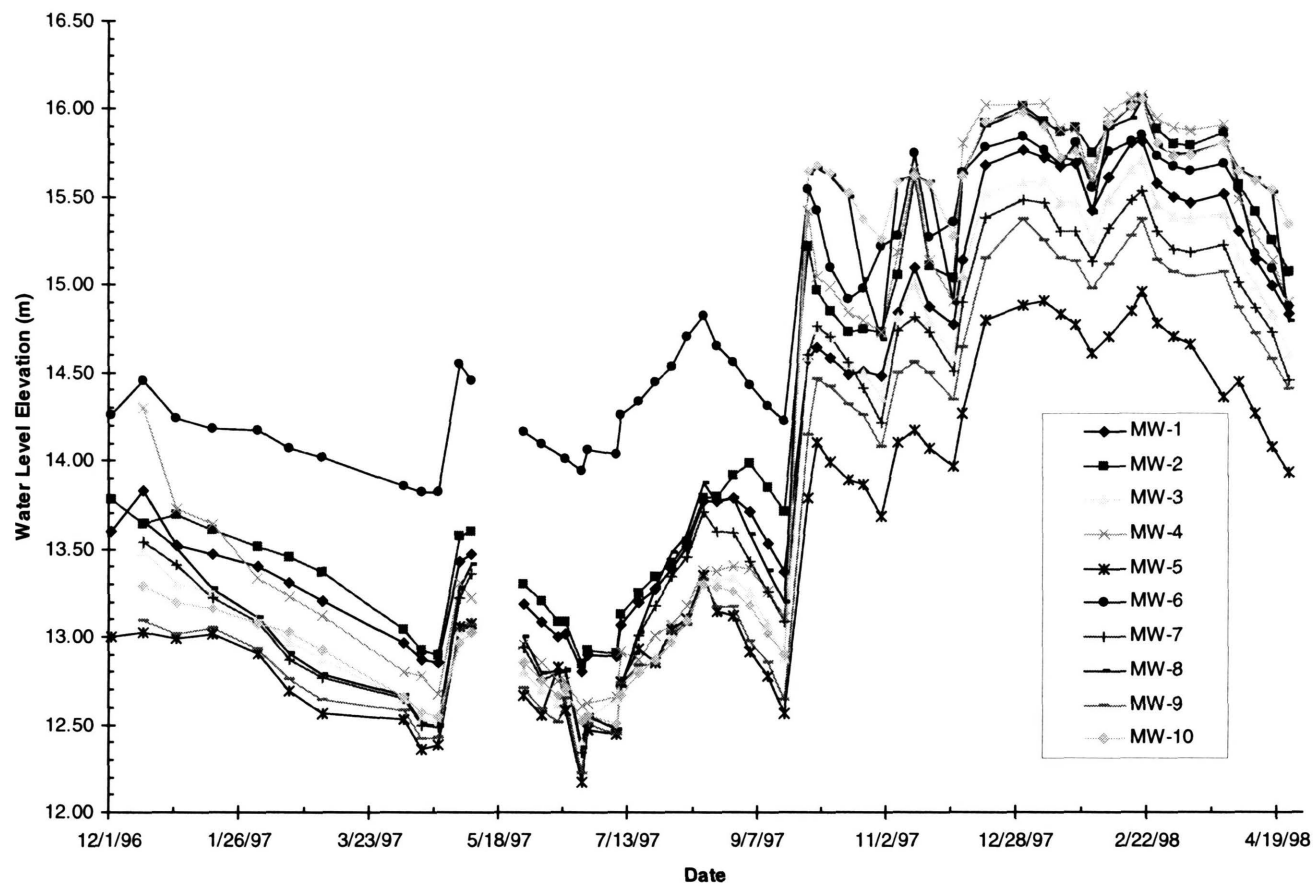


**Figure 14. Water level hydrographs for monitoring wells in the surficial aquifer.**



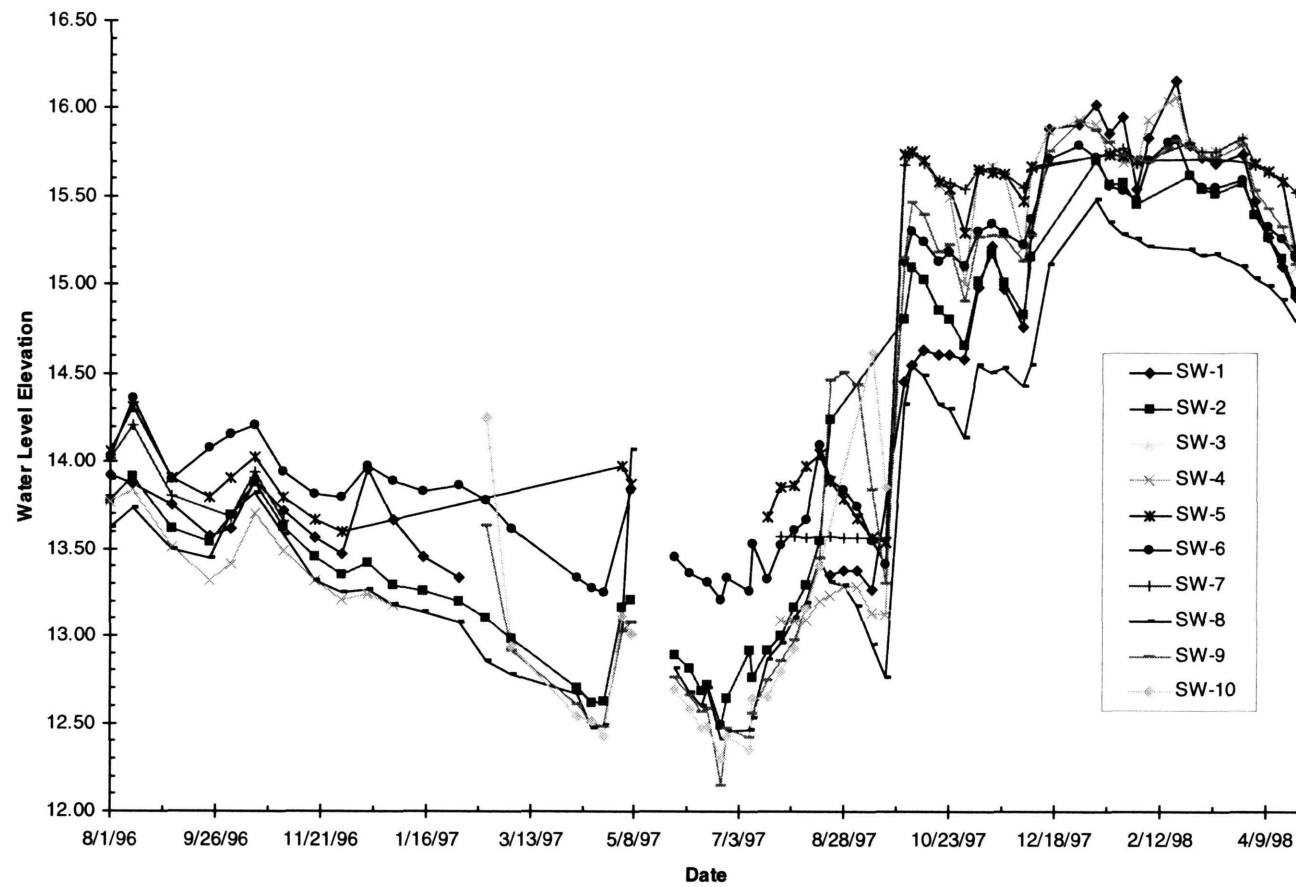


Figure 14. (Continued).

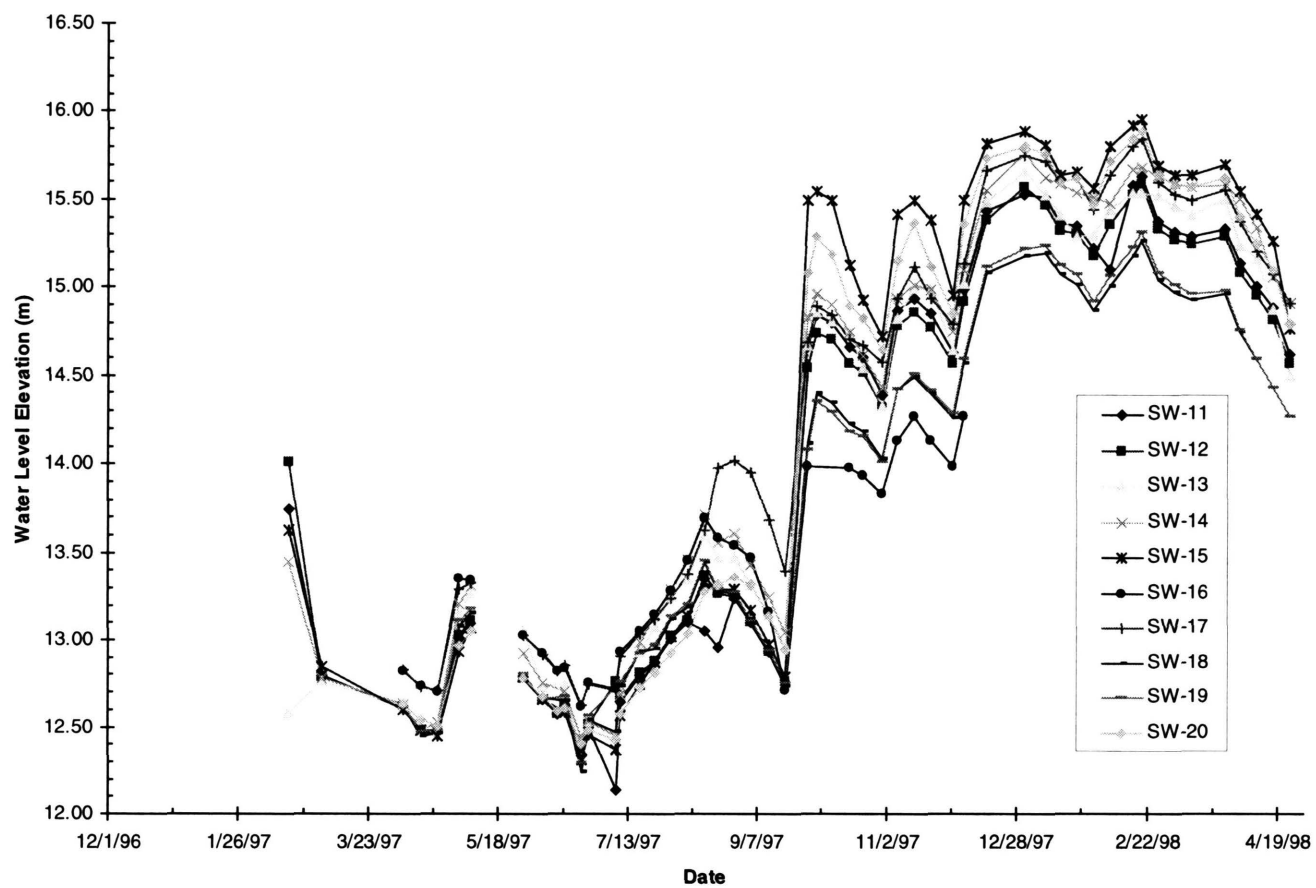


Figure 14. (Continued).

1997 they rise very quickly to elevations greater than 14 m above sea level. The rapid rise in water-table elevations is primarily the result of above-normal rainfall conditions. These above-normal rainfall conditions were the result of the El Niño weather patterns that occurred during the end of 1997.

From the shape of the water-level hydrographs, the data record can be separated into two periods. The first period, from August of 1996 to August of 1997, represents a period with relatively low water-table elevations. The second period, from September of 1997 through the end of the data record, represents a period of relatively high water-table elevations. Water-table maps are constructed at two different times (July of 1997 and March of 1998) to show the difference in hydraulic gradient between the two time periods (Figure 15a and Figure 15b). In July of 1997, it appears that the largest gradient of the water table was in the south-central portion of the wetland (Figure 15a). The hydraulic gradient in this area is about 0.015. In March of 1998, water-table elevations were relatively high (Figure 15b). At this time, most of the area within the wetland had standing water. The berm prevented the standing water from flooding the park area to the south. The maximum hydraulic gradient in Figure 15b is approximately 0.01.

#### *Floridan Aquifer*

Water-level hydrographs for the Floridan aquifer also exhibit relatively low and high periods of water levels (Figure 16). Low water levels are observed prior to September of 1997. From September of 1997 through the period of record, the potentiometric surface is relatively high. Water levels for the two time periods are also different in that, during the low period, hydrographs for each Floridan monitoring well are nearly identical in shape and magnitude (Figure 16). This means that the potentiometric surface of the Floridan aquifer is nearly flat, and, therefore, there is little horizontal groundwater flow. During the second time period when water levels are relatively high, hydrographs for the various wells tend to separate. This indicates that the potentiometric surface is no longer as flat, and groundwater flow is faster during this time period relative to the period with lower water levels.

To illustrate the increase in the magnitude of the hydraulic gradient and thus, groundwater flow velocity, the equation for a plane is fit to two different groups of three monitoring wells. The A area is delineated by a triangle between FMW-1, FMW-4, and FMW-5. The B area is delineated by a triangle between FMW-1,

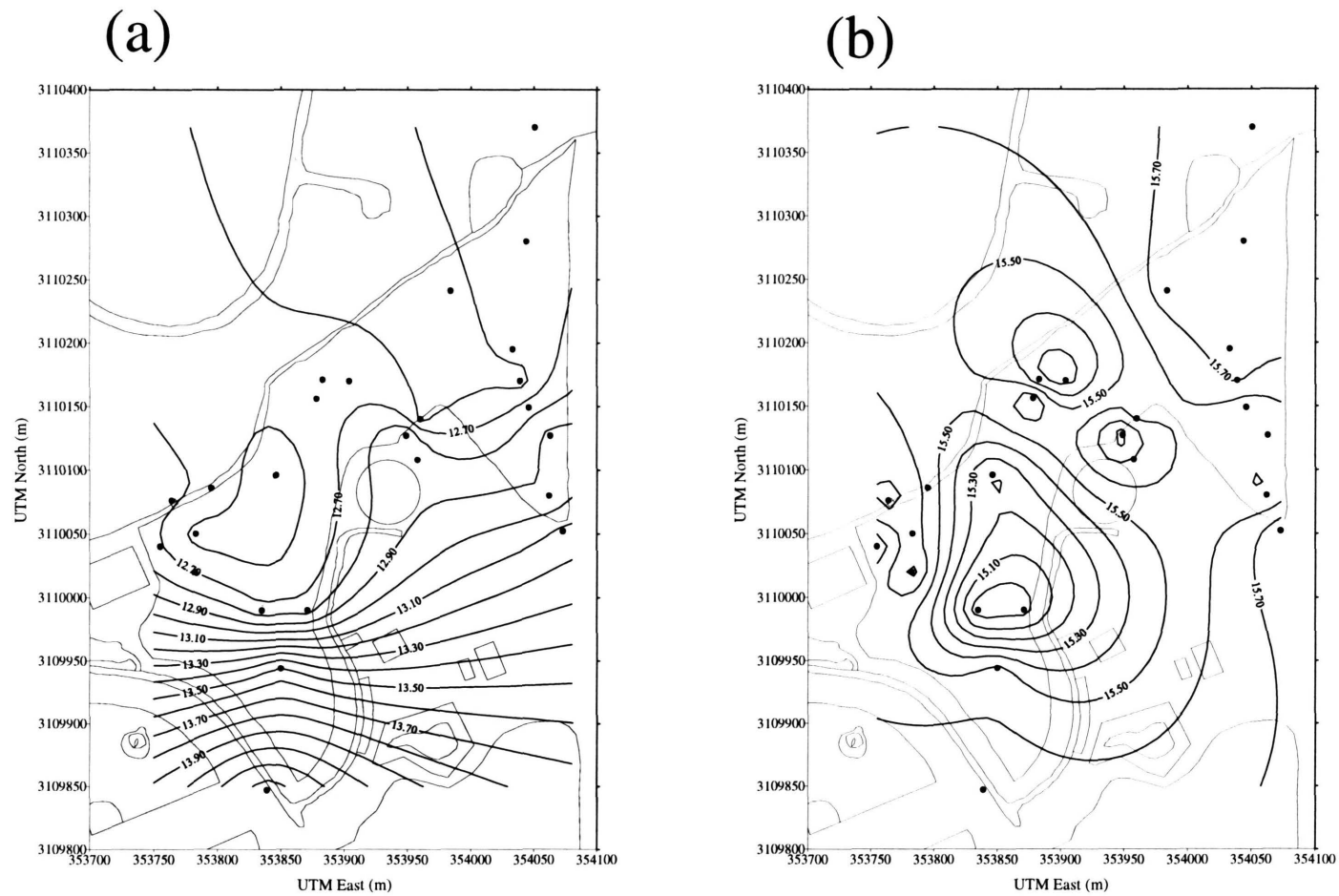


Figure 15. Water table surface for (a) July 10, 1997, and (b) March 13, 1998. Contour interval is 0.1 m.

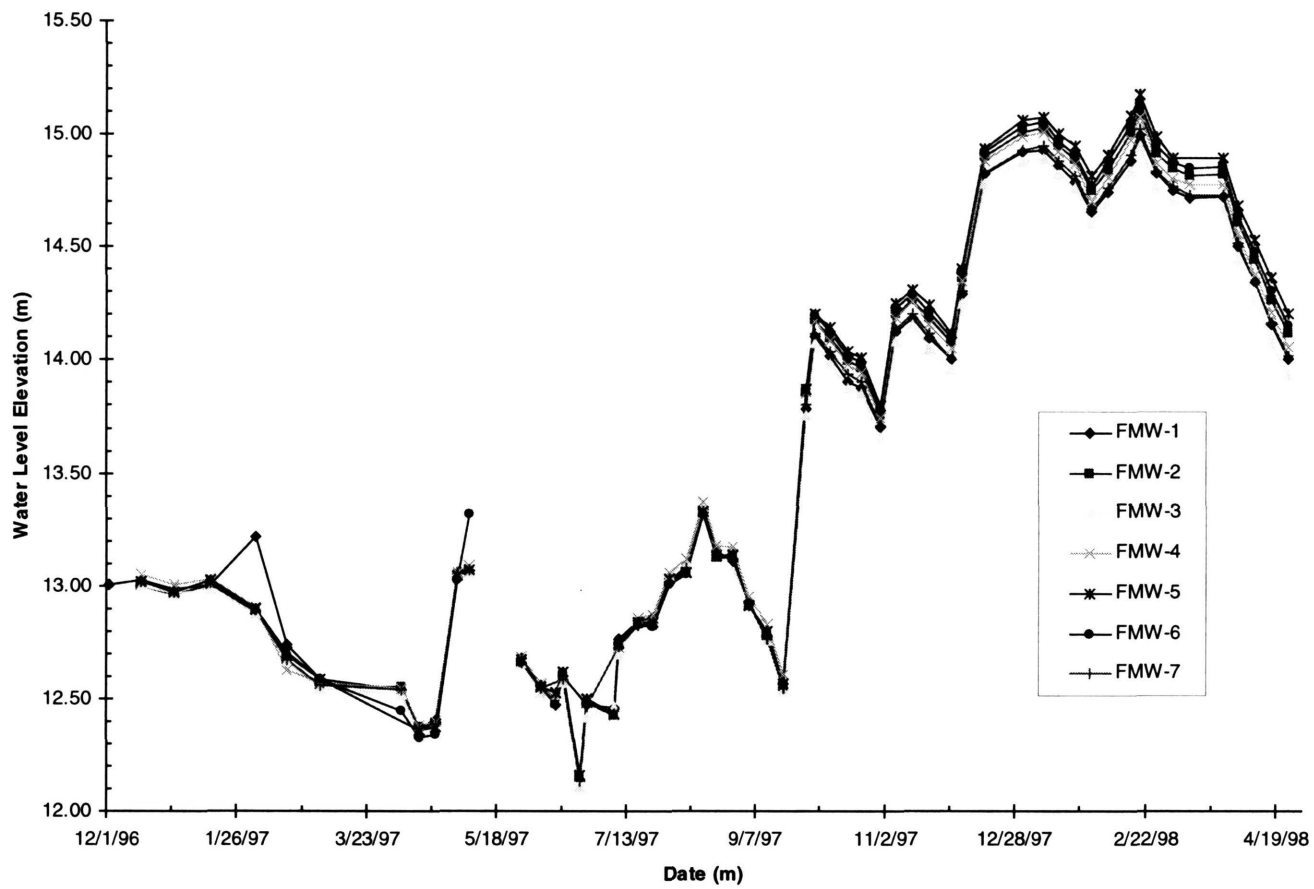


Figure 16. Water-level hydrographs for monitoring wells in the Floridan aquifer.

FMW-3, and FMW-4. Within these two areas, it is assumed that the potentiometric surface is a plane.

From the equation of the plane, it is possible to determine the groundwater flow direction and magnitude of the hydraulic gradient. The flow direction is in the opposite direction of the maximum hydraulic gradient.

The magnitude of the hydraulic gradient ( $\delta h/\delta s$ ) is defined as

$$\frac{\partial h}{\partial s} = \sqrt{\left(\frac{\partial h}{\partial x}\right)^2 + \left(\frac{\partial h}{\partial y}\right)^2}$$

The flow direction is presented as a histogram with respect to azimuth (Figure 17). From this figure, it appears that, most of the time, horizontal groundwater flow in the Floridan aquifer is toward the south. Magnitudes of the hydraulic gradient illustrate the increase in flow during the period with relatively high water levels (Figure 18). Hydraulic gradients increase from less than  $1 \times 10^{-4}$  to more than  $6 \times 10^{-4}$ . This means that horizontal groundwater flow in the Floridan aquifer is nearly six times faster during the second time period than during the first time period.

#### *Vertical Head Differences*

Downward groundwater flow at the North Lakes wetland is driven by head differences between the water table and the potentiometric surface of the Floridan aquifer. Because five of the well locations at North Lakes have three vertically nested wells, it is possible to construct three different plots of head difference. The first plot of head difference represents the total head difference, or the difference in head between the water table and potentiometric surface (Figure 19). This plot is constructed by subtracting water levels in the Floridan aquifer monitoring wells from water levels in shallow surficial aquifer monitoring wells. As with the water level elevations, total head differences can be separated into two different periods. Before September of 1997, the head difference is relatively low and ranges between 0.0 and 0.6 m (Figure 19). After September of 1997, the head difference ranges between 0.8 and 1.6 m (Figure 19). This increase in the total head difference suggests that the downward component of groundwater flow increased in velocity by a factor of approximately two.

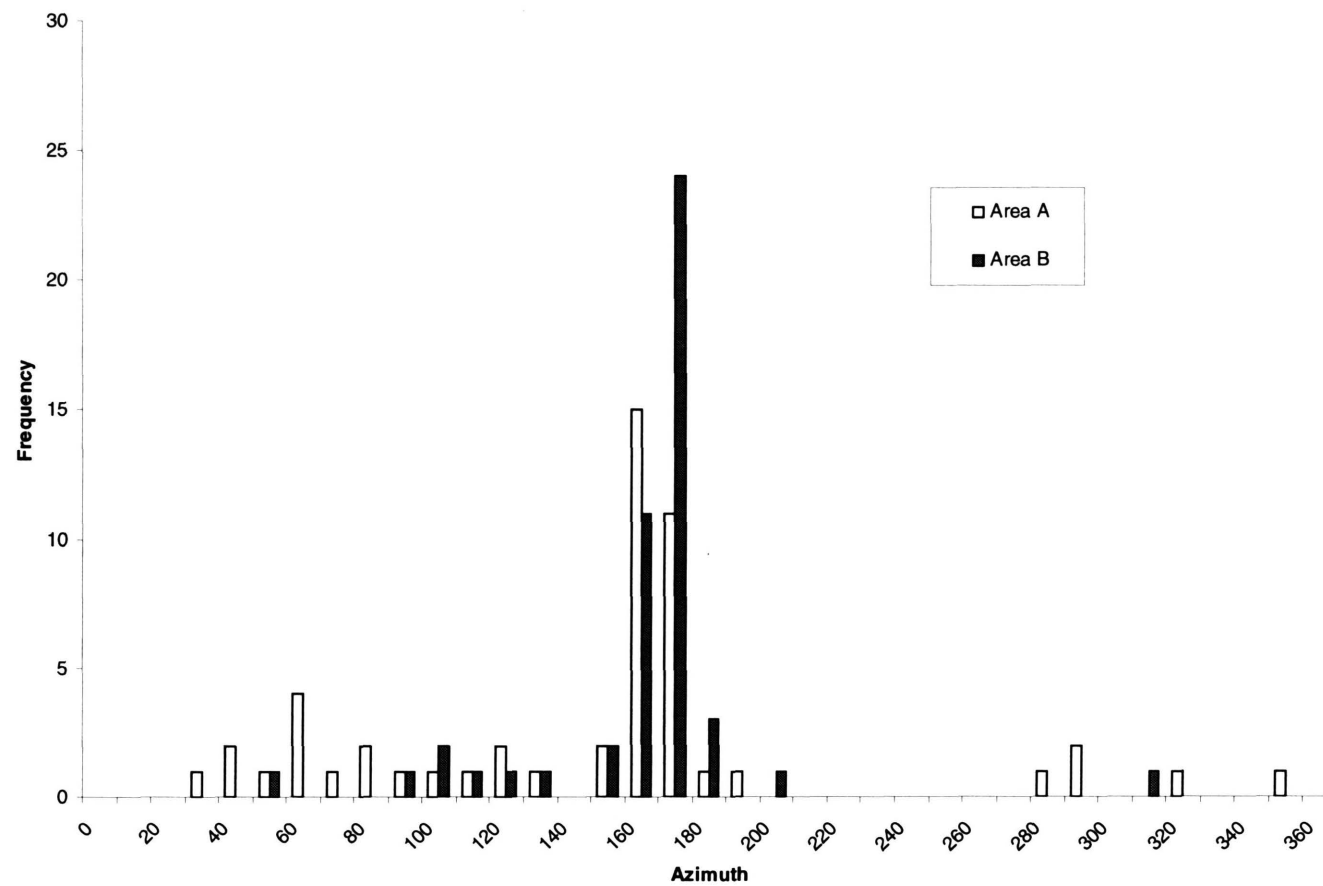


**Figure 17. Azimuth of groundwater flow direction in the Floridan aquifer. Area A is located in the triangular region between FMW-1, FMW-4, and FMW-5.**

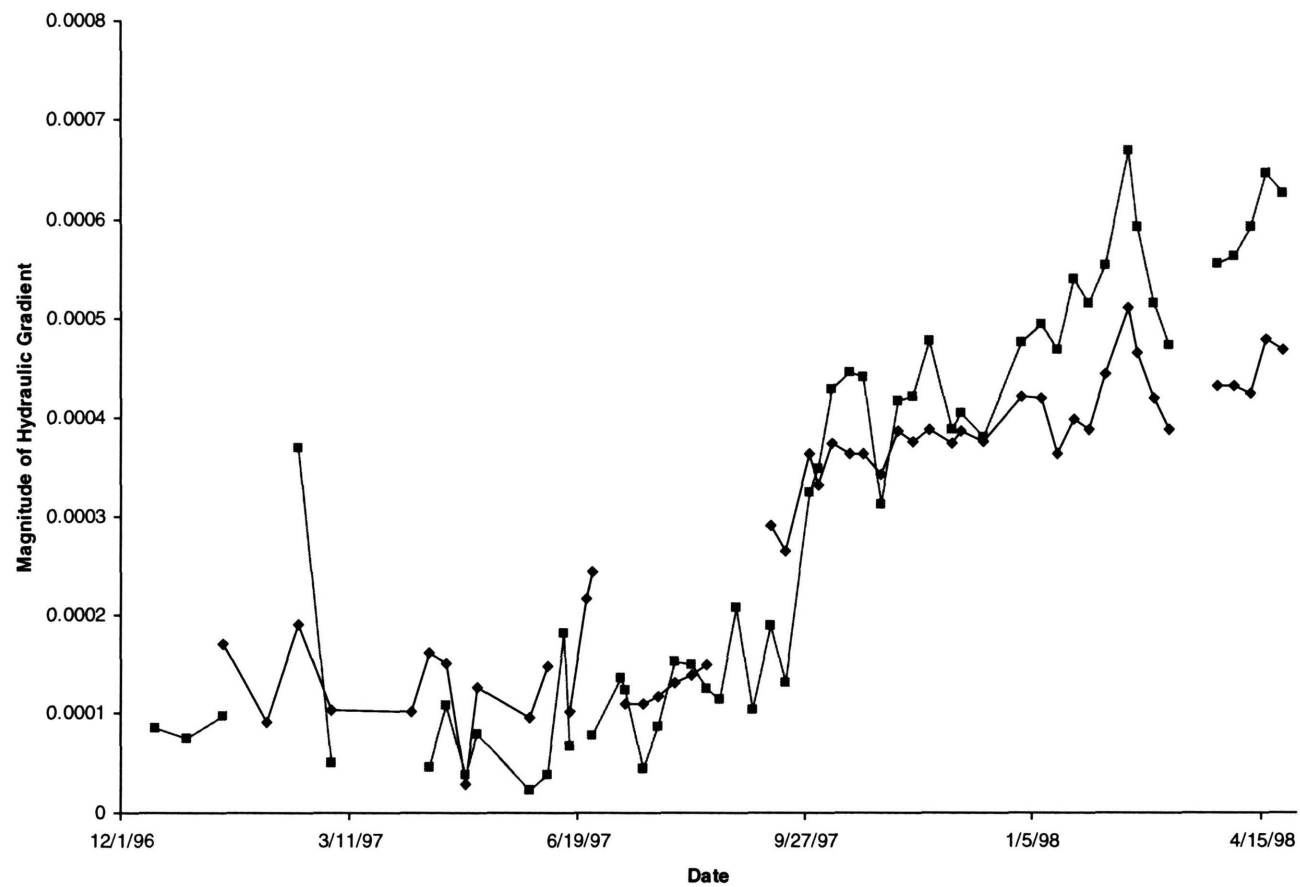
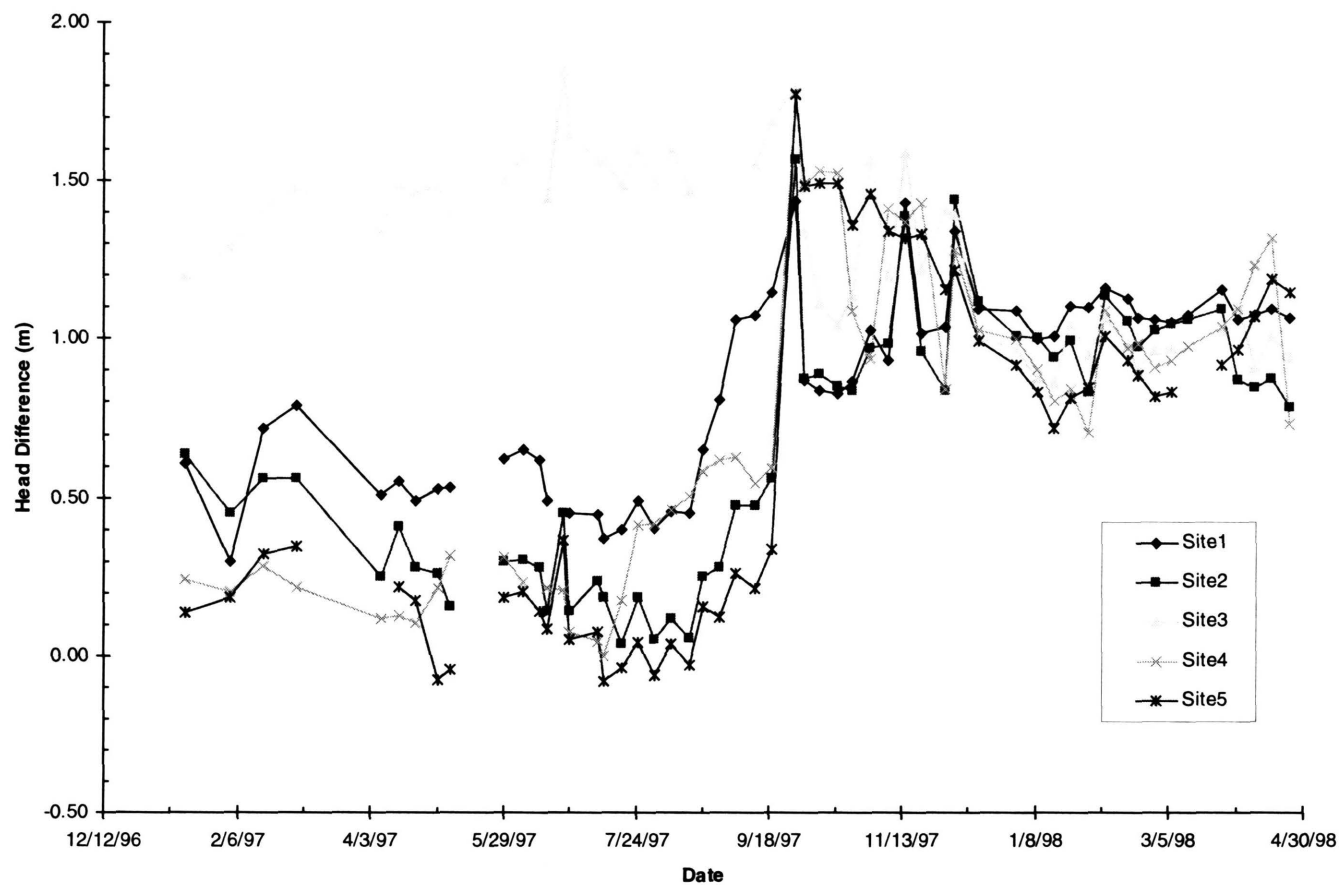


Figure 18. Maximum hydraulic gradient versus time for Areas A and B.





**Figure 19. Total head difference between the shallow surficial aquifer monitoring wells and the Floridan aquifer monitoring wells.**

To understand which aquifer units provide the greatest resistance to flow (or the lowest value of vertical hydraulic conductivity), plots of head difference were constructed by subtracting water levels from the deep surficial aquifer wells from water levels in the shallow surficial aquifer wells (Figure 20). In addition, water levels from the Floridan aquifer wells are subtracted from the deep surficial aquifer wells (Figure 21). From these plots, some qualitative observations can be made. For example, the total head difference at Site 3 is the result of low-permeability material in the surficial aquifer (compare Figure 20 with Figure 21) rather than hydraulic resistance in the Floridan aquifer.

A table of total head difference was constructed for both of the time periods (Table 5). With the exception of Site 3, average head differences during the second part of monitoring period are 2 to 9 times higher than average head differences from the first part of the record. These data clearly suggest that the high values of rainfall had significant effects on the vertical component of groundwater flow.

### ***Estimation of Groundwater Flow Velocities***

#### ***Horizontal Flow in the Surficial Aquifer***

There is concern that reclaimed water added to the North Lakes wetland will travel horizontally in the surficial aquifer to a nearby wellfield. For this reason, the horizontal groundwater flow velocity in the surficial aquifer is estimated using the Dupuit form of Darcy's Law:

$$v = \frac{K_x}{2n} \frac{(h_1^2 - h_2^2)}{L}$$

where  $v$  is velocity,  $K_x$  is the value of hydraulic conductivity in the horizontal direction,  $n$  is porosity, and  $dh/dx$  is the hydraulic gradient. A value for  $K_x$  (5 m/day) is selected from the results of the empirical relationship between grain size and hydraulic conductivity (Table 2). A porosity value of 0.4 was also estimated with an empirical relationship. The maximum value for  $(h_1^2 - h_2^2)/L$ , estimated from the contour

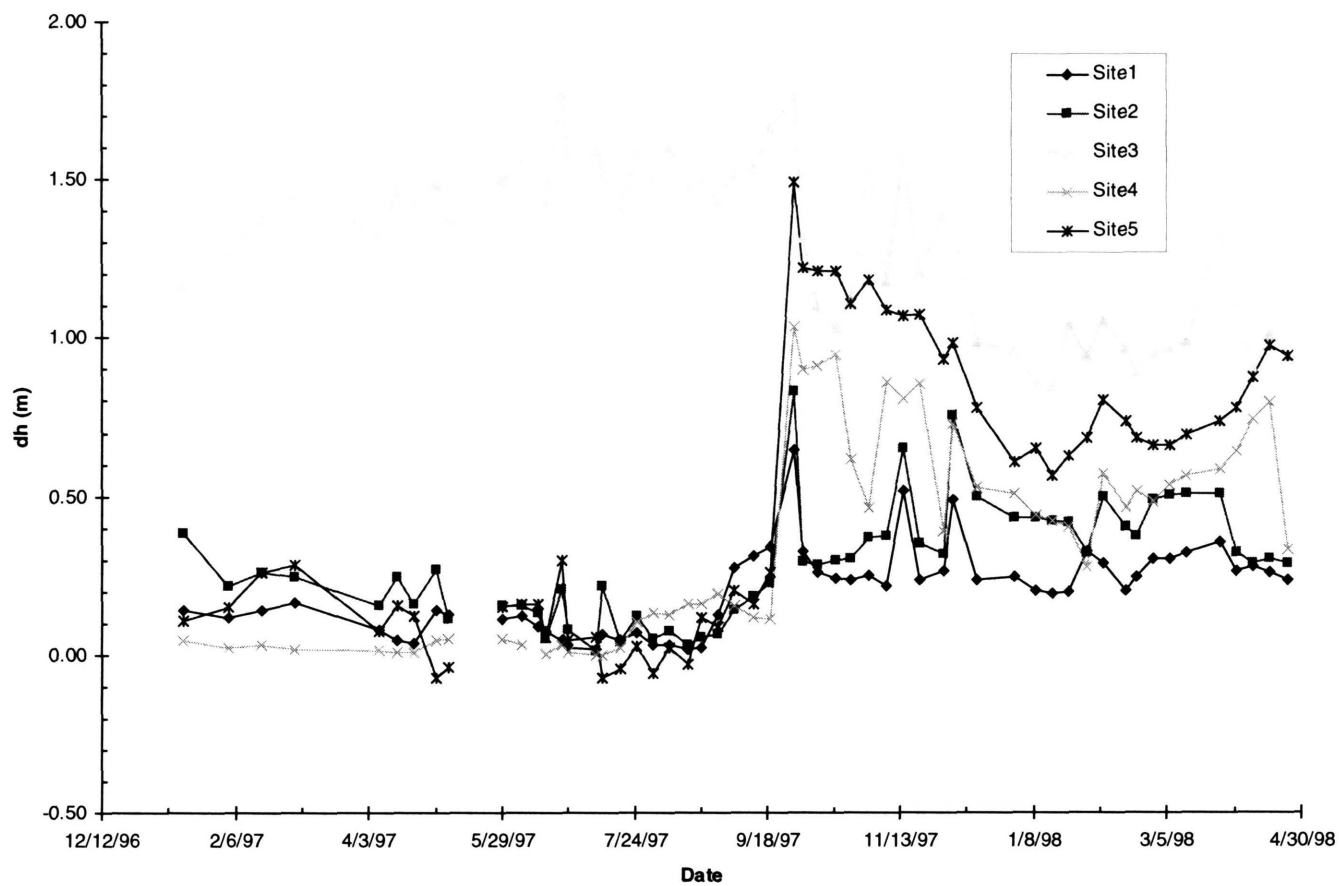


**Figure 20. Vertical head difference versus time for the surficial aquifer. The head difference was calculated by subtracting the water level in the deep surficial aquifer monitoring wells from the water level in the shallow surficial aquifer monitoring wells.**

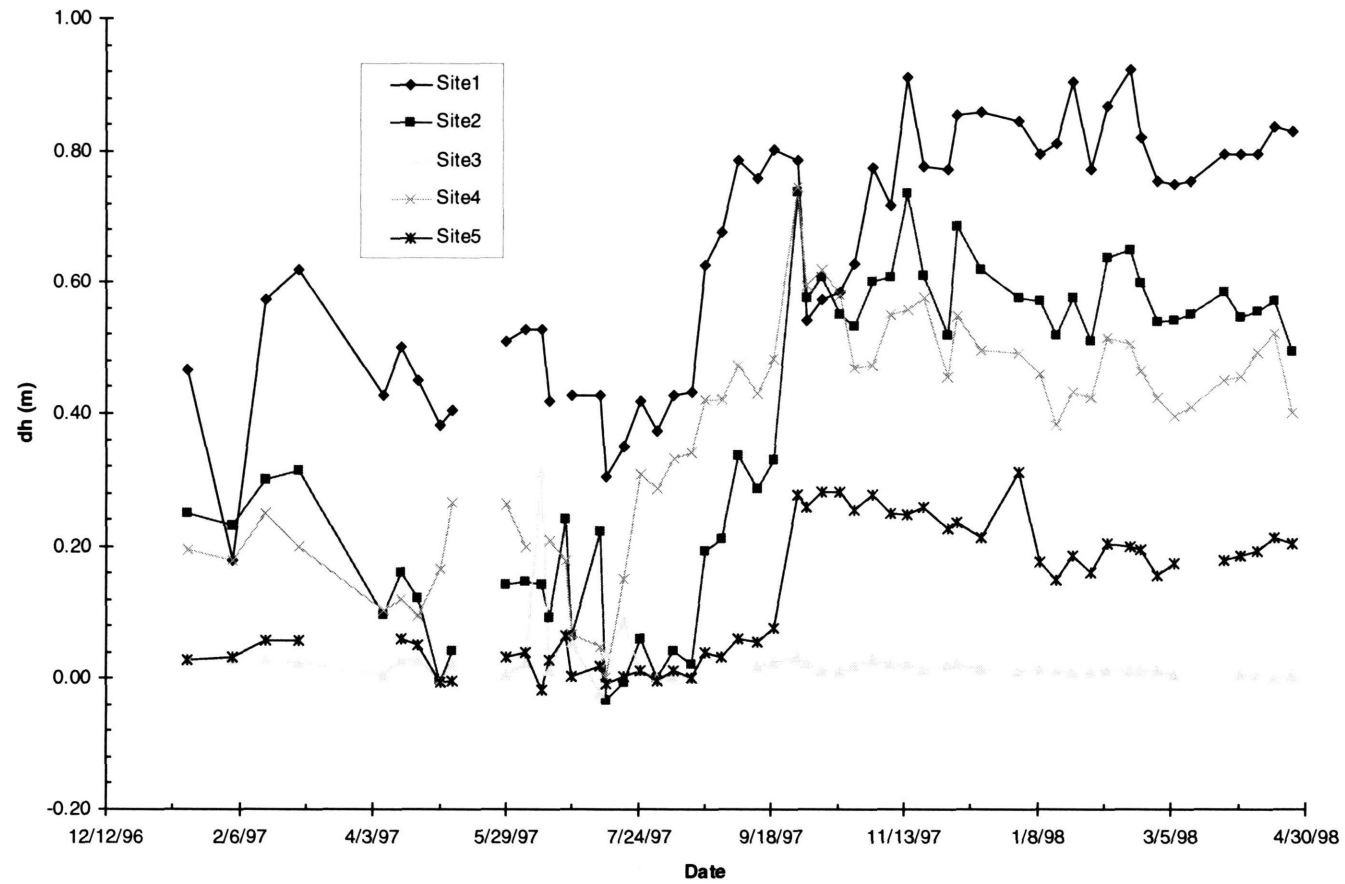


**Figure 21. Vertical head difference versus time for the uppermost 17 m of the Floridan aquifer. The head difference was calculated by subtracting the water level in the Floridan aquifer monitoring wells from the water level in the deep surficial aquifer monitoring wells.**

**Table 5. Summary of the total head differences between the surficial and Floridan aquifers.**

	Head Difference (m)				
	Site 1	Site 2	Site 3	Site 4	Site 5
<i><b>Time period 1</b></i>					
minimum	0.30	0.04	1.19	0.00	-0.08
maximum	1.14	0.63	1.84	0.63	0.36
average	0.60	0.30	1.50	0.30	0.13
<i><b>Time period 2</b></i>					
minimum	0.83	0.78	0.86	0.70	0.72
maximum	1.43	1.57	1.79	1.78	1.77
average	1.07	1.01	1.12	1.11	1.12

maps of the water table (Figure 15a and Figure 15b), is 0.1. This estimate was calculated using 6 m above sea level as the elevation for the base of the surficial aquifer. Using these values and Darcy's Law, the maximum horizontal flow velocity in the surficial aquifer is approximately 1 m/day.

#### *Vertical Flow in the Surficial Aquifer*

Vertical groundwater flow rates in the surficial aquifer are estimated with a number of different methods. The most reliable estimate of the vertical flow rate comes from direct measurement during tracer tests in the surficial aquifer. It is also possible to indirectly estimate vertical groundwater flow velocities with various forms of Darcy's Law. Both methods are used to bracket the range of downward flow velocities at the North Lakes wetland.

Vertical groundwater flow rates in the surficial aquifer were measured directly during the surficial aquifer tracer tests. During the surficial aquifer tracer test, the downward flow velocity in the surficial aquifer was estimated to be 0.2 m/day in the sinkhole and less than 0.07 m/day at the other tracer test location. The conductivity breakthrough curve at SW-2 suggests that the downward flow velocity at this well is approximately 0.1 m/day. Analysis of the water budget during the flooding test suggests that the average flow velocity over the entire flooded area is approximately 0.09 m/day. These groundwater flow velocities are surprisingly consistent with one another.

Darcy's Law can also be used to estimate downward flow velocities in the surficial aquifer. By having nested wells at five different locations at North Lakes, the driving potential, or vertical head difference, is known. Using estimates of hydraulic resistance in the forms of vertical hydraulic conductivity and leakance, and an estimate of porosity, it is possible to estimate the vertical flow velocity.

From the groundwater pumping test, values of leakance were estimated for four of the five nested well locations. By using the following form of Darcy's Law, which is written in terms of leakance rather than hydraulic conductivity,

$$v = \frac{L}{n} dh$$

it is possible to calculate a value of groundwater flow velocity for each time water levels were measured at the nested wells. Values of the head difference (dh) used in the equation are the same as those presented in Figure 19. A plot of vertical flow velocity versus time, using the leakance method, suggests that values of velocity range from slightly negative (which indicate an upward flow component) to approximately 0.04 m/day (Figure 22). Both the maximum and minimum flow velocities are located at Site 5. Vertical velocities at the other three sites range from 0.0 to 0.01 m/day. Velocities are not calculated for Site 2 because it was not possible to estimate a leakance value from the data collected during the groundwater pumping test.

Values for downward groundwater flow velocity in the surficial aquifer can also be made in a similar way using estimates of vertical hydraulic conductivity rather than leakance. The equation for velocity with this parameter of hydraulic resistance is written as:

$$v = \frac{K_z}{n} \frac{dh}{dz}$$

where  $K_z$  is the value of vertical hydraulic conductivity. In the following velocity calculations, the distance between head measurements (dz) is assumed to be 10 m. Porosity is set at a constant value of 0.4. Values of head difference across the surficial aquifer are used for dh (Figure 20). Velocities calculated with these values range from 0.00 to 0.12 m/day (Figure 23).

#### *Horizontal Flow in the Floridan Aquifer*

The horizontal flow velocity in the Floridan aquifer was measured directly during the Floridan aquifer tracer test. The average flow velocity during the test is about 270 m/day. This value, calculated by dividing the travel distance by the time to reach the peak concentration, is not representative of the normal flow velocity in the Floridan aquifer because the tracer test was conducted during stressed conditions. During the stressed conditions, the hydraulic gradient was much higher than hydraulic gradients observed during normal conditions.

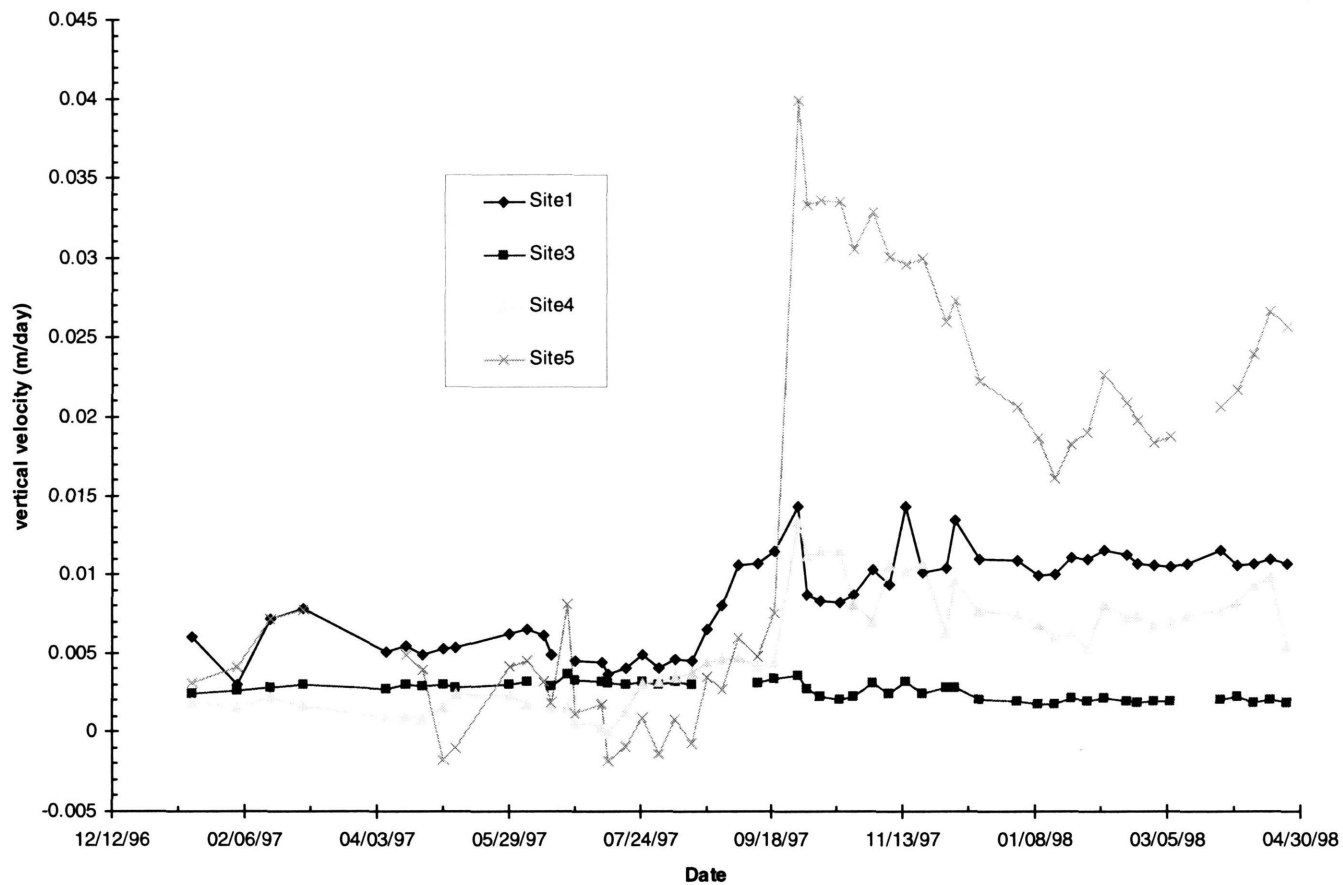


**Figure 22. Vertical flow velocity versus time for the surficial aquifer. The values presented in this graph were calculated using the leakance method.**



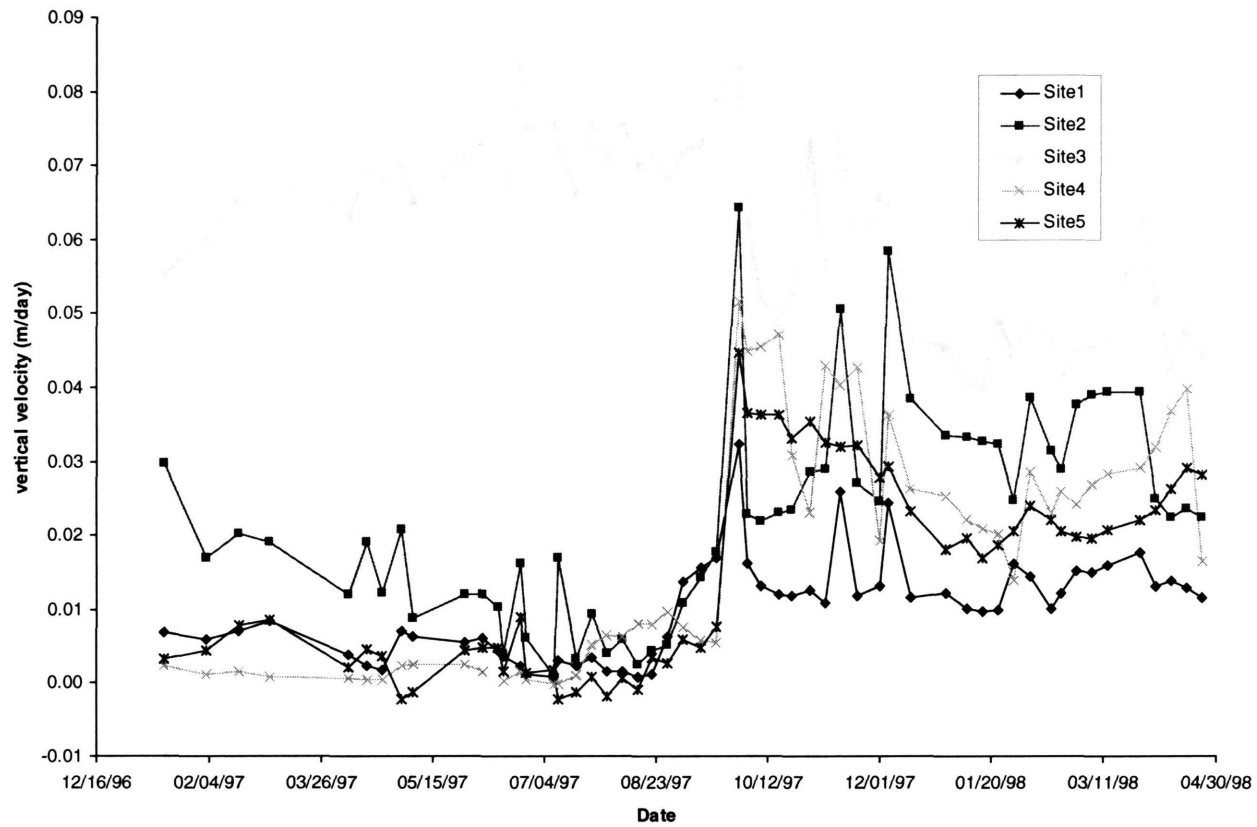


**Figure 23. Vertical flow velocity versus time for the surficial aquifer. Values presented in this graph were calculated using the values of vertical hydraulic conductivity estimated from the grain-size analysis results.**

The maximum value for the hydraulic conductivity in the Floridan aquifer, estimated from the pumping test data, is 22 m/day (Table 3). From the tracer test, the value of effective porosity in the Floridan aquifer is approximately 0.03. Values for the hydraulic gradient in the Floridan aquifer were calculated from water-level elevations (Figure 18). Using these values and Darcy's Law, estimated groundwater flow velocities in the Floridan aquifer range from 0.02 to 0.5 m/day (Figure 24).

## **Discussion**

### ***Reliability of Estimated Groundwater Flow Velocities***

A summary of the groundwater flow velocities estimated for North Lakes is presented in Table 6. The horizontal component of flow in the surficial aquifer is approximately 1 m/day. The reliability of this estimate is unknown because horizontal groundwater flow rates were not measured directly with a tracer test. For horizontal flow in the surficial aquifer, the hydraulic parameter containing the most uncertainty is the hydraulic conductivity in the horizontal direction. It is presumed that the hydraulic conductivity values presented in Table 2 are at least accurate within an order of magnitude. The horizontal velocity estimates for the surficial aquifer, therefore, are also probably accurate within an order of magnitude.

Estimates of vertical flow velocities in the surficial aquifer were made with a number of different methods (Table 6). For the surficial aquifer tracer test, measured velocities are relatively consistent with one another. Due to the direct measurement of tracer movement, these velocities are assumed the most reliable estimates of downward flow rates in the wetland. The velocity of 0.1 m/day, calculated from the conductivity breakthrough curve at SW-2, is especially reliable. SW-2 was installed many months prior to the flooding test. For this reason, the sediment next to the well probably had enough time to fill the annulus that was left during well installation. The probability that there was a short-circuited flow path at SW-2, therefore, is reduced.

The groundwater flow velocities calculated with Darcy's Law and leakance values are an order of magnitude less than velocities calculated with Darcy's Law and hydraulic conductivity values estimated from the grain-size analysis. It is difficult to determine which method provides the most reliable results

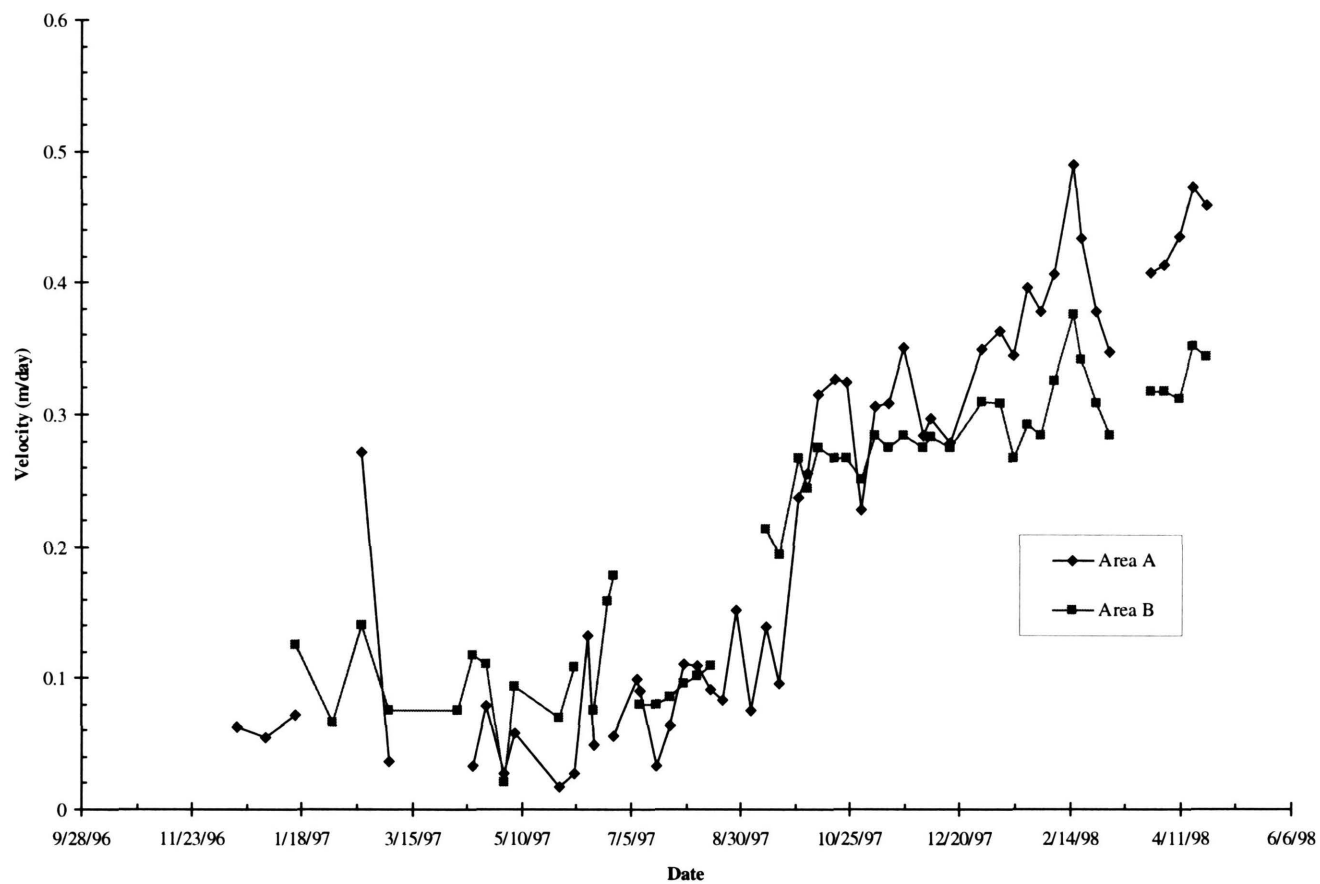


**Figure 24. Estimated values of maximum groundwater flow velocity versus time for the Floridan aquifer.**

**Table 6. Summary of groundwater flow velocities.**

Horizontal Flow in Surficial Aquifer			
Method	Location	Velocity (m/day)	
Darcy's Law Calculation	wetland	1	

Vertical Flow in Surficial Aquifer			
Method	Location	Velocity (m/day)	
breakthrough curve (bromide)	SATT-2 (sinkhole)	0.2	
breakthrough curve (bromide)	SATT-1	< 0.07	
breakthrough curve (fluid conductivity)	SW-2	0.1	
Water balance	flooded area	0.09	

Velocity (m/day) min < avg < max			
Method	Location	Time Period 1	Time Period 2
Darcy's Law Calculation (Leakance)	Site1	0.003 < 0.006 < 0.011	0.008 < 0.011 < 0.014
	Site3	0.002 < 0.003 < 0.004	0.002 < 0.002 < 0.004
	Site4	0.000 < 0.002 < 0.005	0.005 < 0.013 < 0.008
	Site5	-0.002 < 0.003 < 0.008	0.016 < 0.040 < 0.025
Darcy's Law Calculation (Kv from empirical relationship with grain size; dh = shallow surficial - deep surficial)	Site1	0.01 < 0.03 < 0.06	0.04 < 0.05 < 0.07
	Site2	0.00 < 0.02 < 0.05	0.06 < 0.08 < 0.12
	Site3	0.06 < 0.07 < 0.09	0.04 < 0.05 < 0.08
	Site4	0.00 < 0.02 < 0.03	0.04 < 0.06 < 0.09
	Site5	0.00 < 0.00 < 0.01	0.02 < 0.03 < 0.05

Horizontal Flow in Floridan Aquifer			
Velocity (m/day) min < avg < max			
Method	Location	Time Period 1	Time Period 2
Darcy's Law Calculation	Area A	0.02 < 0.08 < 0.27	0.23 < 0.35 < 0.49
	Area B	0.02 < 0.11 < 0.21	0.24 < 0.30 < 0.37

because tracer tests were not conducted at sites with nested wells. It appears, however, that velocities measured during the tracer tests are most similar to the velocities calculated with Darcy's Law and estimates of vertical hydraulic conductivity from the results of the grain-size analysis. The validity of this conclusion is currently being investigated with a numerical model to determine if the leakance values, estimated with the Hantush method, are in fact low.

The magnitude of the horizontal flow velocity that was calculated for the Floridan aquifer is reasonable. In carbonate aquifers, the effective porosity is usually the parameter that contains the most uncertainty. Fortunately, a reliable estimate for effective porosity was calculated with the data collected during the Floridan aquifer tracer test. The largest problem with the estimate of effective porosity is that it was measured at a small scale (the distance between the two wells used in the Floridan aquifer tracer test was only 7.6 m). Without conducting tracer tests at a larger scale, it is impossible to determine if the value for effective porosity calculated during this study can be applied more generally. The range of values of hydraulic conductivity, also used in the calculation of horizontal flow velocities of the Floridan aquifer, is also considered reliable. The values of hydraulic conductivity were determined from data collected during the pumping test. Results from pumping tests are usually considered reliable because a large volume of the aquifer is stressed. The resulting aquifer values are thus considered reasonable estimates of the site-scale aquifer parameters. The estimates of the hydraulic gradient in the Floridan aquifer are also reliable. One problem that was encountered while calculating the hydraulic gradient was that the potentiometric surface was nearly flat during the first time period. During the second time period, however, the magnitude of the hydraulic gradient increased and better estimates of the magnitude and flow direction were made.

### ***Feasibility of Rehydration***

A portion of this study was conducted during a period with above-normal rainfall conditions attributed to an unusually strong El Niño pattern. During this time, much of the wetland was covered with standing water. The period with standing water in the wetland is considered similar to the conditions that would exist if reclaimed water were used to rehydrate the wetland. The vertical groundwater flow velocities calculated with Darcy's Law have been separated into two different time periods. The velocities estimated

during the first time period are thought to be representative of velocities that occur during a normal year. Estimates of velocity are much higher for the second time period. As the wetland was completely flooded during most of this time, the velocities during the second time period are thought to be representative of the velocities that would occur if the wetland were flooded with reclaimed water. In fact, the velocities that would exist if the wetland were flooded during a normal rainfall year might be even higher. During the study, the potentiometric surface of the Floridan aquifer was much higher than the elevation of the potentiometric surface during a normal year. If the wetland were flooded, water levels in the surficial aquifer would be similar to the water levels that were observed during the second time period. Water levels in the Floridan aquifer, however, would probably match more closely with the water levels observed in the Floridan during the first time period. This suggests that under flooded conditions, head differences between the surficial and Floridan aquifers could be 2 m higher or twice as large as they were during flooding test and the second time period. The resulting velocities would be on the order of 0.2 to 0.4 m/day.

Maximum flow rates, in the horizontal and vertical direction in the surficial aquifer, are within an order of magnitude. As the surficial aquifer is 10 m thick, groundwater will not travel far in the surficial aquifer before flowing into the Floridan aquifer. Travel paths to a municipal wellfield, then, can be described as vertical flow in the surficial aquifer, and horizontal flow in the Floridan aquifer. If reclaimed water is added to the North Lakes wetland, the shortest length of time it will take the reclaimed water to reach the Floridan aquifer is approximately 25 days ( $10 \text{ m} / 0.4 \text{ m/day}$ ). As suggested by the histogram of flow directions of Figure 17, groundwater in the Floridan aquifer will most likely flow south at velocities between 0.2 and 0.5 m/day. These velocities are based on the aquifer parameters and hydraulic gradient observed at North Lakes. If groundwater in the Floridan aquifer is diverted towards the Section 21 wellfield, then velocities may increase as the hydraulic gradient increases near the municipal wells. If the assumption is made that the hydraulic gradient at North Lakes is representative for a distance of only 365 m, then the travel time from North Lakes to the 365 m travel distance is approximately two years.

Compared to the surrounding area, the Floridan aquifer is poorly confined at the North Lakes wetland, as the Upper Confining unit is thin to absent beneath much of the wetland. The absence of the Upper

Confining unit at North Lakes introduces some concern over the feasibility of rehydration for two reasons. The first reason is that residence time of reclaimed water in the surficial aquifer will be shorter than the residence time for a site with better confinement. The other reason is that the North Lakes wetland will require more reclaimed water for successful rehydration than a site with better confinement, the same distance from the wellfield.

### ***Significance of Karst Conduits***

One of the initial hypotheses of this study was that karst features, such as sinkholes, act as preferential conduits for vertical groundwater flow. Results from this study suggest that this is not necessarily the case at the North Lakes wetland. Of the five sinkholes that were monitored during the groundwater pumping test, only two sinkholes (A and B) experienced drawdown greater than a nearby monitoring well. This suggests that sinkholes C, D, and E probably do not act as preferential conduits for flow to the Floridan aquifer. Data from the groundwater pumping test conflicts with the data collected during the surficial aquifer tracer test. During the tracer test, the maximum groundwater flow velocity (0.2 m/day) was measured in sinkhole E. A possible explanation for this relatively large velocity is that the bromide tracer migrated along the side of the multi-level sampling tubes. This short-circuiting effect would result in a velocity that is higher than the velocity that would exist in undisturbed portions of the aquifer.

The model of sinkholes acting as vertical conduits for groundwater flow can be refined with the results from this study. One explanation for the sinkholes that experienced little drawdown during the pumping test is that low-permeability soil layers have plugged the sinkholes. Consider a sinkhole early in its development. Through the process of raveling, a preferential flow pathway forms vertically in the upper aquifer. If the length of time between subsidence events is relatively large, or the subsidence rate is slow relative to the rate of soil formation, low-permeability material may collect in the base of the sinkhole. As the sediment continues to subside, these low-permeability layers are carried downward into the aquifer, choking the hydraulic connection of the sinkhole. Based on this notion of sinkhole development, then, the hydraulic significance of a sinkhole depends on the subsidence rate and the depositional rate of low-permeability material in the base of the sinkhole. There is some further evidence to support this model of

sinkhole development. Data from the groundwater pumping test suggests that Sinkhole B may act as a preferential pathway for groundwater flow. The entire development of Sinkhole B occurred during the course of this study. The fact that this sinkhole formed rapidly may explain why this sinkhole responded the way it did to the groundwater pumping test and why this sinkhole appeared to have hydraulic significance.

## **Conclusions**

Groundwater flow at the North Lakes wetland is predominantly downward in the surficial aquifer, and horizontal in the Floridan aquifer. The maximum velocity of lateral flow in the surficial aquifer is approximately 1 m/day. Maximum values of downward flow in the surficial aquifer range from 0.1 to 0.2 m/day. Because vertical flow velocities are within an order of magnitude of the horizontal flow velocities, and the surficial aquifer is relatively thin (10 m), groundwater does not travel far in the surficial aquifer before flowing into the Floridan aquifer. For this reason, horizontal flow in the surficial aquifer is not an important mechanism for advective transport.

During the second part of the North Lakes study, El Niño weather patterns produced above-normal rainfall conditions. As a result of the extreme rainfall conditions, water levels in the surficial aquifer increased by as much as 3 m. Water levels in the Floridan aquifer increased as much as 2.5 m. The effect of the elevated water table and potentiometric surface is to increase groundwater flow rates. During the second part of the study, estimated vertical groundwater velocity in the surficial aquifer increased from about 0.04 to 0.08 m/day, a factor of about 2. The estimated horizontal velocity in the Floridan aquifer increased from 0.09 to 0.3 m/day, a factor of about 3.

The shortest predicted residence time for reclaimed water in the surficial aquifer is on the order of 25 days. Results from this study cannot be used directly to estimate how long it will take groundwater to flow from the North Lakes wetland to the Section 21 wellfield. It is possible that reclaimed water used to rehydrate the North Lakes wetland would not travel to the Section 21 wellfield. This is because horizontal flow directions in the Floridan aquifer appear to be due south. The Section 21 wellfield is northwest of the North Lakes wetland. It is possible that flow lines downgradient of North Lakes could be diverted towards



the Section 21 wellfield because of the large pumping rates. If the assumption is made that the results from this study can be extrapolated more than 400 m, then the travel time from North Lakes to the Section 21 wellfield is much longer than 2 years. If groundwater in the Floridan aquifer traveled the shortest possible path between the North Lakes wetland and the wellfield, the results of this study suggest the travel time would be about 8 years.

The hypothesis that sinkholes act as preferred conduits for vertical flow is not necessarily true at the North Lakes wetland. In fact, results from this study indicate that downward velocities in some of the sinkholes may be less than velocities outside of the sinkholes. One possible explanation for this is that during rainfall events, low-permeability, fine-grained sediments are washed into the base of the sinkhole. Future subsidence within the sinkhole would then carry the low-permeability material into the aquifer causing the conduit to become plugged.

## **CHAPTER 3. INCORPORATING LARGE-SCALE, VERTICAL FRACTURES IN GROUNDWATER FLOW MODELS**

### **Introduction**

Supply wells located within linear features on an aerial photograph, or photolineaments, tend to have higher yields than wells located away from photolineaments (Lattman and Nickelson, 1958; Lattman and Parizek, 1964; Moore, 1976; Parizek, 1976; Siddiqui and Parizek, 1977). The hydraulic significance of photolineaments can be explained in terms of the intersection of a zone of increased density of vertical fractures with the land surface (Lattman and Parizek, 1964). A well located in a photolineament, therefore, has a better chance of intersecting a permeable fracture and producing more water. Recent advances in identifying photolineaments are presented by Mabee et al. (1994). The general model for a fractured aquifer is characterized by blocks and fractures. Blocks represent portions of the aquifer that are not intersected by fractures and tend to have lower values of transmissivity. Conversely, fractures tend to have high values of transmissivity and act as preferential pathways for groundwater flow.

There has been much effort to understand the effects that fractures have on groundwater flow because the effects can be so large. In general, there are two different ways fractures can be modeled. The approach used by most practicing hydrogeologists is to assume that the aquifer can be represented with an equivalent porous medium (EPM). The EPM approach, also known as the continuum approach, works well for quantifying groundwater fluxes at regional scales and, in some cases, can be applied with success to local and site scales. The EPM approach, however, does not work well for predicting advective transport because in most cases, the location of the highly permeable fractures is unknown.

The other approach used to simulate flow in fractured rocks is the discrete-fracture model (DFM). With the DFM approach, flow is simulated in each fracture using solutions to the Navier-Stokes equation (Bear, 1993) or Kirchoff's laws for electrical circuits (Kraemer and Haitjema, 1989). A finite-element DFM has

also been developed in which boundaries for selected elements act as fractures (Geotrans, 1988a). This finite-element model has been applied to the karst aquifer in west-central Florida (Geotrans, 1988b). The complexity of the DFM approach can increase rapidly as simplifying assumptions are eliminated. For example, some DFM models assume flow through two parallel plates. In reality, the aperture of a fracture is variable. Simulating flow in single fracture with variable apertures is possible (Bear, 1993; Wilson and Witherspoon, 1985), but the simulation of flow in many fractures with variable apertures is much more complicated. The biggest problem with using DFM's is that the properties are never known for each fracture in the model domain. Fracture properties, therefore, contain a high degree of uncertainty.

Stochastic methods are the best available tools for quantifying uncertainty in model predictions. It is no surprise, therefore, that stochastic methods are widely used for studies of groundwater flow (Peck et al., 1988; Freeze et al., 1990; Chiles and de Marsily, 1993; Gelhar, 1993). Many of these studies are performed with Monte Carlo (MC) analyses because the method is conceptually straightforward and works well with numerical models (Freeze et al., 1990). Peck et al. (1988) provide an excellent discussion of MC analysis.

There are two basic steps to conducting MC analysis. The first is to randomly generate statistically reasonable values for one or more model parameters. This is done by formulating a probability density function, or pdf, for the parameter that contains uncertainty. The pdf describes the probability that the parameter will assume some value. It is not possible to know for certain the pdf that exactly describes the statistical behavior of the uncertain parameter. One assumes that the pdf, which is fit to a number of observations, is representative of the population. This assumption is known as ergodicity and is required for stochastic analysis.

Another assumption that is commonly made with statistical generation of model parameters, though it is not required, relates to parameters that are spatially or temporally variable. This assumption, known as statistical homogeneity, allows a single pdf to represent the variability for many times or locations. Some of the better-known pdf's include the uniform, normal, and lognormal distributions. From the pdf, a value for the uncertain parameter is randomly selected. Random values are selected for each parameter that contains uncertainty. The collection of random values from one sampling of the pdf's is termed a realization.

The second step in MC analysis is to use the realization as input to the numerical model. The results from one run of the numerical model, therefore, are considered one statistically reasonable prediction. Each statistically reasonable prediction is also referred to as a realization. The collection of many statistically reasonable predictions is termed the ensemble. Statistics performed on the ensemble are used to quantify the probability that a particular result will occur.

For the study of fracture flow, MC analysis is performed to quantify the uncertainty in model predictions that results from uncertainty in one or more of the properties that describe fractures. These properties include fracture orientation, length, aperture, and density. Pdf's are formulated, from field observations if available, for the fracture properties that are assumed to contain uncertainty. A DFM is then used to simulate many realizations of randomly generated fractures. A summary of MC analysis with fractures is presented by Chiles and de Marsily (1993).

The problem with the DFM's described thus far is that they are relatively complex and, as a result, are not widely used by the modeling community. Moreover, most of the current models are limited to geologic conditions where the blocks are assumed to be impermeable. In this chapter, a method is developed for incorporating discrete fractures into grid-based numerical models of groundwater flow. The method is particularly attractive because it uses widely accepted numerical models (such as MODFLOW) that are familiar to most practicing hydrogeologists. The method is extended to simulate advective transport with a simple particle-tracking model that links with the DFM. To quantify the predictive uncertainty, MC analysis is performed with the model. The basic procedure is to generate realizations of random fractures, incorporate the fractures into the grid-based DFM, perform MC analysis, and then evaluate the uncertainty in groundwater travel times. To illustrate the approach, the method is applied to a simplified problem in west central Florida that involves predicting groundwater travel times in a fractured aquifer.

### **Method for Conducting Monte-Carlo Analysis with a Grid-Based Discrete-Fracture Model**

The methods developed in this paper apply to fractures that are relatively large with respect to the study area. To determine if this approach will work for a specific problem, one must first decide if discrete fractures can be incorporated into a grid-based model of groundwater flow. This determination is based on

the average width of the fracture aperture, or thickness of the fracture zone, the density of the fractures, and the level of model resolution that will be required to address the specific problem. This method should not be applied to relatively dense fracture networks that can be adequately simulated with an EPM model. Because the approach inserts fracture zones into model cells, a fracture transmissivity, rather than fracture aperture, is used to quantify the hydraulic significance of fractures.

### ***Fracture Statistics***

If the fractures are relatively large compared to the study area, they may be described with four properties: length, orientation, density, and transmissivity (or hydraulic conductivity if the aquifer is unconfined). For transient applications, there is an additional property: storativity (or specific yield for unconfined aquifers). In the following discussion, the methods that apply to fracture transmissivity also apply to fracture storativity.

It is assumed that uncertainty in model prediction results from uncertainty in one or more of the fracture properties. The first step in quantifying this uncertainty is to develop an understanding of the statistical nature of the fracture properties. Based on field data or an intuitive understanding of the fracture system, pdf's are formulated for each fracture property that is assumed to contain uncertainty. The procedure for fitting pdf's to field data is relatively straightforward. A description of the more commonly used pdfs are presented by Yevjevich, (1976).

Representing fracture length and orientation is relatively straightforward (Chiles and de Marsily, 1993). There are several options, however, for representing the fracture transmissivity. In the literature, the relationship between block transmissivity and fracture transmissivity is usually represented by a ratio. This ratio can be used as a multiplier for calculating the transmissivity of a fracture. The alternative is to specify the transmissivity for each fracture. Regardless of the approach, the multiplier or value of transmissivity may be described with a pdf.

The hydraulic significance of a fracture pattern is controlled primarily by connectivity (Kraemer and Haitjema, 1989; Cacas et. al, 1989). Connectivity is the property that describes how well a fracture system

is connected. Fractures that are well connected have a much larger influence on groundwater flow in an aquifer than the same number of fractures that are unconnected. It is, therefore, very important that the random sampling of the fracture properties results in a fracture pattern that is similar in connectivity to field connectivity.

### ***Equivalent Porous Media Site Model***

Before incorporating discrete fractures into a numerical model of groundwater flow, an EPM model is developed for the domain of interest. The EPM model may be either steady state or transient and should contain square cells that are similar in size to the average width of the fracture zone.

Several codes can be used to simulate groundwater flow. The finite-difference code, MODFLOW (McDonald and Harbaugh, 1988) is arguably the best code for simulating groundwater flow and is certainly the most widely used. The model should be calibrated to site-specific data in order to represent, in general, the flow patterns observed from the field data. If a numerical model of groundwater flow has already been developed at a regional scale, telescopic mesh refinement (TMR) can be used to “zoom in” on the domain of interest (Anderson and Woessner, 1992). TMR is also a practical method for assigning boundary conditions to subregional-scale models.

To simulate advective travel times, two main codes have been accepted by the modeling community and are widely used. These codes are PATH3D (Zheng, 1989) and MODPATH (Pollock, 1989).

### ***Bulk Transmissivity versus Block Transmissivity***

If highly permeable fractures are incorporated into the calibrated EPM model of the site, the bulk transmissivity of the layer containing the fractures will increase. It is unlikely, then, that the discrete fracture model will be able to match observed conditions. It is necessary to determine what the value of the block transmissivity should be in the discrete fracture model so that the resulting bulk transmissivity is the same as the bulk transmissivity in the EPM model.

The relationship between bulk transmissivity and block transmissivity is evaluated using the properties of the fractures. A simple, two-dimensional model is developed at the same scale as the EPM model. Along two opposite sides of the model, constant-head cells are inserted to impose a hydraulic gradient across the model domain. No-flow boundaries are used for the other two boundaries. Within the model domain, random fractures are inserted. Transmissivity for the fractures may be specified with a value or multiplier. The value or multiplier may be deterministic or stochastic.

The box model is run using the basic MC approach. Separate MC analyses are run for different values of the block transmissivity. For each run of the flow model, bulk transmissivity is calculated by summing the total flux into or out of the constant head cells on one side of the box model and dividing the total flux by the model width and imposed hydraulic gradient. Median values of bulk transmissivity are then plotted against the specified values of block transmissivity. This relationship will be used to adjust the block transmissivity in the site model so that the bulk transmissivity is the same as the EPM site model.

#### ***Monte-Carlo Analysis with Discrete-Fracture Model of Site***

The final step is to quantify the uncertainty in model predictions that result from uncertainty in fracture properties. A realization of randomly-generated fractures is incorporated into the transmissivity array of the flow model. First, the block transmissivity in the discrete fracture model is adjusted. The adjustment is made to the values of block transmissivity using the relationship derived with the box model. This ensures that the bulk transmissivity of the discrete fracture model is the same as the bulk transmissivity of the EPM model. Next, the flow and particle tracking models are run with the transmissivity array that contains the fractures. The predictions of interest, simulated with the numerical models, are stored for later analysis.

This sequence of generating random fractures, running the numerical models, and storing the predictions is repeated until the uncertainty in model predictions is quantified. Robinson and Hodgkins (1986) estimate that 10,000 runs are required to adequately describe the uncertainty in model predictions. The number of required simulations may be reduced by using advanced schemes for generating realizations, such as the latin-hypercube method (Peck et al., 1988).

### ***Implementation***

A FORTRAN code, FRACMOD, was written to implement the methods described above. The objective of the implementation stage was to develop a robust code that could be used with most grid-based models of groundwater flow and particle tracking. FRACMOD was developed specifically for MODFLOW and PATH3D but can be modified to work with most flow and particle-tracking models. FRACMOD uses existing MODFLOW and PATH3D models.

MODFLOW was written so that each of the data arrays may be removed from the specific package, such as the block-centered flow (BCF) package, and located in another file. This freedom in array location is used to remove the transmissivity array from the BCF package and place it in another file. FRACMOD works by reading this transmissivity file and writing a new one that contains randomly generated fractures. FRACMOD then calls a DOS Batch program to run MODFLOW and PATH3D. No modifications are required to MODFLOW or PATH3D because the models are run outside of the FRACMOD program.

Prior to running the DOS Batch program, fractures are randomly generated and placed in the transmissivity array. The general procedure for incorporating the linear fractures is as follows. First, the fracture properties that are treated stochastically, such as initial position, orientation and length are selected from their respective pdf's. Selection of the random values uses the latin-hypercube approach. Orientation and length define a line in two-dimensional space. A subroutine was written to select all model cells that intersect the line. It is very important that selected cells along a fracture connect at cell faces, rather than at diagonals. Cells that connect along the diagonal cannot transmit the proper volume of water. The value for hydraulic conductivity or transmissivity in the selected cells is determined in either of two ways: from a multiplier with the original value, or as an explicit value. The multiplier or explicit value may be selected from a pdf. Fractures are generated with this procedure until the simulated fracture density is equal to the desired fracture density. The desired fracture density may also be selected from a pdf or stated explicitly.

FRACMOD runs a loop that generates fractures and runs the numerical models. The total number of simulations is determined by the user. To store the model results, FRACMOD runs two additional batch files immediately before and immediately after the batch file that calls MODFLOW and PATH3D. The



first batch file, PRE.BAT, is used to move the file(s) that contain the model results from the previous simulations to a temporary file. POST.BAT, which is run after MODFLOW and PATH3D, appends the new results to the old and gives the files the appropriate names. Other routines are also included in FRACMOD to generate SURFER grids for head and realizations of transmissivity.

### **Application to North Lakes Wetland Project**

To illustrate the procedure, the method is applied to a problem in west-central Florida, which involves the estimation of groundwater travel times in a fractured aquifer. The objective of this application is to illustrate the procedure so a number of assumptions are made to simplify the problem. For example photolineament statistics from a previous study at a nearby wellfield are assumed to be representative of the fracture zone statistics at North Lakes. The assumptions add uncertainty to the North Lakes results but they do not detract from the objective of this chapter, which is to present the method and illustrate the benefits for using this approach.

### ***Background***

The North Lakes wetland has been selected as a potential candidate for rehydration with reclaimed water. The main concern with rehydration at North Lakes is that the residence time of reclaimed water in the aquifer system will not be long enough for sufficient renovation. Located approximately 1.4 km from the wetland, the Section 21 wellfield is permitted to withdraw groundwater at an average annual rate of 40,000 m<sup>3</sup>/day (10 million gallons per day; Figure 25). The Section 21 wellfield is operated by the City of St. Petersburg and supplies potable water to the residents of Hillsborough County. Environmental managers at the Southwest Florida Water Management District have determined that reclaimed water added to the wetland must reside in the aquifer system for at least two years before being withdrawn by a municipal supply well.

### ***Fracture Statistics***

The goal of the North Lakes project is to develop an estimate of the advective travel time from the North Lakes wetland to the Section 21 wellfield. Clearly, the presence of highly permeable, vertical fracture

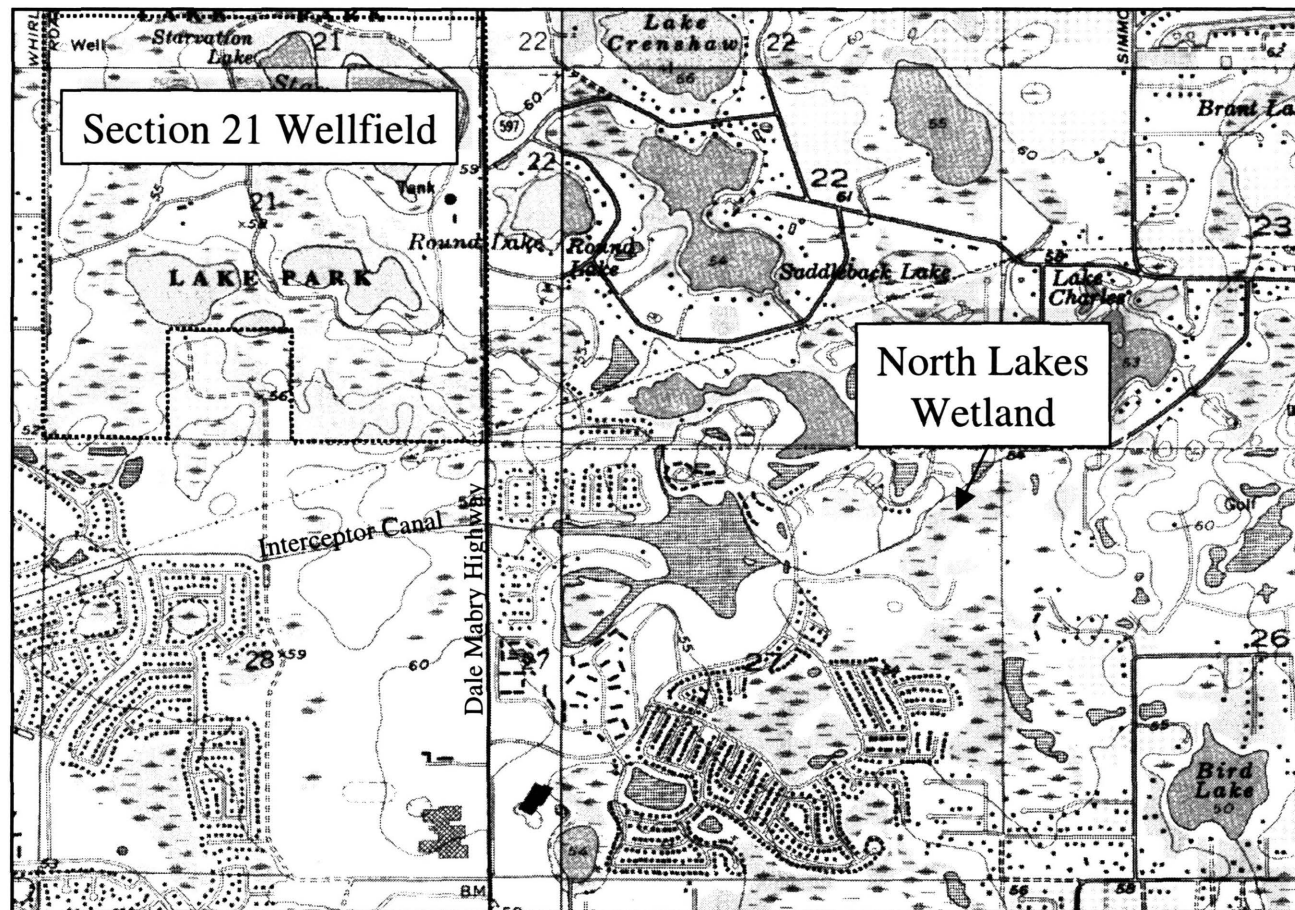


Figure 25. Location of the North Lakes wetland and Section 21 wellfield.

zones will affect the groundwater travel time. There is, however, a great deal of uncertainty in locating these highly permeable fracture zones and describing their properties. For this reason, selected fracture zone properties are treated stochastically.

Williams (1985) conducted a detailed study of the photolineaments at the Cross Bar Ranch wellfield. Included with her analysis are histograms of fracture length and orientation. It is assumed herein that the statistical properties of the photolineaments mapped by Williams (1985) are also representative of the length and orientation statistics of the fracture zones within the North Lakes study area. William's study was conducted relatively close to North Lakes (20 km) and her data is supported by other local studies of photolineament length and orientation. For these reasons, the use of Williams orientation and length data to represent fracture zone properties at North Lakes is assumed to be reasonable.

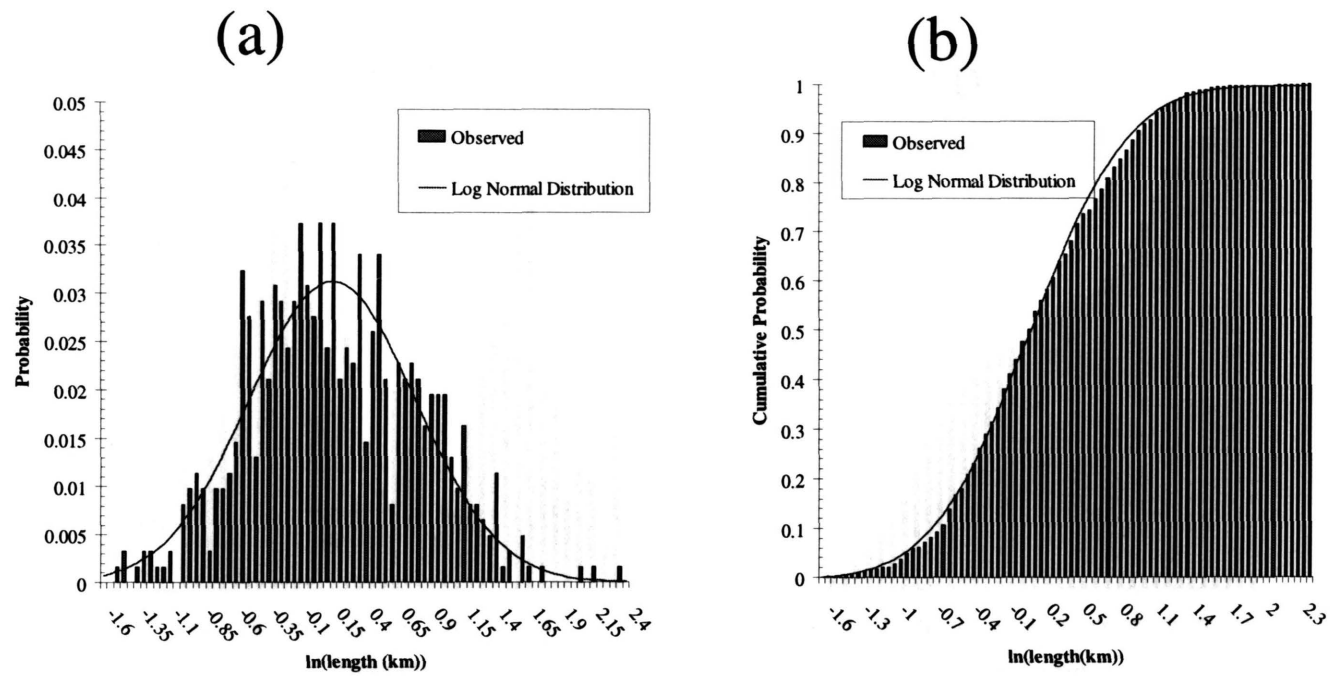
The criteria used by Williams to define the lineaments were soil tone, presence of sinkholes, elongation of sinkholes, sinkhole alignment, tree alignment, vegetation bodies, elongation of vegetation bodies, alignment of vegetation body, and straight water-course segments. The 618 photolineaments that were identified in her study are presented in Figure 26.

Photolineaments range in length from 0.2 to 10 km. A normalized frequency histogram suggests that fracture length may be lognormal (Figure 27a). The mean and standard deviation of the natural logarithm of length (km) are 0.14 and 0.64, respectively. These statistics do not imply that the standard deviation of photolineament length is greater than the mean length, because the values are based on the natural log of length. A lognormal function with these values for mean and standard deviation is also presented in Figure 27 to illustrate the match between the pdf and the observed data.

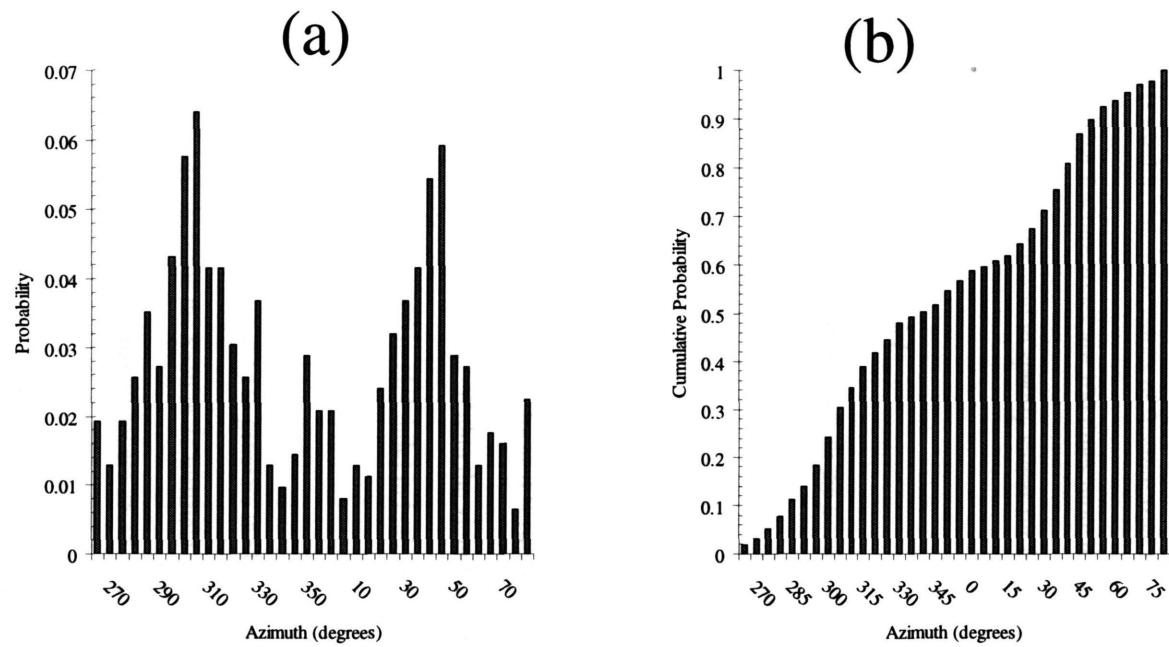
The orientation of a fracture is defined on the north half of a compass by an azimuth ranging between 270 and 90 degrees. A frequency histogram of azimuth suggests that fracture orientation is bimodal and possibly tri-modal (Figure 28). The statistical distributions of azimuthal data pose a particular problem because it is difficult to fit a pdf to circular data. For this reason, it is assumed that the azimuth histogram of Williams (1985) is representative of the entire population. With this assumption, it is not necessary to fit a pdf to the observed histogram.



Figure 26. Photolineaments at the Cross Bar Ranch Wellfield (modified from Williams, 1985).



**Figure 27. Frequency histogram for fracture length of the photolineaments mapped by Williams (1985).**



**Figure 28. Frequency histogram for photolineament orientation as mapped by Williams (1985).**

The sum of all of photolineament lengths is 876 km. The study area for the Cross Bar Ranch wellfield is 13.3 km by 14.9 km. The fracture density, therefore, is 4 km/km<sup>2</sup>. For the North Lakes application, the density of fracture zones is treated as a deterministic parameter. The assumption is made that half of the photolineaments mapped by Williams (1985) are hydraulically significant. To incorporate this assumption, a fracture density of 2 km/km<sup>2</sup> is used rather than the mapped value of 4 km/km<sup>2</sup>.

A deterministic multiplier is used to calculate values of fracture zone transmissivity from values of block transmissivity. It is assumed that fracture zones are 100 times more transmissive than blocks. The simulations are steady state, so there is no need to specify values for fracture zone storativity.

#### ***Development of Equivalent Porous Media Model***

To develop a groundwater flow model that incorporates both the Section 21 wellfield and the North Lakes wetland, TMR is used to generate a local-scale model from a larger, regional-scale model. The regional-scale, MODFLOW model was developed and calibrated by SDI Environmental (1994) to simulate groundwater flow in west central Florida from 1971 to 1993. The model contains two layers. The upper layer represents the surficial aquifer. The lower layer represents the Upper Floridan aquifer. The model is quasi-three-dimensional in that the semi-confining unit, located between the surficial and Upper Floridan aquifers, is simulated with a vertical resistance term. Within the vicinity of the Section 21 wellfield, cell size for the regional model is approximately 400 m (1/4 mile) in both the east-west and north-south directions.

A commercially available software package was used to generate the local-scale model from the regional-scale model. The local-scale model includes the Section 21 wellfield and the North Lakes wetland. The model is 160 rows by 192 columns. The cells in the model are 25.15 m x 25.15 m square. This means that there are 256 cells in the local-scale model for each cell in the regional-scale model. The TMR software assigns constant-head boundary conditions around the local-scale model with head values interpolated from the regional-scale model. The local-scale model is run to steady state using average annual hydrologic conditions for calendar year 1993.

Within the North Lakes and Section 21 area, two values for transmissivity were used for the Floridan aquifer to calibrate the regional-scale model. The transmissivity zonation from the regional-scale model is included in the local-scale model. The western half of the local-scale model has a transmissivity value of 5570 m<sup>2</sup>/day. The eastern half of the model has a transmissivity value of 1860 m<sup>2</sup>/day. The value for porosity is held constant at 3 percent. This porosity value for the Floridan aquifer was estimated from a tracer test that was conducted at the North Lakes wetland (Chapter 2). Initially, the local-scale model is run as an EPM model. This means that the transmissivity values for the two zones represent bulk transmissivity and include the effects of any fractures that may be present. The result of running the EPM model is that the particle migrates from North Lakes to the Section 21 wellfield (Figure 29). After 9 years, the particle is withdrawn by the supply well at the southeast corner of the wellfield.

#### ***Effects of Fractures on Bulk Transmissivity***

A simple, two-dimensional MODFLOW model was used to ascertain the effect that fractures have on the bulk transmissivity of the aquifer. The model domain is 4753 m x 4753 m. Constant heads were assigned to the east and west boundaries. No-flow boundaries were used for the north and south edges of the model. Each cell in the model is 25.15 m x 25.15 m. Therefore, the model consists of 189 rows and 189 columns. Values for the constant-head cells were selected in such a way that the resulting hydraulic gradient is  $1 \times 10^{-3}$  and groundwater flows from east to west.

MC analysis was run seven times using FRACMOD. For the seven MC analyses, fracture length and orientation were treated as stochastic parameters using the statistical descriptions of Williams (1985). For each MC analysis, a different value was specified for the block transmissivity. The ratio between block transmissivity and fracture transmissivity, however, was held constant at 100. The seven values used for block transmissivity were 1000, 2000, 3000, 4000, 5000, 5700, and 7000 m<sup>2</sup>/day. The resulting values of bulk transmissivity plot as a straight line against values of block transmissivity (Figure 30). Error bars represent one standard deviation. This linear relationship will be used later to determine block transmissivity values for the North Lakes model.



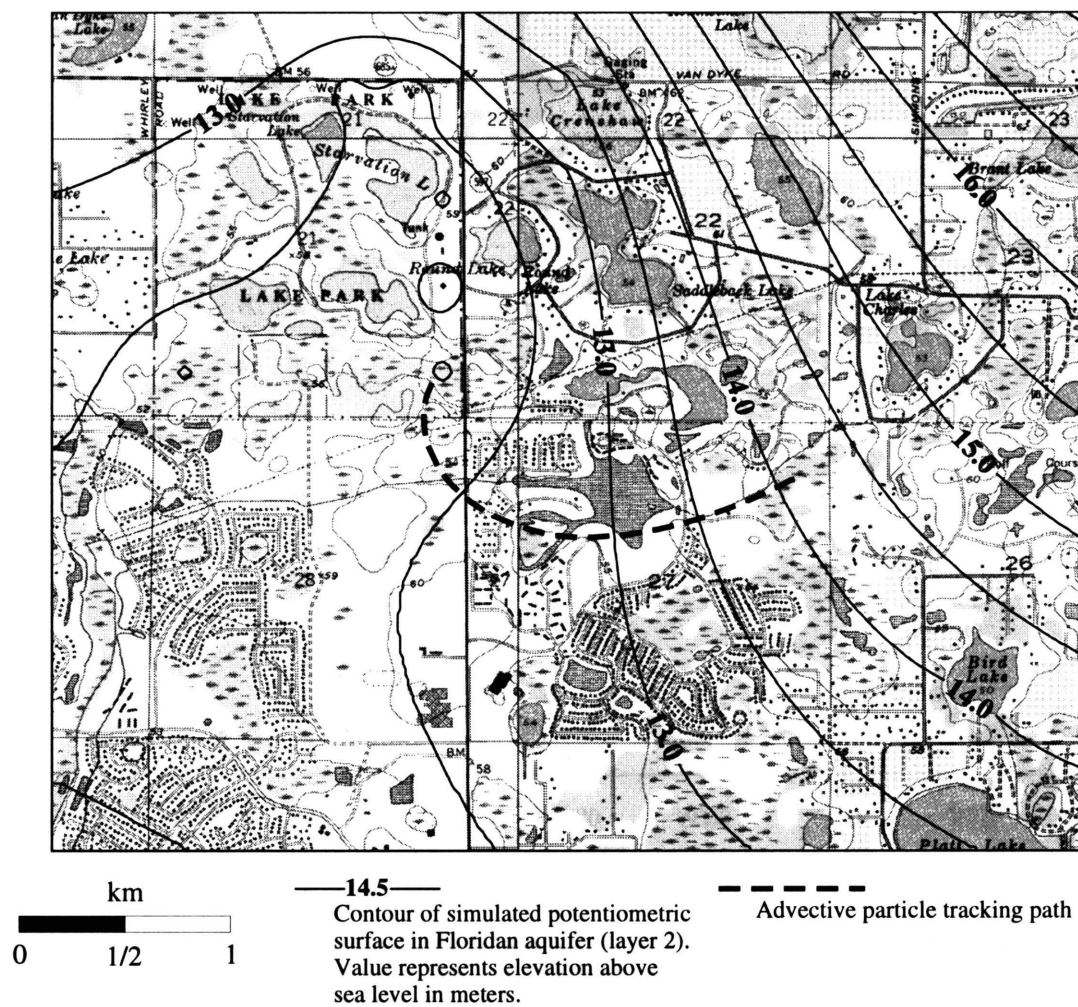
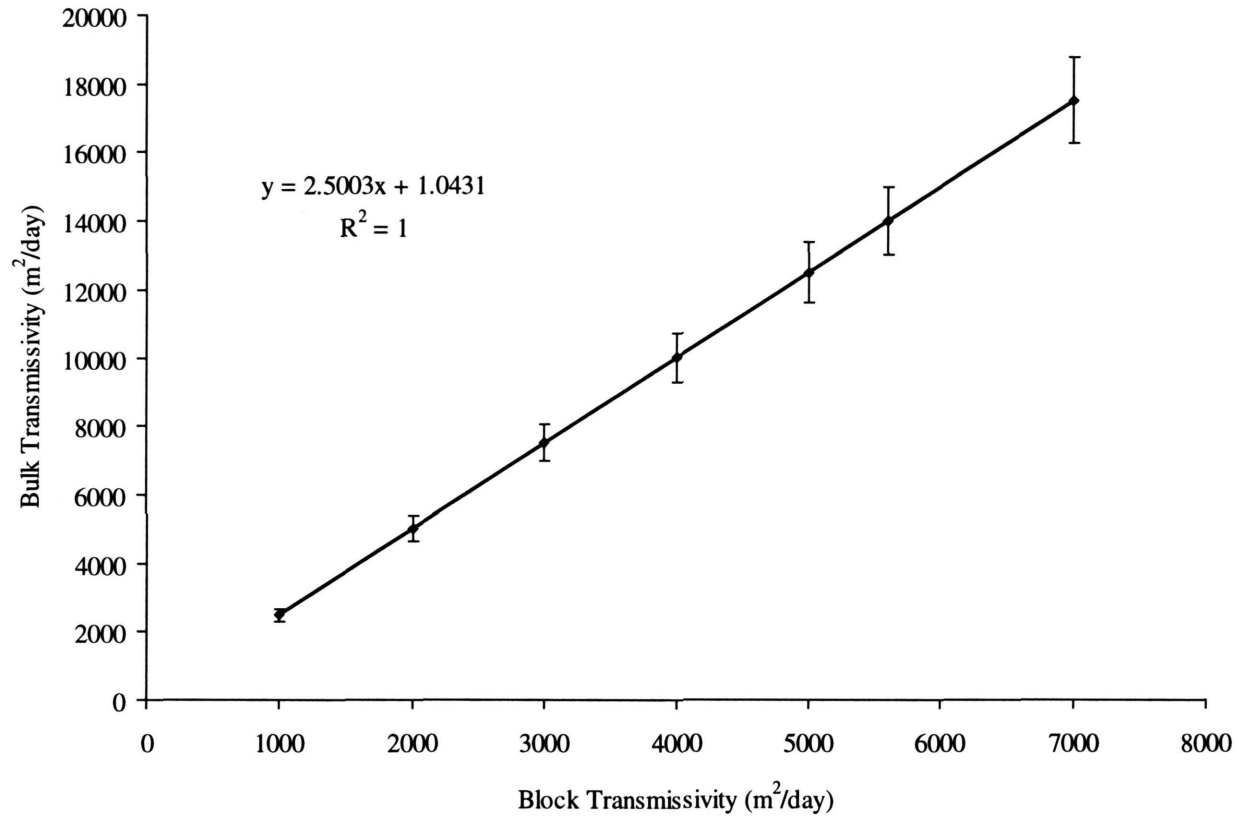


Figure 29. Path of particle simulated with the equivalent porous media model.



**Figure 30. Relationship between bulk transmissivity and block transmissivity. The relationship is based on fracture zones that are 100 times more transmissive than blocks. Values for orientation and length of each fracture zone are selected randomly using the data from Williams (1985). Fracture density is specified with a single, deterministic value of 2 km/km<sup>2</sup>.**

For these first simulations, the general flow pattern was from east to west. If the model orientation is rotated, however, calculated values for bulk transmissivity may in fact be different even though the value for block transmissivity is the same. It is possible that if flow were forced in a direction in which fractures have a highly probable orientation, the bulk transmissivity will be higher than suggested by Figure 30. To investigate the potential for this error, MC analysis was run 18 times with different rotation angles. The block transmissivity was held constant at 5700 m<sup>2</sup>/day. All other parameters were the same as the previous analysis. Results from the 18 MC analyses are presented as a polar plot of bulk transmissivity (Figure 31). Median values for transmissivity are not significantly affected by rotation of the model domain. Azimuths of 310 and 50 degrees exhibit slightly increased values for transmissivity. This increase, however, is less than 10 percent when compared with the average value for the median transmissivity. Results from this analysis suggest that the relationship between bulk transmissivity and block transmissivity does not need to be adjusted for flow direction.

#### ***Monte-Carlo Analysis with North Lakes Model***

In the previous simulations, a simple box model was used to derive the relationship that allows the conversion from an EPM model into a stochastic DFM. In the next analysis, the results from the box model are used to develop a stochastic DFM model for the North Lakes study area. This new model is used to quantify the probability of various travel times from the North Lakes wetland to the Section 21 wellfield.

The EPM model for North Lakes was converted to a DFM using the derived relationship between bulk and block transmissivity (Figure 30). To maintain the appropriate values for bulk transmissivity and incorporate highly permeable fractures, the values of bulk transmissivity from the original model are adjusted according to the equation in Figure 30. Using bulk transmissivity values of 5570 and 1860 m<sup>2</sup>/day (from the EPM model), values of block transmissivity (for the DFM) are 2200 and 740 m<sup>2</sup>/day, respectively.

FRACMOD was used to run 1000 simulations with the North Lakes DFM. The fracture statistics described for the box model were also used for the North Lakes DFM. The results from one realization, which include both flow and particle-tracking simulations, are presented in Figure 32. This figure clearly

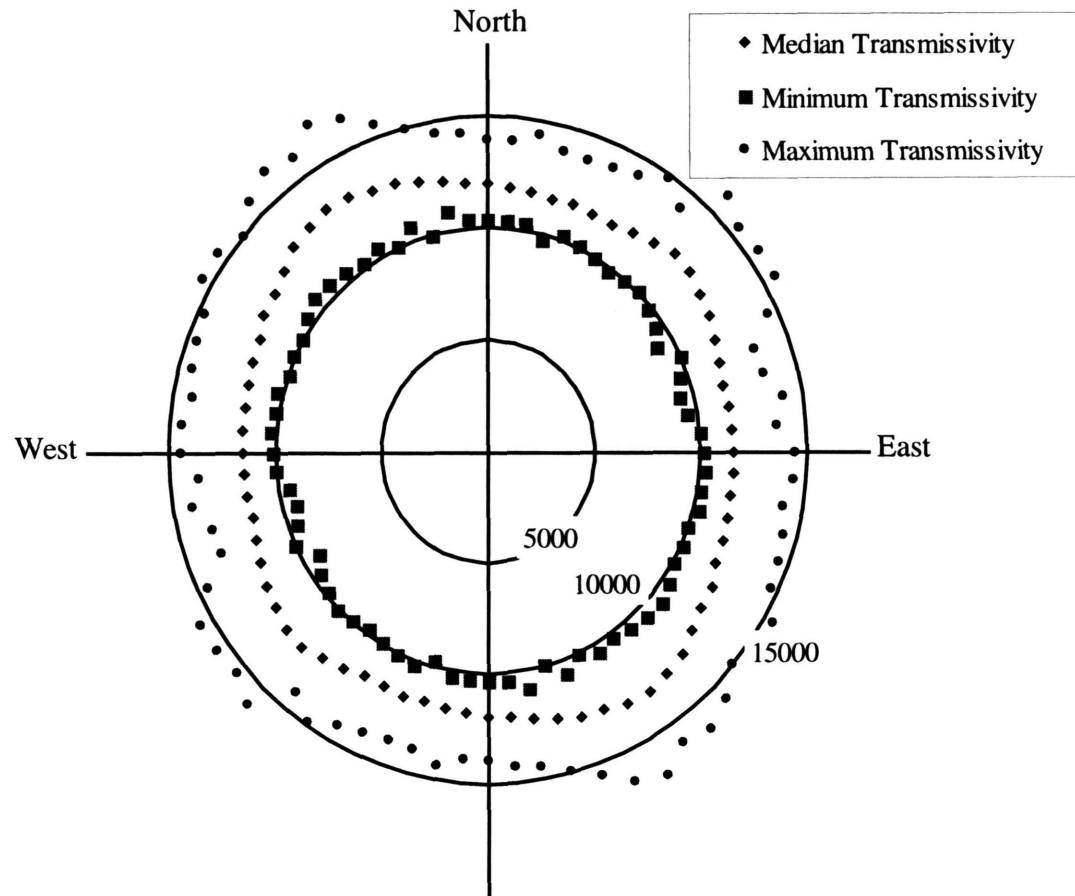


**Figure 31. Transmissivity “ellipse” calculated from Monte-Carlo analysis with rotated model domain. Model is rotated in 5 degree increments.**

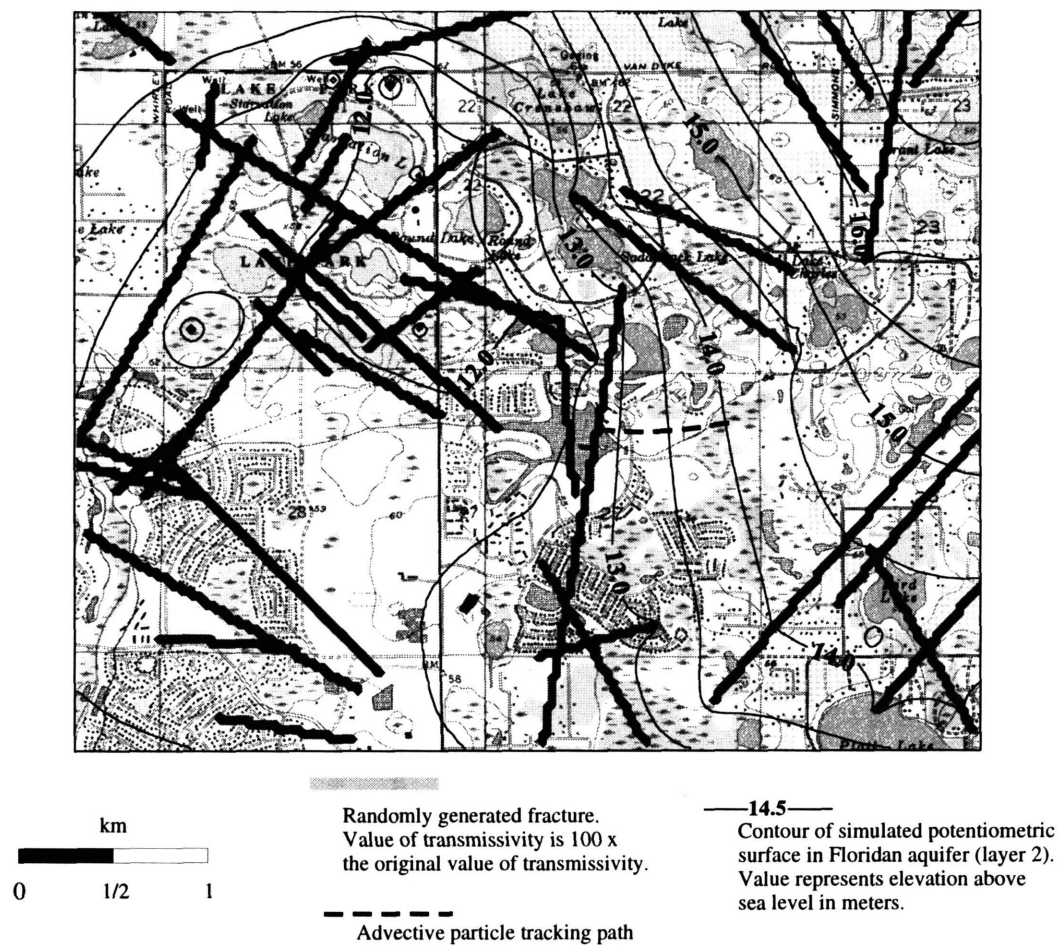


**Figure 32. Results from one simulation with randomly generated fractures.**

illustrates the significant effect that fractures have on a groundwater travel path. The particle tends to remain in the highly permeable fracture until it is forced into a lower-permeability block.

Most flow paths lead from the wetland to the Section 21 wellfield (Figure 33). The particle paths in Figure 33 represent the results from the first 100 simulations. This figure illustrates the variability of the simulated travel paths. The variability results from the uncertainty in fracture length and orientation. The effect of this variability on groundwater travel times is illustrated as a plot of cumulative probability versus travel time (Figure 34). Of the 1000 simulations, 820 result in the capture of the particle by a Section 21 supply well. The probability that the travel path is from the North Lakes wetland to the Section 21 wellfield, therefore, is 82 percent. This graph is used to estimate the probability associated with different travel times. For example, there is less than a 10 percent chance that the advective travel time from North Lakes to the Section 21 wellfield is less than two years (Figure 34).

## **Discussion**

### ***Benefits and Limitations***

There are several benefits to the approach presented in this paper. The greatest benefit applies to stochastic methods in general. Freeze (1975) was the first to apply stochastic methods to groundwater problems. Since then, the use of stochastic methods has grown rapidly (Dagan, 1986) because researchers realize how important it is to quantify the uncertainty in model results. In addition, deterministic approaches cannot be used successfully for fracture simulations because the properties of each fracture are unknown. Discussions of the benefits that can be achieved with stochastic analysis are presented by Freeze et. al (1990), Gelhar (1993), Neuman (1982), and Peck et. al (1988).

The EPM approach may work well at regional scales for groundwater flow problems, but cannot simulate advective and dispersive transport, especially at local and site scales. To the practicing hydrogeologists, there are few options for simulating fracture flow. Most models that are designed to simulate fracture flow are mathematically complex and restricted to research purposes. Also, many of the existing fracture models assume impermeable blocks (Chiles and de Marsily, 1993).

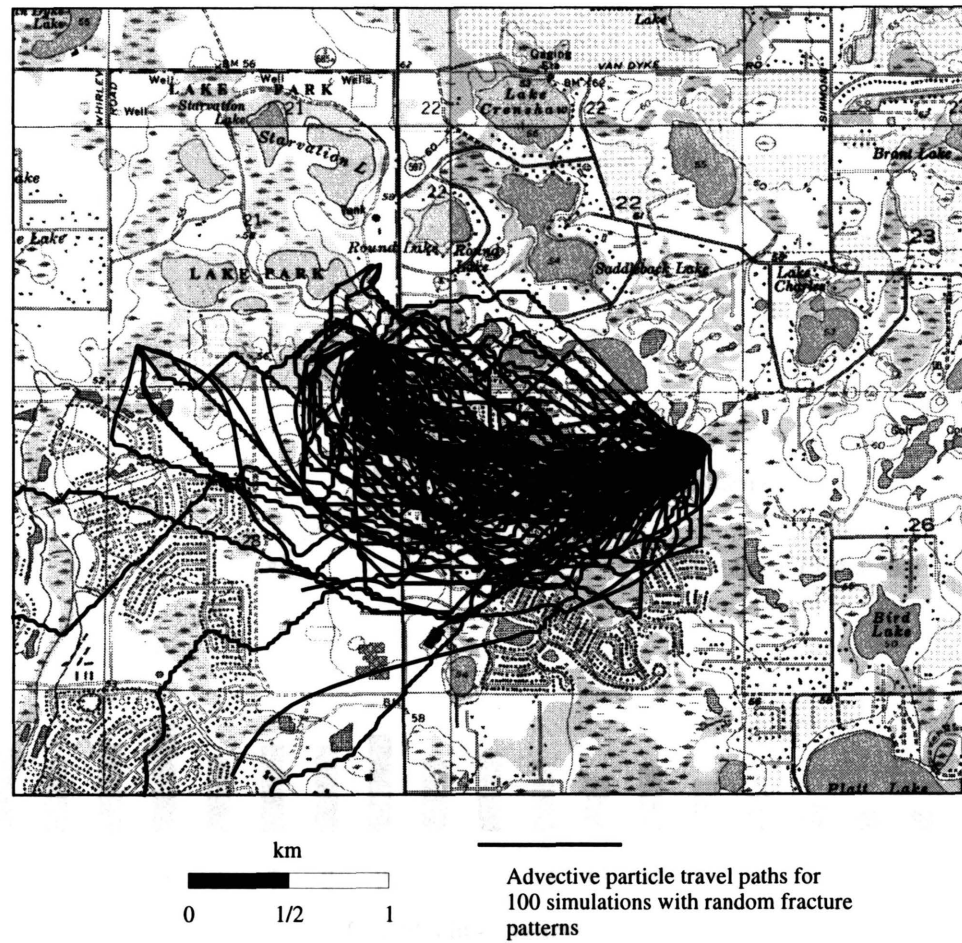


Figure 33. Travel paths for the first 100 Monte-Carlo simulations.

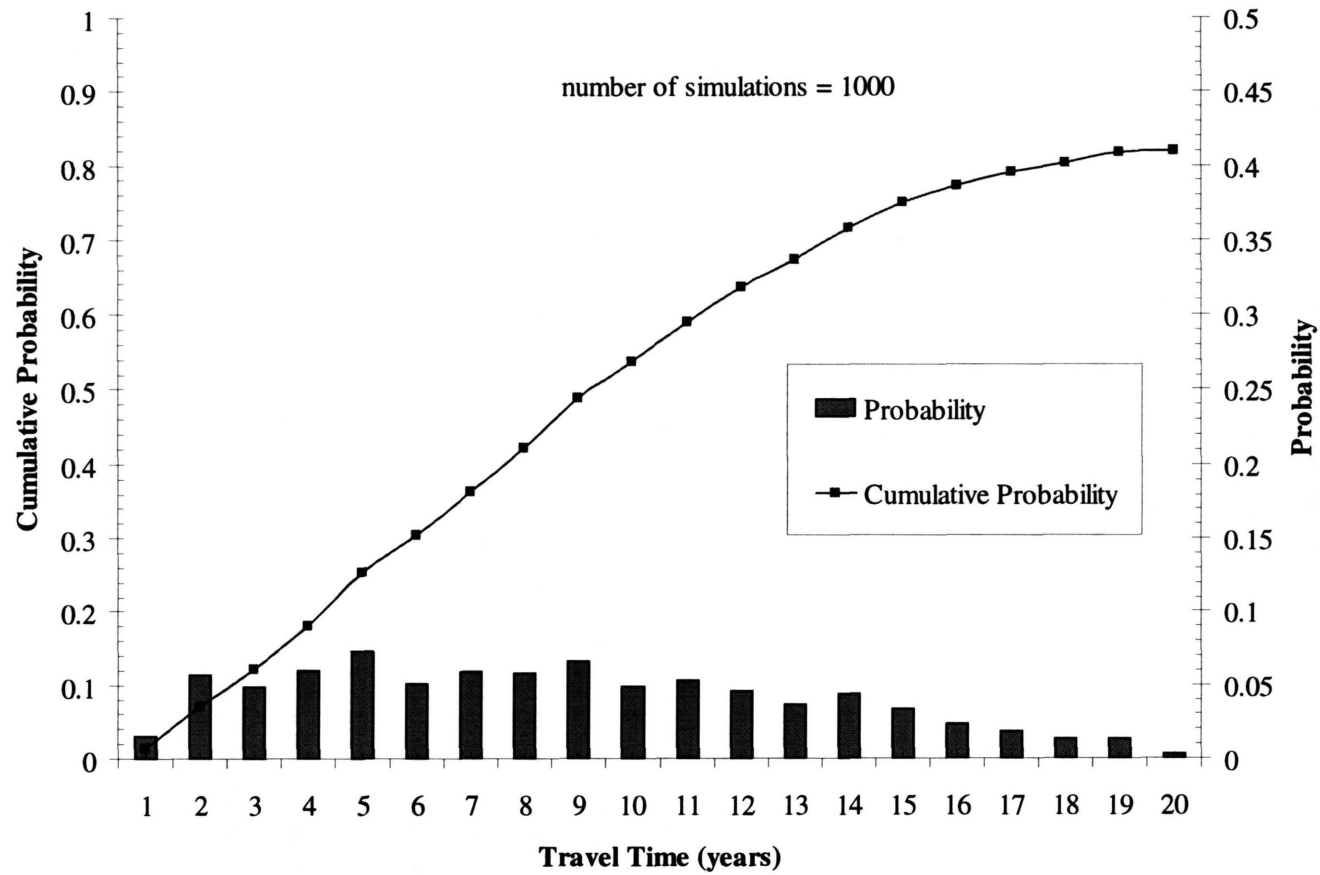


Figure 34. Plot of cumulative probability versus advective travel time.



The intuitive approach developed in this paper links fundamental statistics with traditional finite-difference modeling. The result is a method that is conceptually straightforward and easy to implement. The method works with existing models of groundwater flow and particle tracking, such as MODFLOW and PATH3D, so that the results from the simulations are precise. Another advantage to using traditional codes is that pre- and post-processors are available to help with model design and calibration.

The main limitation to this method is that model cells must be of the same width as the fracture zones. This means the method is best suited for wide fractures and relatively small model domains. The method will not work well for narrow fractures in large model domains because the number of cells required to characterize the system is limited by computer speed and memory.

### ***North Lakes Application***

The application of the stochastic fracture model to the North Lakes study illustrates the utility of this method. From the EPM flow and particle-tracking model, it appears that the advective travel time from the North Lakes wetland to the wellfield is 9 years. The problem with the deterministic EPM model, however, is that there is no way to quantitatively estimate the confidence of the predicted travel time. This limitation poses a severe problem for the prediction because there are potential health risks associated with advective travel times of less than two years. It is misleading for scientists to present 9 years as the predicted travel time, knowing that fractures may act as highly permeable pathways for groundwater flow. It must be concluded that the estimate of 9 years contains a large degree of uncertainty; however, there is no way to quantify the uncertainty within a deterministic model. Sensitivity analysis can be performed with the numerical model, but sensitivity analyses are usually conducted by changing global values of one or more model parameters.

Results from the stochastic model provide a much better representation of the prediction of advective travel time. Results indicate that there is a 50 percent chance that the travel time will be less than 9 years. The results also indicate that there is a 10 percent chance that the travel time will be less than 2 years. This is new information, beyond the reach of the original EPM model.

The North Lakes simulations are an example of how to apply the method developed in this chapter. The results are not reliable because assumptions about the fracture zone properties were made to simplify the problem. The assumptions are

1. the width of each fracture zone is equal to the width of the finite-difference cell;
2. orientation and length properties from the Williams study are representative of the North Lakes area;
3. fracture zone transmissivity is 100 times the block transmissivity;
4. only half of the photolineaments mapped by Williams contain hydraulic significance.

Although these assumptions are limiting, their effects could be examined with additional MC simulations. The utility of stochastic analysis lies in the ability to bracket all reasonable possibilities and run the model with each possibility. For example, it is very difficult to determine the transmissivity of a fracture zone. If one reasonably infers, for example, that the transmissivity value for a fracture zone lies between 100 and 100,000 m<sup>2</sup>/day, then MC analysis could be performed to improve the estimate of uncertainty in groundwater travel times. In this case, the uncertainty in travel time would significantly increase, but the uncertainty would be quantified and based a reasonable bracket of fracture zone transmissivity. The effects of the other limiting assumptions could be evaluated in a similar manner.

#### ***Importance of Adjusting for Bulk Transmissivity***

Adjusting the values of block transmissivity is a very important step for the procedure outlined in this chapter. To illustrate the importance, MC analysis was rerun with the block transmissivity values equal to the transmissivity values from the original EPM model. Fracture transmissivity was calculated with the same multiplier value of 100. Results from the first 100 simulations are presented in Figure 35. Note that the capture zone of the wellfield is much narrower because the value of bulk transmissivity is higher. The result is that most travel paths do not lead from the wetland to the wellfield (Figure 35). The pdf of travel time for this MC analysis illustrates the magnitude of this potential misapplication (Figure 36). The

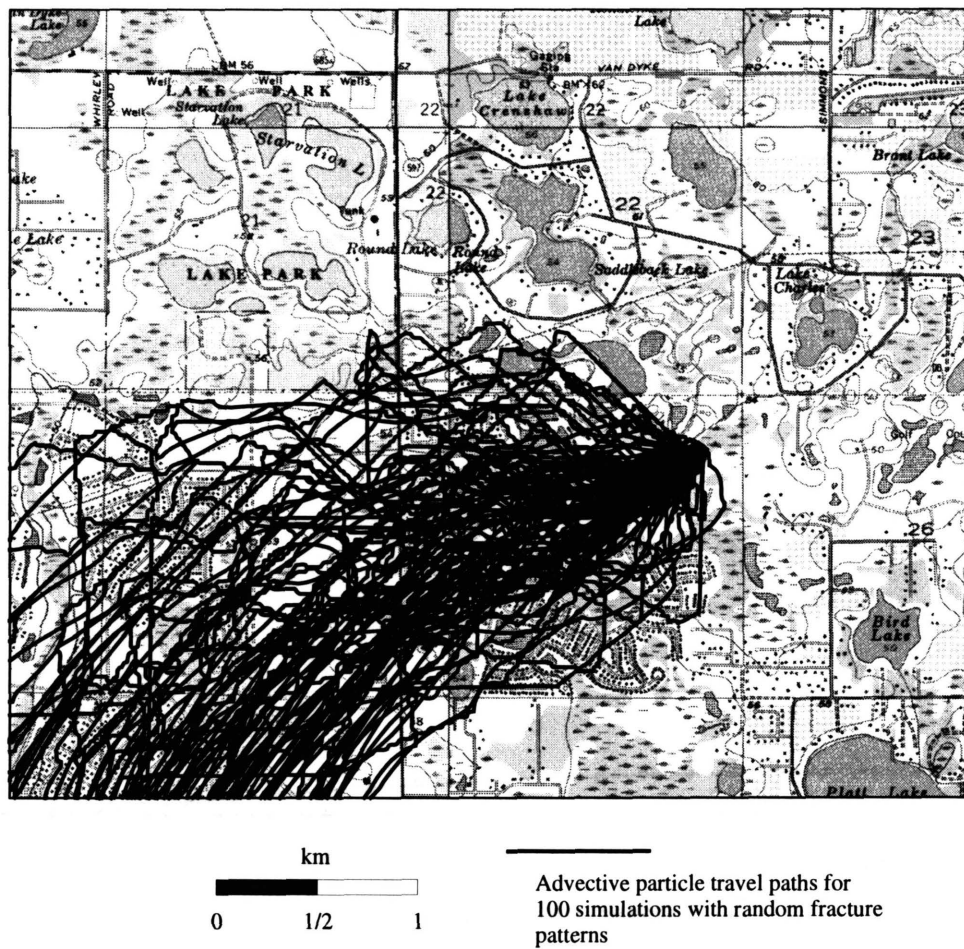


**Figure 35. Results from the first 100 Monte-Carlo simulations where the block transmissivity has not been adjusted to reproduce the appropriate value for bulk transmissivity.**

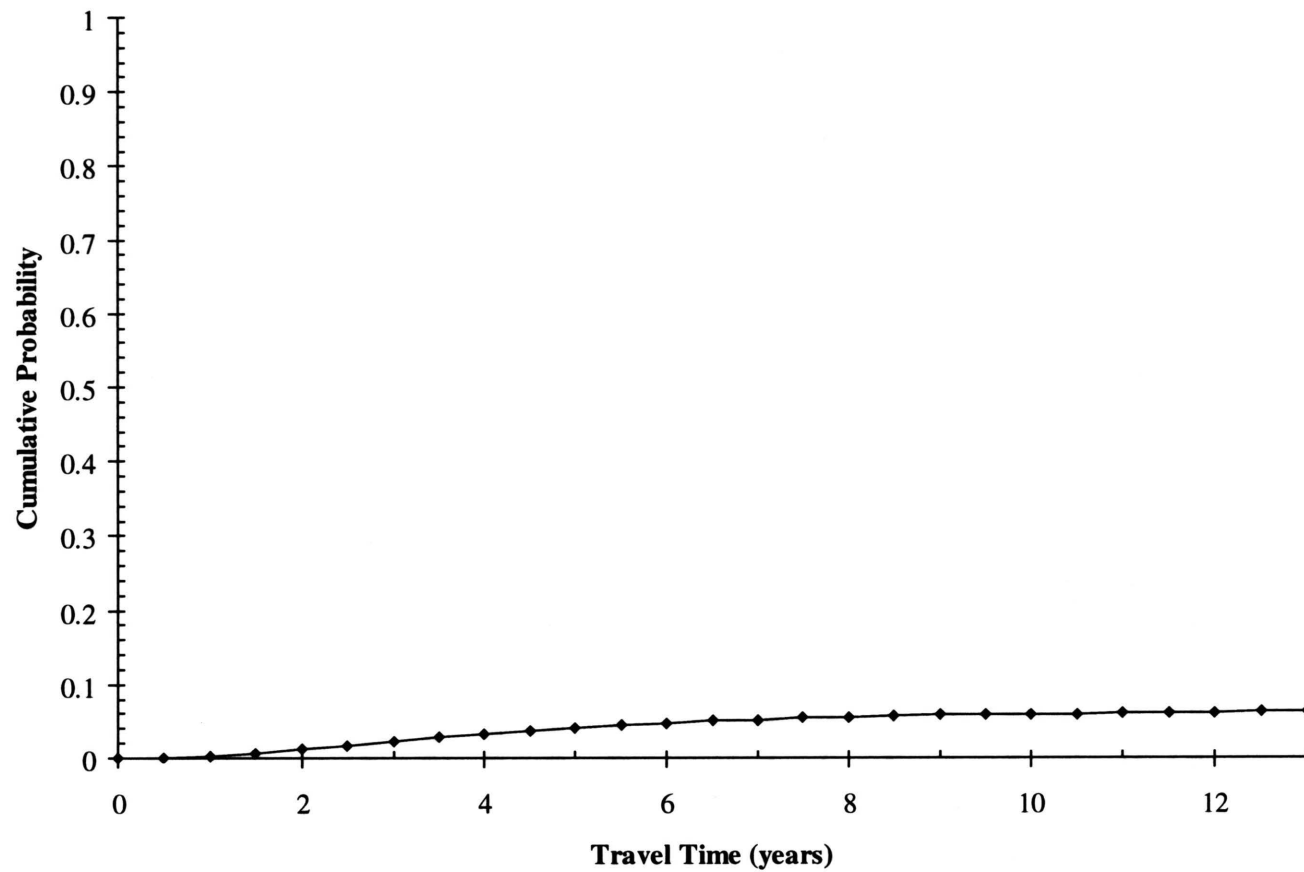


**Figure 36. Cumulative pdf for the case where block transmissivity has not been adjusted to reproduce the appropriate value for bulk transmissivity.**

probability that an advective travel path will lead from the wetland to the wellfield is reduced to less than 10 percent. Clearly, bulk transmissivity in the DFM must be the same as the bulk transmissivity in the original EPM model or severe errors will result.

### ***Future Applications***

Linking a contaminant transport model to the flow model is a reasonable extension of this method.

Because the numerical models are separate from the code that runs the MC analysis, incorporation of a transport model is seamless. The problem with running a transport model is the additional processing time required by the computer. For example, the transport model, MT3D, was applied to the North Lakes EPM model. Processing time for the transport model is approximately two to three times longer than processing time for the groundwater flow model. It takes approximately 12 hours to complete 1000 simulations with the North Lakes DFM. If the transport model were included in the MC analysis, 1000 simulations would take 1 to 2 days. However, as computer processing speeds increase, the inclusion of a transport model with the MC analysis will not be difficult.

To apply the stochastic fracture model to three-dimensional applications, several of the routines will have to be modified. In two dimensions, the spatial location of a fracture is described by a line. This line can also be thought of as a random strike direction with a specified dip angle of 90 degrees. In three dimensions, a plane is used to represent fractures zones. This means that the dip angle would be allowed to change. For three-dimensional applications, the current algorithm would be adjusted to select cells that are intersected by the plane. As for the two-dimensional case, it would be required that fracture cells be connected at cell faces rather than along diagonals.

There are several different models for representing fractures in three dimensions (Chiles and de Marsily, 1993). The most common models are circular disks and rectangles. Algorithms for selecting cells in a three-dimensional grid could be developed for either of these fracture models. In general, applying the method to three dimensions should be relatively straightforward. The main limitation to using this approach in three dimensions is that the computer processing speed would severely restrict the size of the

model domain. The power of MC analysis relies on the ability to run the model many times. Very large model grids would prohibit efficient application of this methodology.

Another logical use for the model would be to run a parameter estimation program during each run in the MC analysis. A parameter estimation routine could be used to adjust the transmissivity values for the blocks and fractures, for example, so that simulated heads match observed values of head. At the end of the MC analysis, the user could select the fracture realizations that best reproduce observed conditions. Again, the limitation with this approach is processing speeds. It is conceivable, however, that by restricting the adjustable parameters to fracture and block transmissivity, the parameter estimation code would not require many flow simulations.

## **Summary**

In this chapter, a stochastic method is developed for simulating the effects that large-scale vertical fracture zones have on groundwater flow and advective transport. Groundwater flow and particle tracking are simulated with MODFLOW and PATH3D, respectively, though the approach could be used with many of the existing codes. Fracture zones are discretely incorporated in the flow and particle-tracking models by including linear patterns of high transmissivity (or hydraulic conductivity for unconfined aquifers). This approach requires that fracture zones are similar in width to the dimensions of a model cell. The stochastic component of this method allows for uncertainty in one or more of the properties of the fracture zones. Monte Carlo analysis is used to quantify the uncertainty in model results by running numerous simulations with statistically reasonable fracture properties.

To illustrate the procedure and benefits for using this approach, the method is applied to a problem of fracture flow in west-central Florida. Though simplifying assumptions limit the direct interpretation of the model results, the example problem illustrates the advantages to using this approach. For example, groundwater travel times are presented as functions of probability rather than single, deterministic values.

## **CHAPTER 4. THE PROBABILITY OF RESTORING WATER LEVELS IN A DAMAGED WETLAND**

### **Introduction**

Stochastic analysis is rapidly becoming a widespread and accepted technique for estimating the errors associated with predictions that are based on numerical or analytical models. Historically, the development of a mathematical model has focused on deterministic approaches for predicting response of a system to various conditions, stresses, or perturbations. With the deterministic approach, factors used as input to a model do not contain uncertainty, and thus their values are assumed known. As a result, there is only one solution to a mathematical model based on deterministic factors. The power of stochastic analysis lies in the ability to incorporate uncertainty, or statistical variability, in the factors used as input to a mathematical model. Consequently, the solution to a stochastic model includes an estimate of the predictive uncertainty resulting from uncertainty in the input factors.

For groundwater problems, the application of stochastic analysis began in the 1970's with the work of Freeze (1975). Since then, the number of studies applying the concepts of stochastic analysis has increased rapidly (Dagan, 1986). While the power of stochastic methods is acknowledged by many groundwater hydrologists, routine application of stochastic methods to hydrological problems has been limited. The purpose of this paper is to illustrate the power of stochastic analysis and show how easily the concepts can be applied to the problem of wetland restoration.

Northwest Hillsborough County, Florida, is the site of significant withdrawals of groundwater from the Floridan aquifer. Four major municipal wellfields (South Pasco, Section 21, Cosme-Odessa, and NW Hillsborough) withdrew an average of  $1.39 \times 10^5 \text{ m}^3/\text{day}$  for calendar year 1993 (SWFWMD, 1996). As a result, the surficial aquifer has experienced water-level declines as great as 3 to 4 m, affecting local lakes and wetlands.

Current initiatives by the Southwest Florida Water Management District (SWFWMD) focus on developing sustainable water use practices. One practice, which has received much attention, involves replenishing aquifer supplies with highly treated wastewater, or reclaimed water. This concept is appealing because it “closes the water loop”. Water withdrawn from the system is used and then returned, promoting a sustainable practice. Currently, much of the reclaimed water is discharged to streams and coastal waters. SWFWMD is exploring ways to return the reclaimed water to areas where it was originally withdrawn. The concept of using reclaimed water to rehydrate damaged wetlands is appealing because the practice has the potential to restore the environment as well as close the water loop.

This paper will show how stochastic analysis can be used to estimate the probability of restoring a damaged wetland. The mathematical model used to simulate water levels in a wetland is based on the water balance equation, but the stochastic methods could also be used with a numerical model of surface or groundwater flow. To illustrate the procedure, the method is applied to a wetland in west-central Florida. Input variables, such as rainfall, are treated stochastically to quantify the uncertainty in predicted time series of water levels.

### **Description of Study Site**

The North Lakes wetland, located approximately 1 km from the Section 21 wellfield in Northwest Hillsborough County (Figure 37), has been selected as a potential site for rehydration with reclaimed water. During the past few decades, water levels within the wetland have declined to levels that cannot support wetland vegetation. Consequently, cypress trees are dying and much of the wetland is being invaded by upland vegetation. To help with the decision on whether to proceed with rehydration at North Lakes, the University of South Florida was contracted by SWFWMD and Hillsborough County to conduct a feasibility study. The objectives of the feasibility study were to 1) determine the amount of reclaimed water that will be required to restore optimal water levels, and 2) assess the potential risks of using reclaimed water by predicting flow patterns and estimating travel times. The objective of this paper is to address objective (1) of the feasibility study by applying the methods of stochastic analysis to estimate the probability of successfully restoring beneficial water levels.



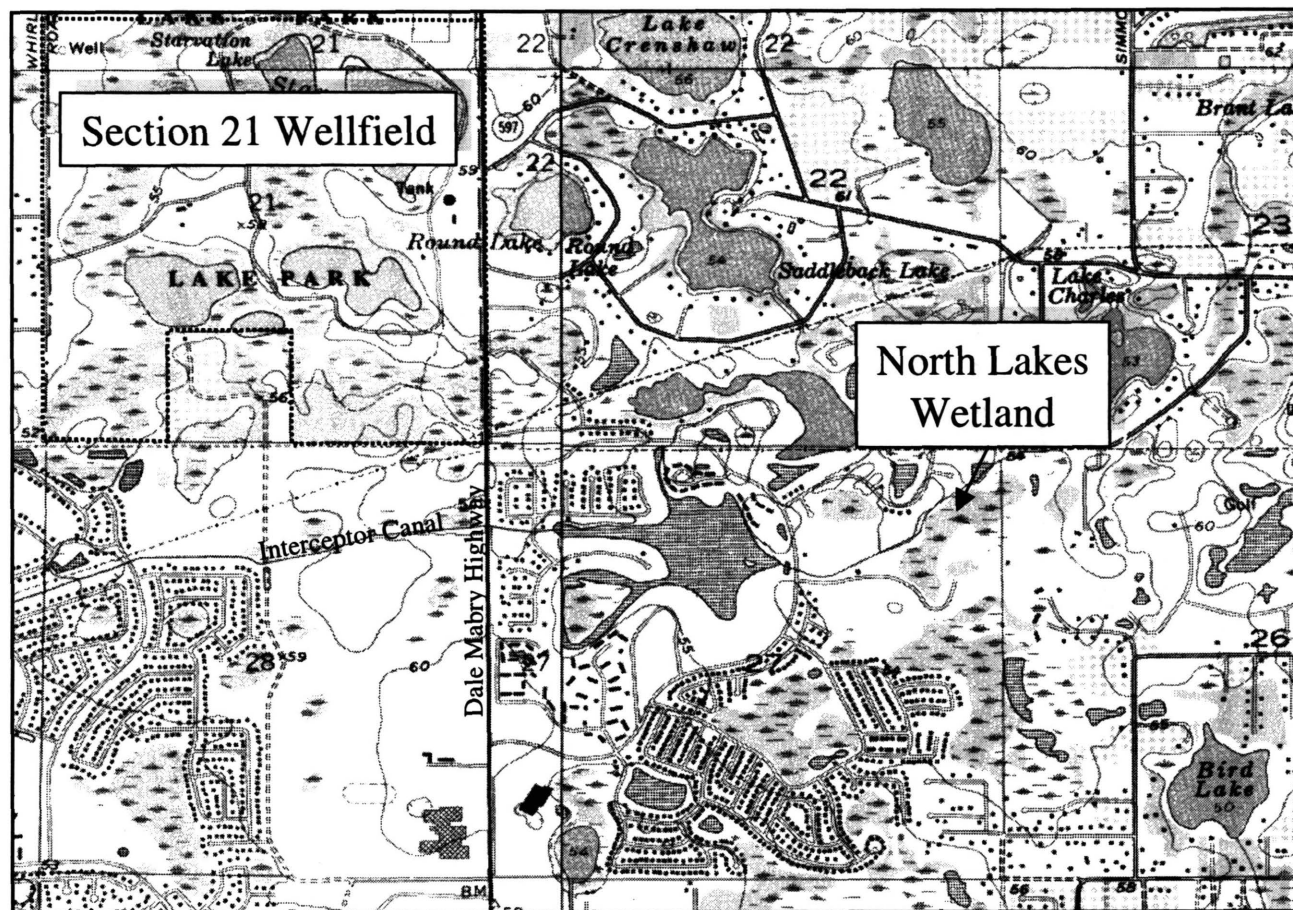
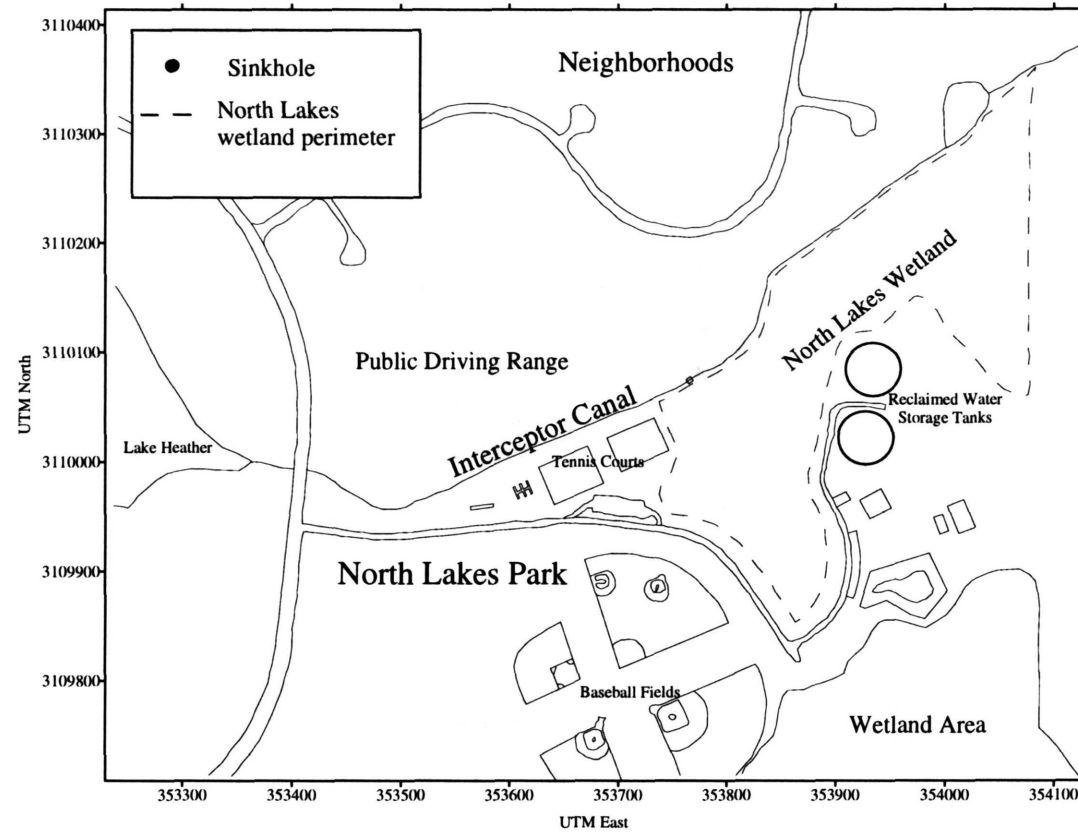


Figure 37. Location of the North Lakes wetland and Section 21 wellfield.

The North Lakes wetland covers 65,000 m<sup>2</sup> (16 acres) and is located within North Lakes County Park (Figure 38). Surface-water drainage in the vicinity of the park has been altered through the construction of the Interceptor Canal, weir, North Pond, and the berm (Figure 38). The Interceptor Canal was constructed in 1960 to keep local areas from flooding. The canal continues westward to Lake Heather and eventually connects with Brushy Creek on the west side of Dale Mabry Highway (Figure 37). The presence of the Interceptor Canal may be partly responsible for lowered water levels in the area by providing a discharge zone for shallow groundwater. In an effort to rehydrate the North Lakes wetland, a weir was constructed in the Interceptor Canal, just north of the tennis courts. The elevation of the weir crest is 15.64 m above sea level, 0.12 m higher than the average elevation in the wetland (15.54 m). The purpose for constructing the weir was to dam surface water flowing west within the canal and flood the wetland (Florida Land Design and Engineering, 1987). A one-meter high berm was constructed around the wetland to prevent the park from flooding. The plan to rehydrate the wetland failed, however, due to low surface water flows from the east.

The geology of west-central Florida is characterized by unconsolidated deposits overlying a thick sequence of carbonate units (Miller, 1986). Throughout much of west-central Florida, the base of the unconsolidated deposits is marked by the presence of clay, up to several meters thick. The boundaries of the hydrogeologic units correlate well with the boundaries of the geologic units. The surficial aquifer corresponds with the unconsolidated sediments, and the Floridan aquifer corresponds with the thick sequence of carbonate units. Where present, the clays at the base of the unconsolidated deposits act as a semi-confining unit that retards vertical flow between the surficial aquifer and the Floridan aquifer.

To determine the site-specific geologic and hydrogeologic properties at the North Lakes wetland, a large volume of field data was collected at the site. Details of the field study and data interpretation are presented in Langevin et. al (1998). Nine wells are installed in the Floridan aquifer, and 30 wells are installed in the surficial aquifer. At five locations, nested wells are installed to evaluate the hydraulic gradient that controls vertical groundwater flow. The locations of these five sites are presented in Figure 39. At the five nested sites, split-spoon samples were collected continuously from land surface to the top of the limestone surface. In general, the geology at the site corresponds well with the geology of west-central



**Figure 38. North Lakes Park and surrounding area.**

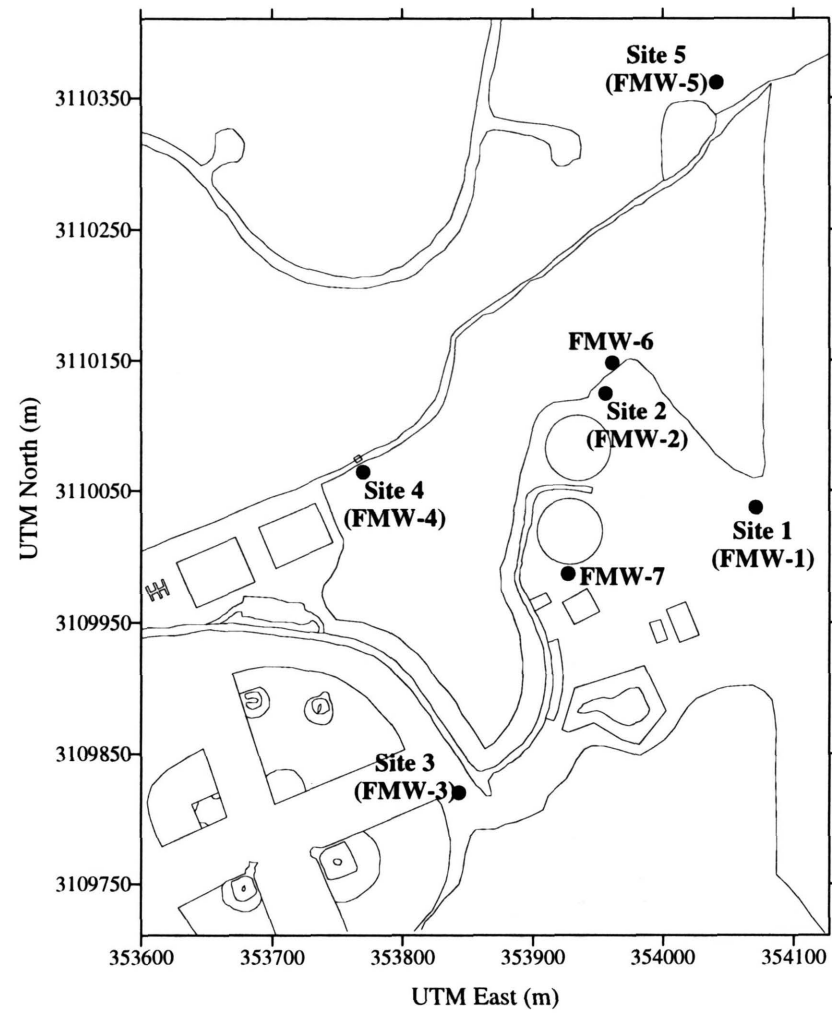


**Figure 39. Locations of the five sites with nested wells. The site number also refers to the number of the monitoring well located in the Floridan aquifer.**

Florida with one exception. The clay unit normally found at the base of the unconsolidated deposits is not present beneath much of the wetland.

Detailed sediment analyses, performed on the split-spoon samples, indicate that the unconsolidated deposits can be separated into three distinct layers (Figure 40). The upper layer (S1), consists of a fine-grained sand and has an average thickness of about 3.0 m. The average porosity of S1, determined from the results of the grain-size analysis (Vukovic et. al, 1992), is 0.45. Beneath S1 is a fine-grained sand unit with approximately 20 percent silt and clay. The average thickness of S2 is 2.3 m. The average porosity of S2 is 0.25. The bottom layer, S3, consists of clean, fine-grained sand with little silt and clay. The average thickness of S3 is 3.1 m, and its average porosity is 0.42.

An aquifer performance test was performed at the North Lakes wetland to better determine the leakance, storage, and transmissive properties of the aquifers. Groundwater from the Floridan aquifer was withdrawn from FMW-2 (Figure 39) at a nearly constant rate of 5000 m<sup>3</sup>/day (1000 gallons per day) for 3 days. Recorded drawdowns in monitoring wells open to the Floridan aquifer were analyzed with the Hantush-Jacob analytical solution. Estimated values of leakance range from 0.0008 to 0.04 day<sup>-1</sup> (Table 7). The arithmetic average of the six estimated leakance values is 0.009 day<sup>-1</sup>. Values of storativity and transmissivity, also estimated from the drawdown curves, are presented in Langevin et. al (1998).

Water levels in the 39 monitoring wells were recorded each week with a water-level indicator for the calendar year, 1997. At the five nested well locations, the time series of head differences illustrates the change in the vertical hydraulic gradient during the course of a year (Figure 41). Under typical conditions, head differences are highest during the summer months when rainfall is the highest. During 1997, however, water levels were strongly influenced by El Niño weather patterns. The large head differences towards the end of 1997 are attributed to the above-normal rainfall values from El Niño.

West-central Florida receives, on average, approximately 140 cm of rainfall per year. This average was calculated for rainfall data from the weather monitoring station at St. Leo, Florida, where rainfall totals range from 90 to 210 cm per year (Figure 42). Under normal conditions, most of the precipitation occurs during the summer months of June, July, August, and September, when convective weather patterns

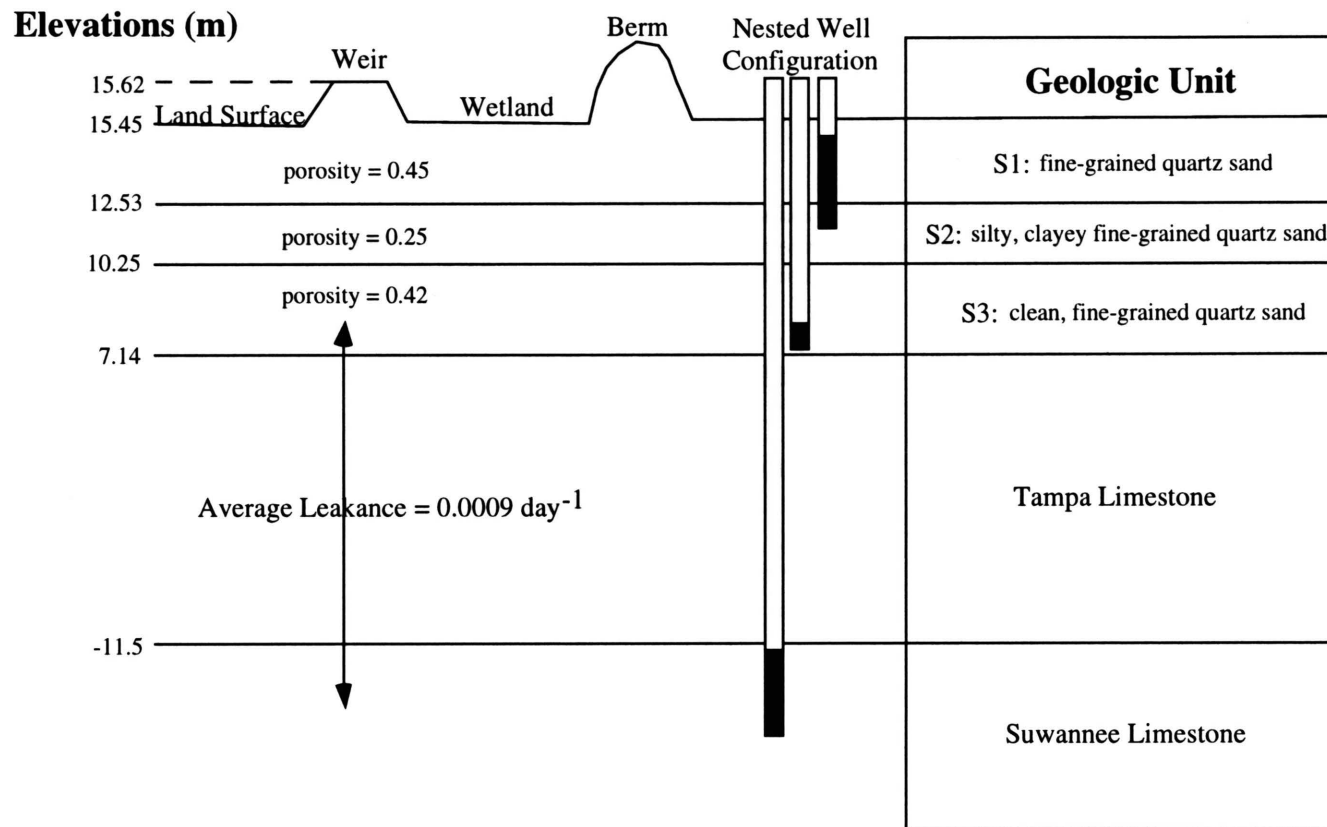


**Figure 40. Geologic section of the North Lakes wetland.**

**Table 7. Leakance values estimated from the North Lakes aquifer performance test (from Langevin et al., 1998). The Hantush-Jacob method was used to match drawdown curves and estimate values of leakance for the six monitoring wells.**

<b>Well</b>	<b>Leakance (<math>\text{day}^{-1}</math>)</b>
FMW-1	0.004
FMW-2	
FMW-3	0.0008
FMW-4	0.003
FMW-5	0.009
FMW-6	0.04
FMW-7	0.001

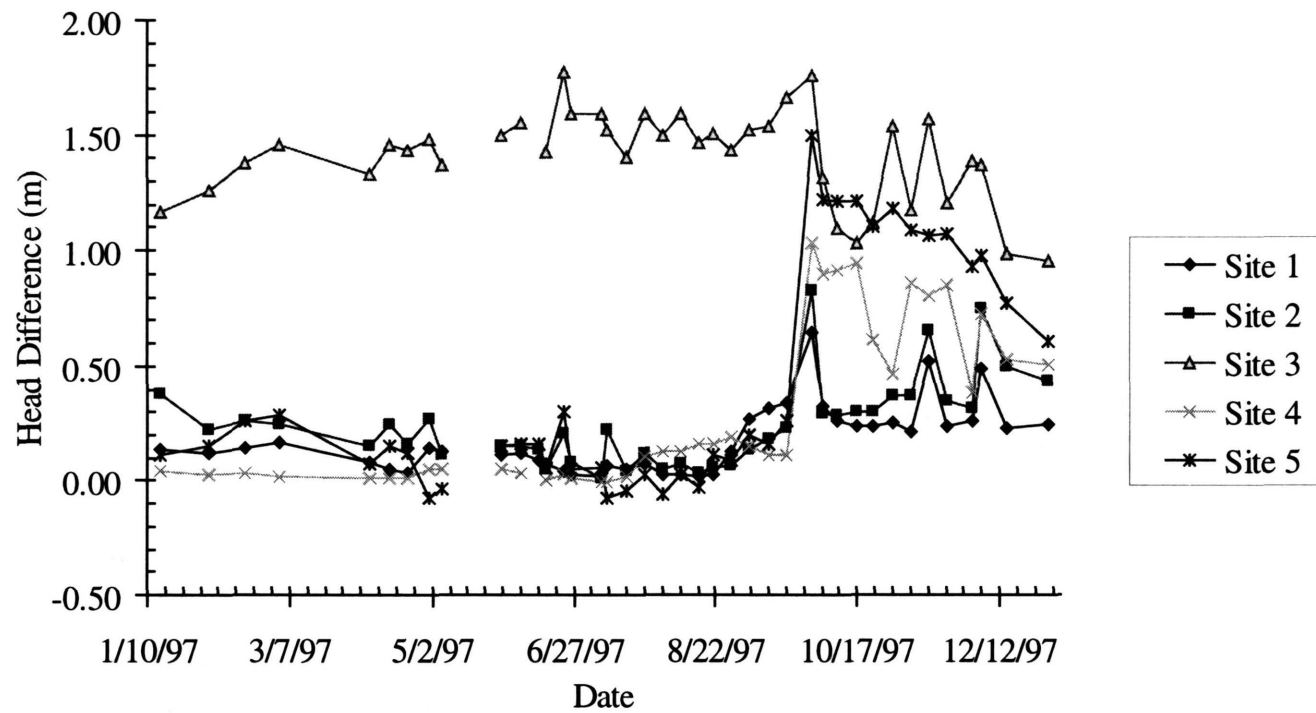


**Figure 41. Differences in head between the surficial and Floridan aquifers. Head differences are calculated for the five well nests at the North Lakes wetland.**



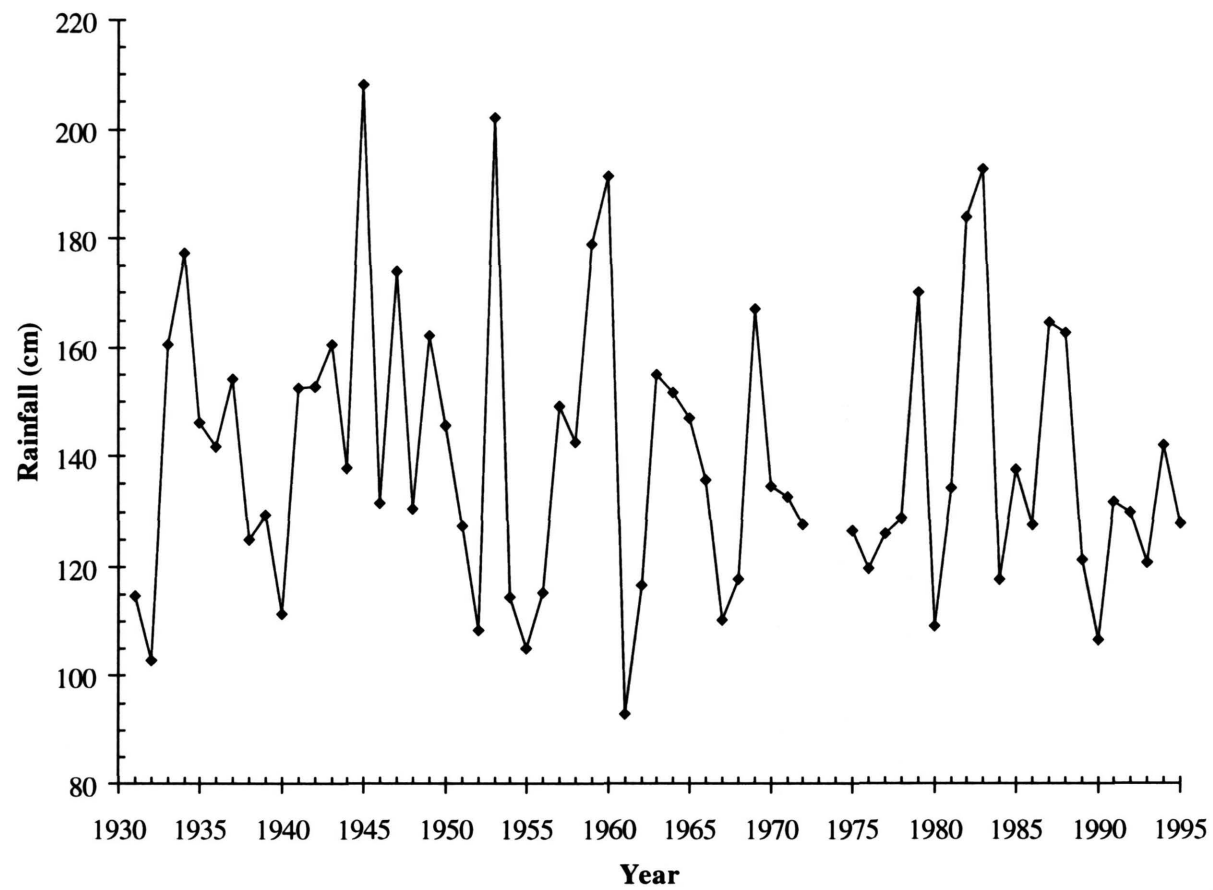


**Figure 42. Annual rainfall totals measured at the St. Leo monitoring station.**

dominate. During the rest of the year, most of the precipitation results from frontal systems, which produce less precipitation than convective weather systems.

## **Background Theory**

### ***Random Variables***

Input to a mathematical model is referred to as a factor. The terms for three quantifiable factors are variables, parameters, and constants (Edwards and Hamson, 1990). The value of a constant does not change, regardless of the problem, location, or time frame. Parameters may change for different problems, but remain fixed for a specific problem. As the name suggests, variables are allowed to change. For example, hydraulic conductivity is a parameter when used in a groundwater flow model. If the flow model is linked to a geochemical model and values of hydraulic conductivity change in response to dissolution or precipitation, the hydraulic conductivity field acts as a variable.

Variables and parameters may be either random or deterministic. A deterministic variable or parameter has a constant, set value that includes no uncertainty. The value for a random variable or parameter, however, is not explicitly known. Instead, the probability that the variable will assume some value,  $x$ , is described by a probability density function (PDF), mathematically referred to as  $f(x)$ . The integrated form of the PDF,  $F(x)$ , is written as:

$$F(x) = \int_{-\infty}^x f(u) du$$

$F(x)$  is also called the cumulative PDF or CPDF. The CPDF is important for generating random values of a random variable from the PDF. To generate random values for  $x$  from a known PDF, a random number between 0 and 1 (RND) is drawn. A random value of  $x$ , conforming to the PDF, is found by setting  $\text{RND} = F(x)$  and solving for  $x$ .

The PDF's used in this study are the normal distribution, the lognormal distribution, and the Weibull function. The most widely used PDF is the normal distribution, which is characterized by its bell-shaped curve (Figure 43a). The mathematical formulation for the normal distribution is written as:

$$f(x) = \frac{1}{\sigma\sqrt{2\pi}} \exp\left[-\left(\frac{x-\mu}{\sigma}\right)^2\right]$$

where  $x$  is the random variable of interest,  $f(x)$  is the probability of occurrence of  $x$ ;  $\sigma$  is the standard deviation of the distribution and  $\mu$  is its mean. The CPDF for the normal distribution is presented in Figure 43b. The value of the CPDF,  $F(x)$ , refers to the area under the curve of the PDF up to the value of  $x$ . Unfortunately, there is no analytical solution for the CPDF of the normal distribution.

Another distribution, which is very commonly used in groundwater studies, is the lognormal distribution (Gelhar, 1993). Lognormal distributions result when processes generating the random variable are multiplicative (Yevjevich, 1976). The mathematical equation for the lognormal distribution is:

$$f(x) = \frac{1}{x\sigma\sqrt{2\pi}} \exp\left[-\frac{(\ln x - \mu)^2}{2\sigma^2}\right]$$

With the lognormal distribution, values for  $\ln(x)$ , rather than the values of  $x$  themselves, are normally distributed. As with the normal distribution, there is not an analytical solution for the CPDF of the lognormal distribution.

The Weibull function has been used as a PDF to match rainfall statistics (Perry 1995). The function is defined so that by definition, there is zero probability that the random variable will be negative. This is an important requirement for many natural processes, such as rainfall. The Weibull function is written as:

$$f(x) = \alpha\beta x^{\beta-1} e^{-\alpha x^\beta}$$

where  $\alpha$  and  $\beta$  are constants used to fit the observed data. Unlike the normal and lognormal distributions, there is an analytical solution for the CPDF of the Weibull function, namely:

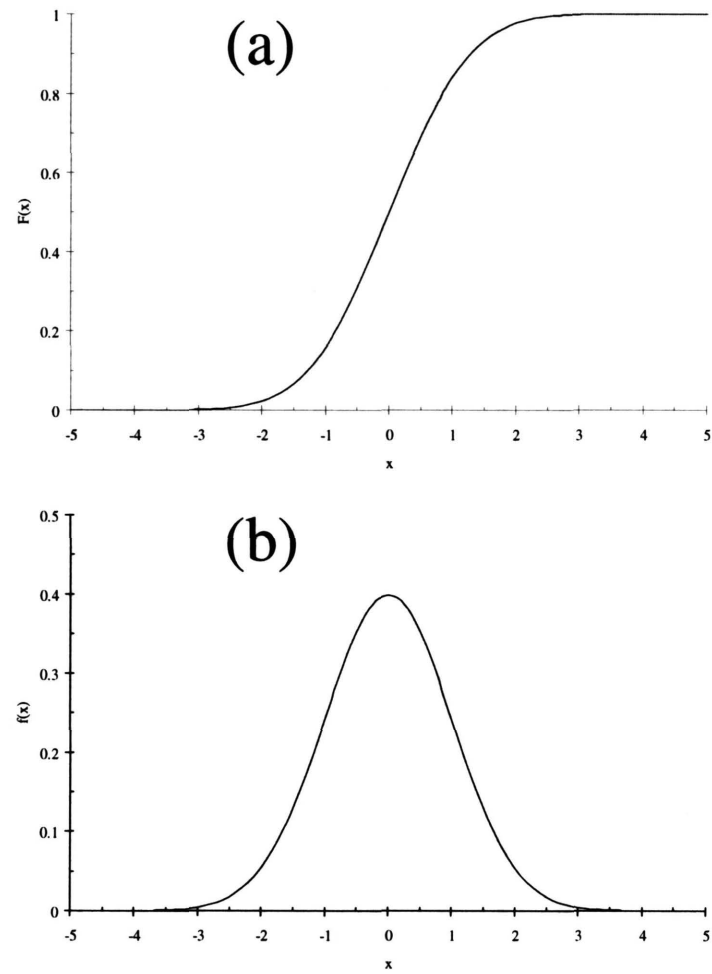


**Figure 43. a) Probability density function for a normal distribution. b) Cumulative probability density function for the normal distribution.**

$$F(x) = 1 - e^{-\alpha x^\beta}$$

To generate a random value from the CPDF of the Weibull function, a uniformly distributed random number from 0 to 1 (RND) is drawn. RND is then used as a replacement for F(x) in the CPDF of the Weibull function, and x is solved as a function of RND. The solution is found through some minor algebraic manipulation as:

$$x = e^{\frac{\ln\left[\ln\left(\frac{1}{RND}\right)\right] - \ln\alpha}{\beta}}$$

### ***Stochastic Analysis***

Stochastic analysis is used to estimate the uncertainty in model predictions that result from uncertainty in model input. Errors and uncertainty in model predictions generally result from three causes (Peck et al, 1988): (1) poor representation of the processes, (2) errors from numerical methods, and (3) parameter averaging errors and errors in input data. The purpose of stochastic analysis is to investigate the uncertainty of model predictions by quantifying the effects of parameter averaging errors and errors in input data. Uncertainty of input data is caused by several factors. Two of the most important are the inability to predict the value of future stresses, and measurement or averaging errors. The first step in stochastic analysis is to determine which parameters have the largest effect on model results, and which of those parameters contain uncertainty. The next step is to mathematically describe the uncertainty associated with them. For predictive uncertainty, this procedure is usually accomplished by fitting theoretical PDF's to histograms of historical data. Obviously, large numbers of historical data points increase the ability to match a PDF. Uncertainty caused by parameter averaging or measurement error is more difficult to quantify.

The next step in stochastic analysis is to determine the method to be used to propagate the statistical descriptions of the parameter through the model to the solution. Three methods presented by Freeze et al. (1990) are first-order analysis, perturbation analysis, and Monte Carlo (MC) analysis. First-order analysis is a simple way to approximate the mean and standard deviation of the output. The main limitation of this

method is that the coefficient of variation, which is the standard deviation divided by the mean, must be much less than one (Peck et al., 1988). Those applying this approach to groundwater problems include Dettinger and Wilson (1981), Townley (1984), Townley and Wilson (1985), Sitar et al. (1987), and Wagner and Gorelick (1987).

Perturbation analysis began with the early works of Gelhar (1976) and Gelhar et al. (1979), and current approaches are reviewed in Gelhar (1993). One difficulty with this approach is that it is limited to infinite domains and works best with analytical solutions. Another limitation is that the mathematics are complex and difficult to apply to practical applications.

The third method, MC analysis, has evolved with perturbation analysis as a method for solving stochastic equations. The method is the most powerful and conceptually straightforward of the three stochastic approaches. The general procedure is as follows. PDF's are determined for one or more of the input parameters. A random number generator is then used to select values from the PDF for the input parameters. Each set of input parameters is used as input to a numerical or analytical model. The model is then run and the model output is recorded. This process is repeated a large number of times. Peck et al. (1988) estimate that a thousand runs will produce a 10% error while 10,000 runs will produce a 1% error. At the end of MC analysis, statistics performed on all of the model runs are used in a probabilistic sense to answer questions about the system.

## **Water Balance Equation and Development of Input Parameters**

### ***Approach***

A lumped-parameter, water balance model was used stochastically to simulate time-series realizations of water levels in a wetland. Selected parameters in the water balance equation were treated stochastically. Values for the stochastic parameters were selected randomly from their respective PDF's. Parameters treated stochastically in this chapter are presented in bold type.

The mathematical formulation of the water balance equation is relatively simple. For a wetland, the water balance equation states that the volume of water entering the wetland less the volume of water leaving the

wetland is equal to the change in the volume of water that is stored in the wetland. The water balance equation is written as:

$$(\mathbf{R} + \mathbf{RW}) - (\mathbf{ET} + \mathbf{GW} + \mathbf{SW}) = \Delta \mathbf{S}$$

where, **R** is rainfall [ $L^3/T$ ]; **RW** is the additional input of water, such as reclaimed water [ $L^3/T$ ]; **ET** is the volumetric discharge of water that is lost to evapotranspiration [ $L^3/T$ ]; **GW** is the groundwater discharge [ $L^3/T$ ] out of the wetland and underlying aquifer; **SW** is the surface water discharge out of the wetland [ $L^3/T$ ], and  $\Delta \mathbf{S}$  is the change in the volume of water in the system with time [ $L^3/T$ ]. As written here, the discharge rates for ET, GW, and SW are positive when out of the wetland. R and RW are positive when into the wetland. The water level is calculated by summing the volume of water that has entered and the volume of water that has left the wetland during one time step. The time step is used to convert the discharges in the water balance equation to volumetric quantities in  $L^3$ . These quantities are then used to calculate the change in storage during one time step. An increase in storage results in an increase in the water level. Conversely, a decrease in storage results in a decrease in the water level.

### ***Rainfall***

Rainfall data are typically reported in dimensions of [ $L/T$ ], as presented above. The water balance equation, however, requires a volumetric discharge with dimensions of [ $L^3/T$ ]. For this reason the following relationship is used:

$$\mathbf{R} = \mathbf{r} \cdot \mathbf{A},$$

where **r** is the rainfall rate [ $L/T$ ], and **A** is the area of the wetland [ $L^2$ ].

Rainfall is treated stochastically because it is not possible to accurately predict future rainfall values. The statistical distribution of rainfall for each month was calculated and plotted from the St. Leo rainfall data (Figure 44). Data are presented as quartiles, rather than mean and standard deviation, because rainfall distributions for each month are not normal. The Weibull function is used as the PDF for each monthly rainfall distribution. Monthly values for  $\alpha$  and  $\beta$  were calculated using an iterative solver from a

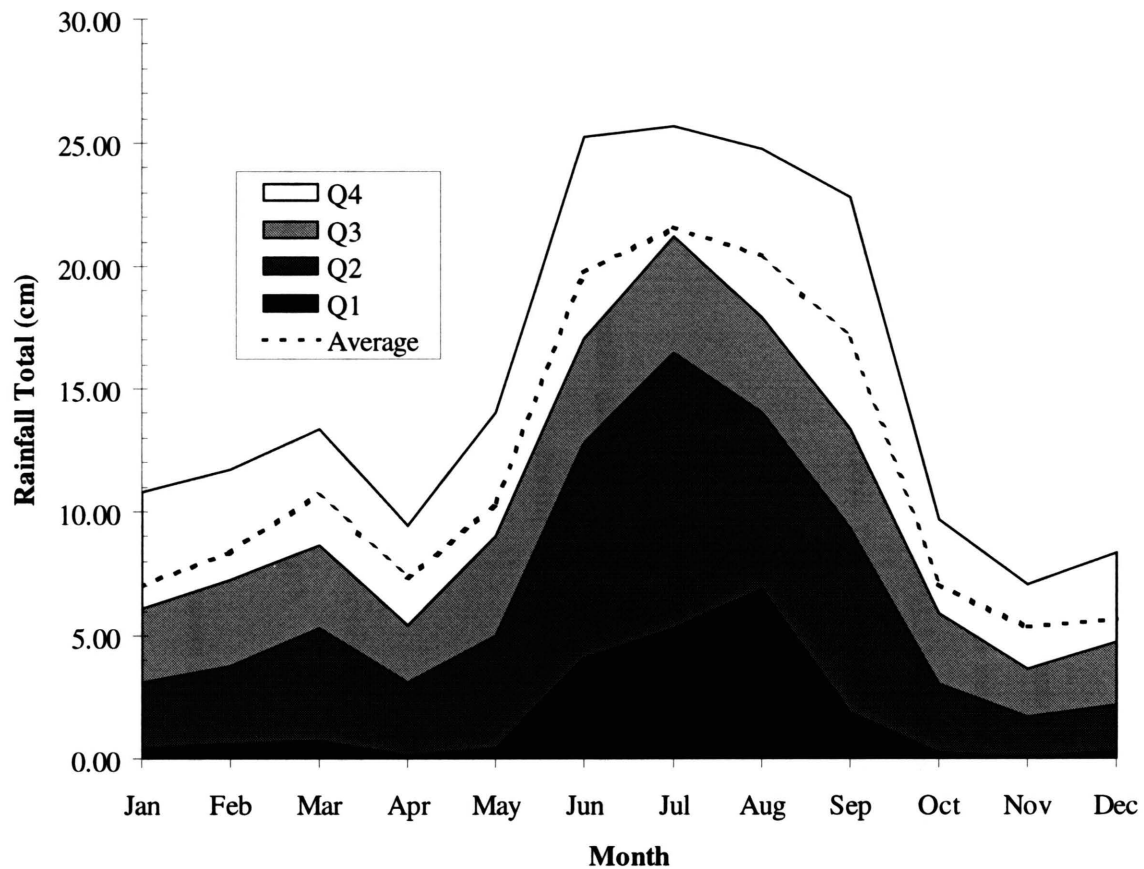


**Figure 44. Monthly statistics from historical rainfall data at the St. Leo weather monitoring station. Shaded areas represent quartiles, or the region on the graph where 25 percent of the rainfall values lie. The lower line of Q2 is also the median. The average and median values are not the same because the rainfall distribution is not normally distributed.**



spreadsheet. Values of  $\alpha$  and  $\beta$  were adjusted until the root mean square error (RMS) between observed and predicted rainfall distributions is minimized. As an example, the observed data are plotted with the cumulative Weibull function for the month of January to illustrate the match between the Weibull function and the observed data (Figure 45). Values of  $\alpha$  and  $\beta$ , for each month, are listed in Table 8.

### ***Reclaimed Water Application Rate***

The allocated reclaimed water rate (RW) is treated as a deterministic parameter. RW is assumed known and has a constant value for each month. To rehydrate the North Lakes wetland, Hillsborough County has allocated reclaimed water at a rate of approximately 5700 m<sup>3</sup>/day (1.5 MGD) for the four summer months. The RW value during the eight remaining months is zero. This is an average yearly rate of 1900 m<sup>3</sup>/day (0.5 MGD).

### ***ET Estimation***

Like rainfall, evapotranspiration is commonly used with dimensions of [L/T]. To represent evapotranspiration as a volumetric discharge, the following equation is used:

$$\mathbf{ET} = \mathbf{et} \cdot A,$$

where **ET** is the volumetric evapotranspiration rate from the entire wetland [L<sup>3</sup>/T]; **et** is the evapotranspiration rate [L/T], and **A** is the area of the wetland [L<sup>2</sup>].

Evapotranspiration is a difficult parameter to estimate because it cannot be measured directly. For this reason, **ET** is treated stochastically. A simple relationship between **et** and **r** is assumed to exist where:

$$\mathbf{et} = \mathbf{C} \cdot r$$

**C** is a normally distributed, random variable with a mean of 0.8 and a standard deviation of 0.2. In other words, evapotranspiration is assumed to be approximately 80 percent of the rainfall value with a standard deviation of 20 percent. There are little data to support this assumption, but by selecting such a large

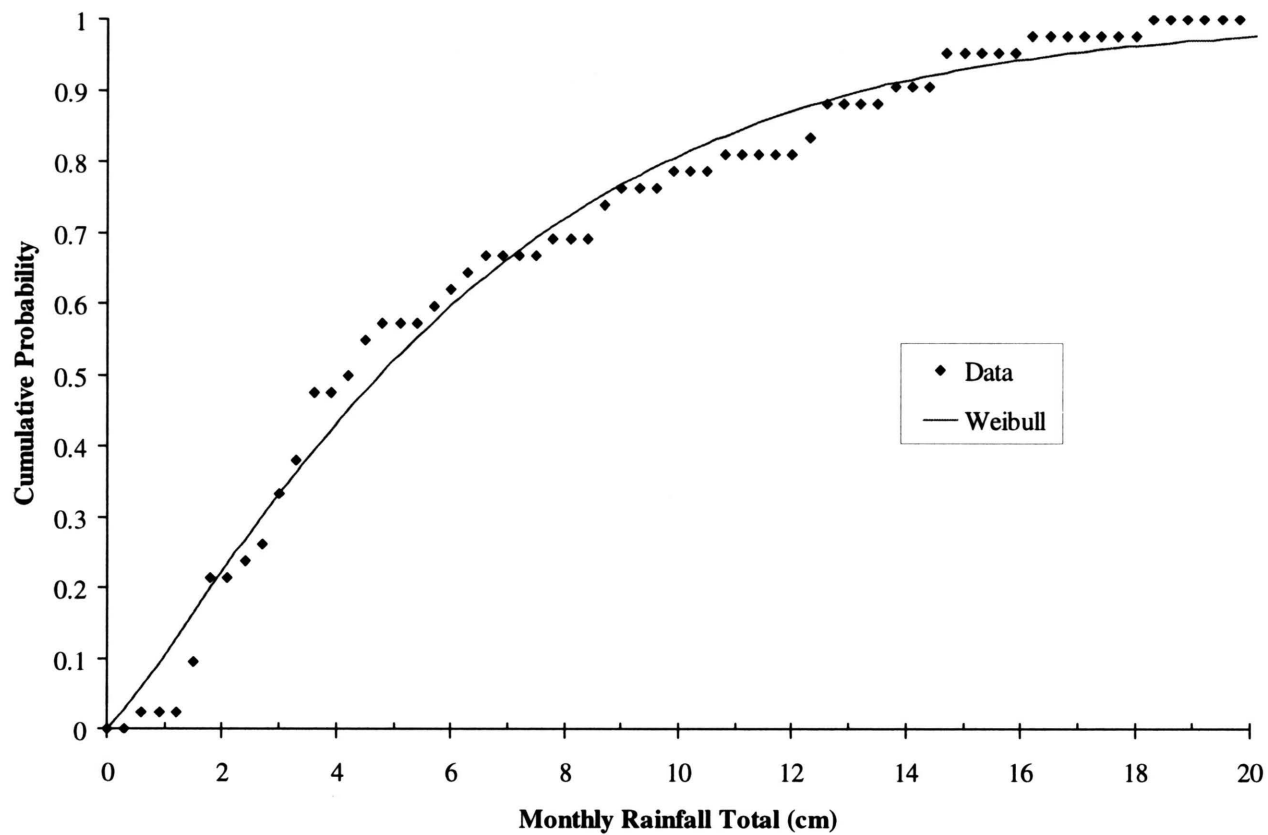


**Figure 45. Cumulative probability graph of rainfall for the month of January. Rainfall data is taken from the weather station at St. Leo, Florida. The solid line represents the fit of the Weibull function to the observed data.**

**Table 8. Summary of rainfall statistics for the St. Leo weather monitoring station. Q1 through Q4 represent the quartiles of the rainfall data. The value of Q2 is the median. The Weibull parameters match the Weibull function to the observed rainfall data. The root mean square (RMS) value indicates how well the Weibull function matches the observed rainfall data.**

	<b>Jan</b>	<b>Feb</b>	<b>Mar</b>	<b>Apr</b>	<b>May</b>	<b>Jun</b>	<b>Jul</b>	<b>Aug</b>	<b>Sep</b>	<b>Oct</b>	<b>Nov</b>	<b>Dec</b>
<b>Q1</b>	0.46	0.64	0.76	0.15	0.43	4.06	5.31	6.91	1.91	0.25	0.05	0.33
<b>Q2</b>	3.10	3.78	5.28	3.12	5.00	12.83	16.43	14.05	9.32	3.07	1.69	2.21
<b>Q3</b>	6.07	7.26	8.66	5.41	9.04	17.07	21.21	17.93	13.34	5.89	3.64	4.74
<b>Q4</b>	10.81	11.71	13.34	9.42	14.00	25.22	25.65	24.77	22.78	9.70	7.09	8.37
<b>average</b>	7.03	8.38	10.72	7.28	10.37	19.74	21.58	20.41	17.02	7.10	5.38	5.66
<b>weibull parameters</b>												
$\alpha$	0.1115	0.0350	0.0222	0.0862	0.0097	0.0006	0.0001	0.0001	0.0085	0.0454	0.2410	0.0832
$\beta$	1.17	1.47	1.57	1.19	1.94	2.40	2.82	2.94	1.61	1.45	0.93	1.36
<b>RMS</b>	0.033	0.032	0.023	0.021	0.020	0.027	0.037	0.040	0.049	0.026	0.021	0.025

standard deviation in  $C$ , the thinking is that the uncertainty in  $e_t$  has been generously incorporated into the model.

### ***Surface Water Flow***

For most wetlands, the water balance equation contains a surface-water component, which includes both inflows and outflows. At the North Lakes wetland, surface water inflows are extremely rare and thus have never been measured. For these reasons, surface-water inflows are not represented in the model. Surface-water outflows, however, are represented in the water balance model. When the water level in the wetland exceeds the elevation of the control structure, water is removed from the wetland at the rate required to keep the water level at the elevation of the control structure. This procedure maintains water balance and ensures that the water level in the wetland is at or below the elevation of the control structure.

### ***Groundwater Flow***

Groundwater flow is separated into horizontal and vertical components. For this study, it is assumed that the horizontal component of flow in the surficial aquifer is negligible. The vertical component of flow, however, is considered significant to the overall water budget and is treated as a stochastic parameter. In the water balance equation, net groundwater flow is defined as positive when out of the wetland. The equation for groundwater flow, therefore, is written so that downward flow out of the wetland is positive, and upward flow into the wetland is negative. The equation describing vertical flow is a form of Darcy's Law and is written as:

$$\mathbf{GW} = \mathbf{L} \cdot \mathbf{A} \cdot \mathbf{dh},$$

where  $\mathbf{GW}$  is the vertical, volumetric flow rate [ $L^3/T$ ];  $\mathbf{L}$  is the leakance between the surficial and Floridan aquifers [ $T^{-1}$ ];  $\mathbf{A}$  is the area of the wetland [ $L^2$ ], and  $\mathbf{dh}$  is the difference in water levels between the surficial and Floridan aquifers [ $L$ ]. The value of  $\mathbf{dh}$  is positive when the water level in the surficial aquifer is higher than the water level in the Floridan aquifer.

The leakance value is treated stochastically. The PDF for leakance is assumed to be lognormal. The mean for the distribution of  $\ln(L)$  is determined through a calibration procedure, described later. The standard deviation for  $\ln(L)$  is assumed to be 1.

The head difference between the surficial and Floridan aquifer,  $dh$ , varies throughout the year. Values of  $dh$  depend on many factors such as rainfall, leakance, groundwater withdrawals, evapotranspiration, and the previous value of  $dh$ . As a result, there is a great deal of uncertainty in predicting future values of  $dh$ . For this reason,  $dh$  is treated stochastically. Ideally,  $dh$  should be handled similarly to rainfall. PDF's should be matched to observed monthly distributions of  $dh$ . Another approach would be to correlate  $dh$  with the parameters that influence its distribution, such as rainfall, leakance, evapotranspiration, etc. For this study, however, there are not enough time-series data to adequately describe the statistical distribution of  $dh$ . Instead, some simplifying assumptions are made about  $dh$  in order to treat this parameter stochastically.

To describe the distribution of  $dh$ , a histogram is constructed with the time-series values of  $dh$  (Figure 46). The values of  $dh$  for Site 3 are suspect and are not included in the construction of the histogram. An assumption is made that the distribution of  $dh$  is normal, and the mean and standard deviation are 0.6 and 0.5 m, respectively. These statistical estimations are used to calculate the normal PDF, also included in Figure 46.

### ***Change in Storage***

The change in water storage with time is described mathematically as:

$$\Delta S = (h - h_{t-1}) \frac{An}{dt},$$

where  $\Delta S$  is the change in the storage of water within the wetland during the time step [ $L^3/T$ ];  $h$  is the water level or stage in the wetland [ $L$ ];  $h_{t-1}$  is the head or stage in the wetland during the previous time step [ $L$ ];  $A$  is the area of the wetland [ $L^2$ ];  $n$  is the porosity [ $L^0$ ], and  $dt$  is the length of the time step. When the surface of the water table is below land surface, specific yield should be used instead of porosity. For the application of this method to the North Lakes project, however, porosity is used for simplicity.

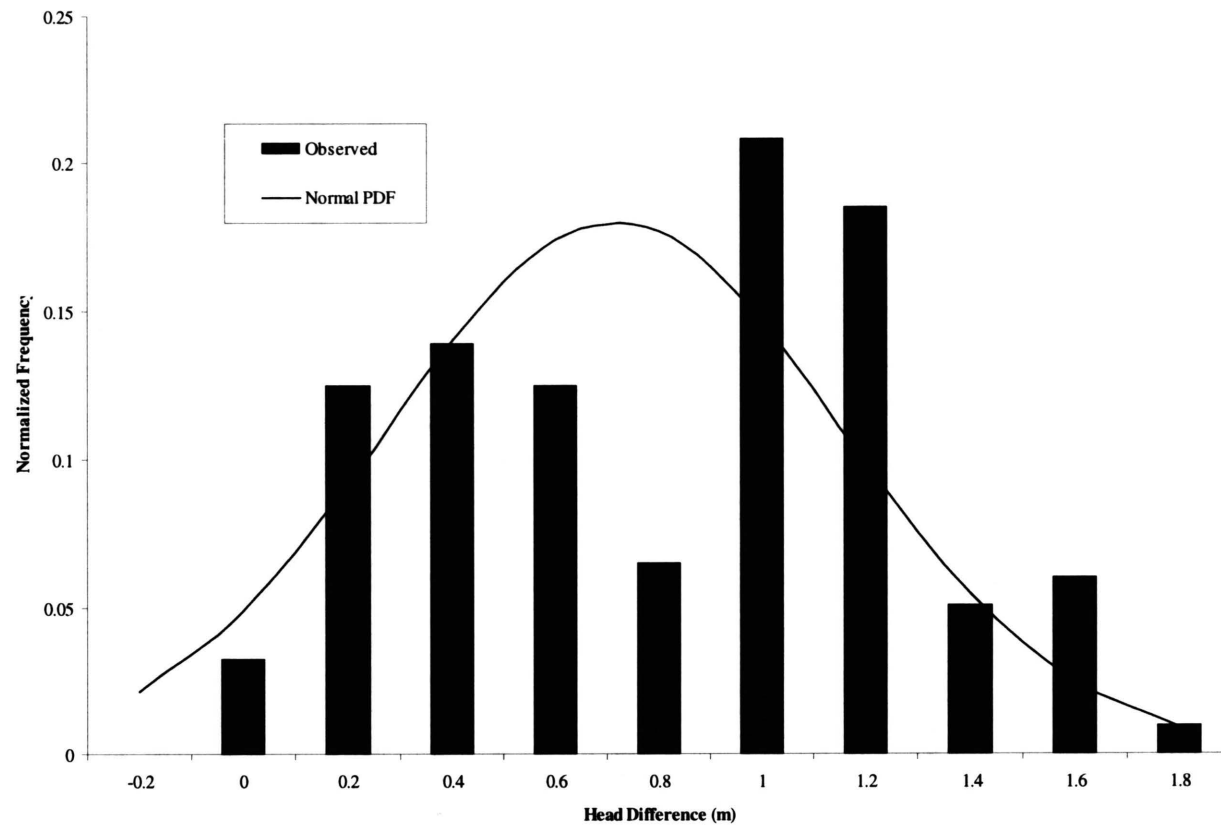


**Figure 46. Histogram of time-series dh values for four of the five nested wells at the North Lakes wetland. The solid line represents the PDF used to represent the distribution of dh.**

The starting water level,  $h_0$ , is selected from a normally distributed PDF. The mean and standard deviation of the PDF are assumed to be 14.50 m and 1.0 m, respectively. The value for porosity is dependent on the elevation of the water table. For this reason, the value of porosity may change during the course of one model run. If the starting water level for a time step is above land surface, the value for porosity is 1.0. If the starting water level for a time step is below land surface, the porosity value is set based on the porosity of the sedimentary layer (S1, S2, or S3; Figure 40) of the water table.

### ***Numerical Formulation***

By substituting equations for  $R$ ,  $RW$ ,  $ET$ ,  $GW$ , and  $\Delta S$  into the water balance equation and rearranging terms, the equation for water level ( $h$ ) is,

$$h = \frac{dt}{n} \left[ r + \frac{RW}{A} - et - L \cdot dh \right] + h_{t-1}$$

A FORTRAN code was written and developed to solve the equation for water level. A flow chart for the program is presented in Figure 47. There are three main loops. The outermost loop runs each stochastic simulation. The next loop runs each month. The monthly loop is required because stochastic values for  $r$  and  $et$  are selected monthly. The innermost loop runs the daily time step for each month. After each daily time step, porosity is reassigned based on the layer in which the water table resides. The total simulation time is 72 months, or six years.

The water balance model is run many times using the Monte Carlo approach. The number of model runs for each Monte Carlo simulation is 8000. It takes approximately 10 minutes to run 8000, 72-month runs on a Pentium II-type personal computer running at 200 megahertz.

### ***Outline of Model Runs***

Two different hydrologic scenarios are investigated with the stochastic model. Each scenario contains more than one stochastic simulation. The first scenario represents normal conditions, or conditions that occur without the addition of reclaimed water. The objective of the first scenario is to reproduce the

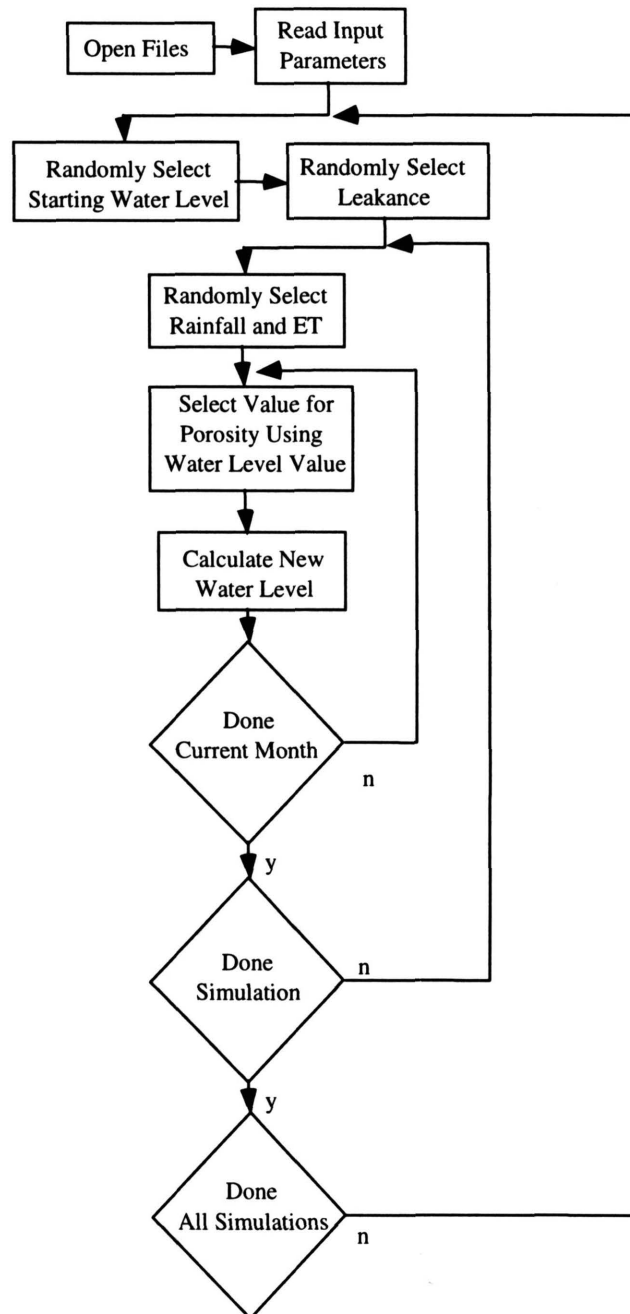


**Figure 47. Flow chart for running Monte Carlo analysis with the water balance equation.**



normal variation in water levels by calibrating the model. The model is considered calibrated when the median value of the starting water level is nearly equal to the median value of the ending water level. This calibration approach assumes that water levels at the wetland have achieved a long-term, steady-state average. The model is calibrated by adjusting the mean of the lognormal PDF for leakance until steady state is achieved over a six-year period.

The objective of the second scenario is to investigate the effects of applying reclaimed water to the wetland. The calibrated leakance distribution is used for these simulations. The stochastic model is run 12 times, each with a different value for the reclaimed water application rate, RW.

## **Results**

### ***Scenario 1. Natural Conditions without Addition of Reclaimed Water***

Calibration of the model is achieved when the mean value for  $\ln(L)$  is set at  $-6.7$  ( $1 \times 10^{-3} \text{ day}^{-1}$ ). Results with this adjustment produce a final, median water level that is nearly equal to the starting median water level (Figure 48). For this simulation, the average water level does not track the median water level (Figure 48) because the statistical distribution of water level elevation is not normal.

### ***Scenario 2. Rehydration with Reclaimed Water***

Many different application rates were used to determine the hydraulic effects of adding reclaimed water to the wetland. As an example, the water level trend for a reclaimed water application rate of  $1400 \text{ m}^3/\text{day}$  is presented (Figure 49). With this application rate, the majority of the simulated water levels are at or near the elevation of the control structure (15.62 m). Notice, however, that some low-probability realizations have water levels that are unrealistically low (Figure 49). For example, the minimum, simulated water level is at an elevation of approximately 2 m.

Results from five stochastic simulations with different values of RW are presented as a cumulative probability plot of water level (Figure 50). Each line on this figure represents the probability that the median water level will be greater than the corresponding elevation along the x axis. The probability for

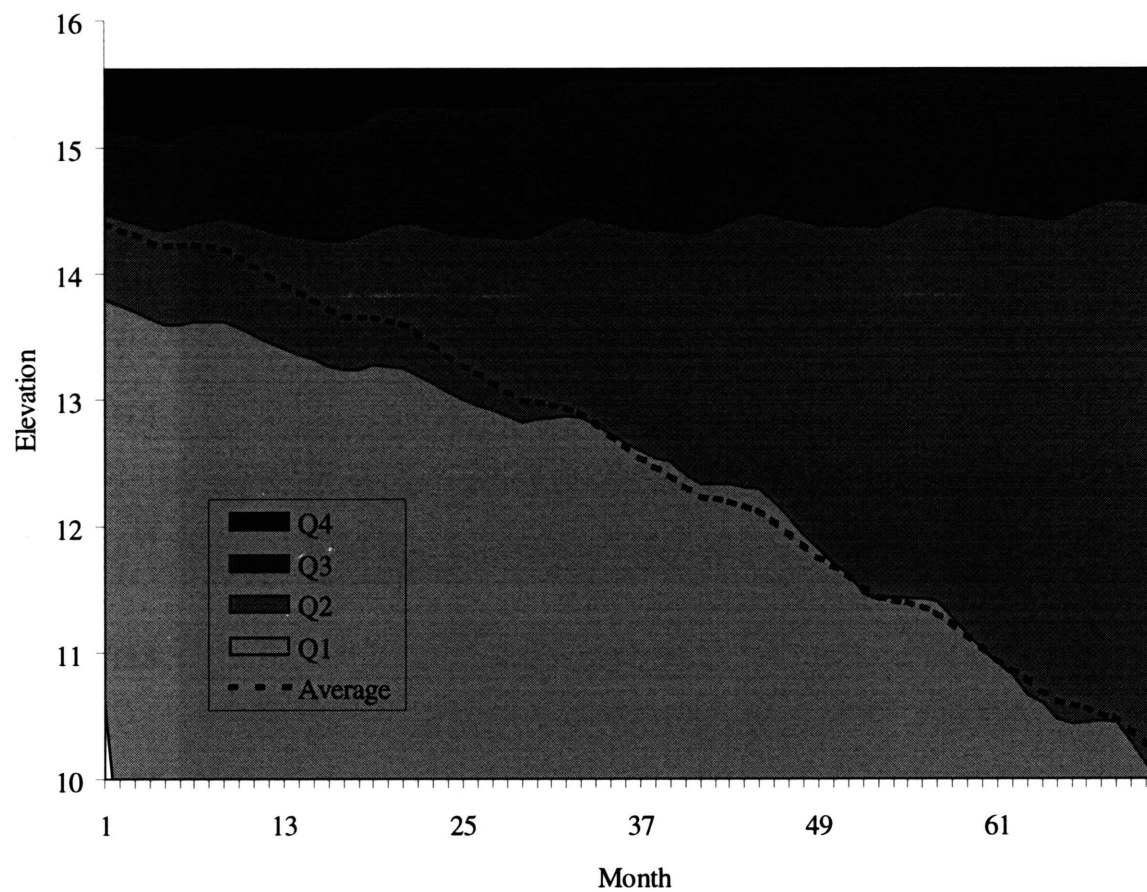


**Figure 48. Results from the stochastic simulation of head versus time for the calibration run that produces an acceptable median water level. Data are presented in quartiles. The upper line is the elevation of the weir.**

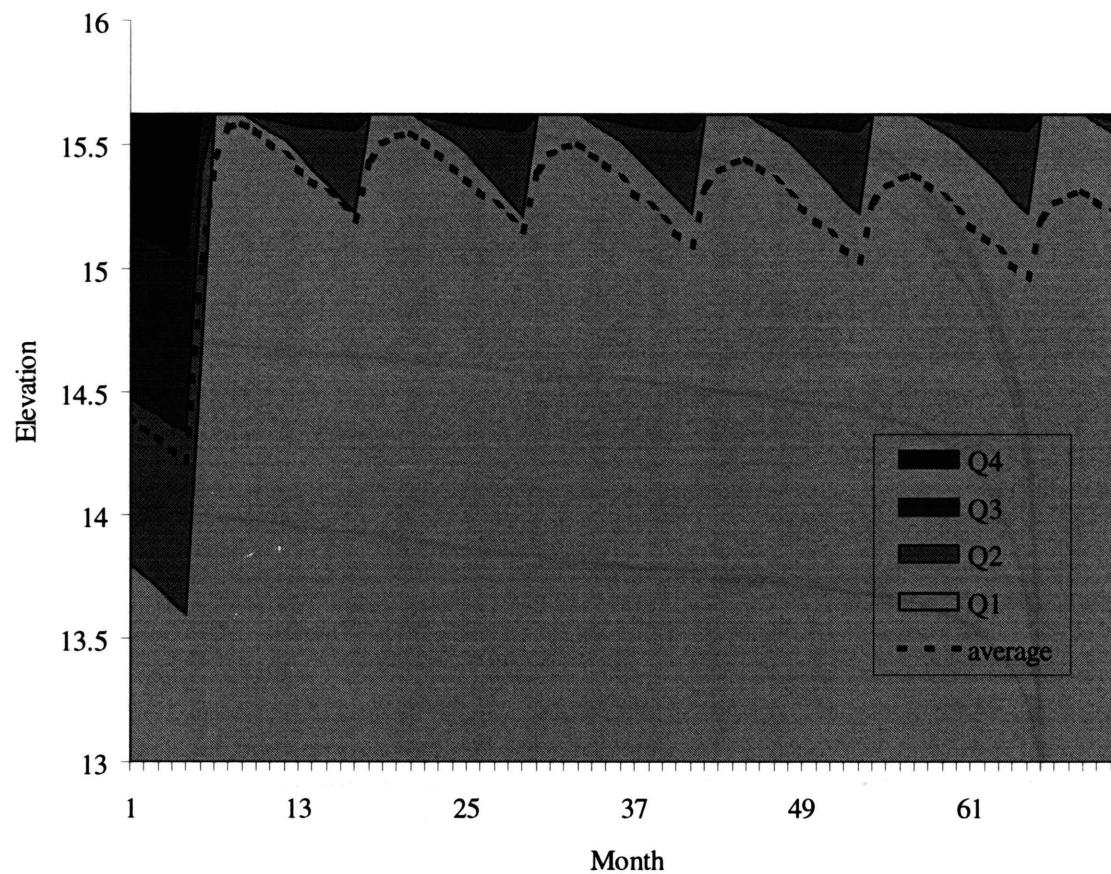


**Figure 49.** Stochastic simulation of head versus time. Water is added to the wetland at a rate of  $1400 \text{ m}^3/\text{day}$  for the months of June, July, August, and September. The median value of  $\ln(Kv)$  is set at  $-4.6$ . Data are presented as quartiles. The upper line is the elevation of the weir. The difference between average water level and median water level (upper limit of Q2) mean that water levels are not normally distributed.

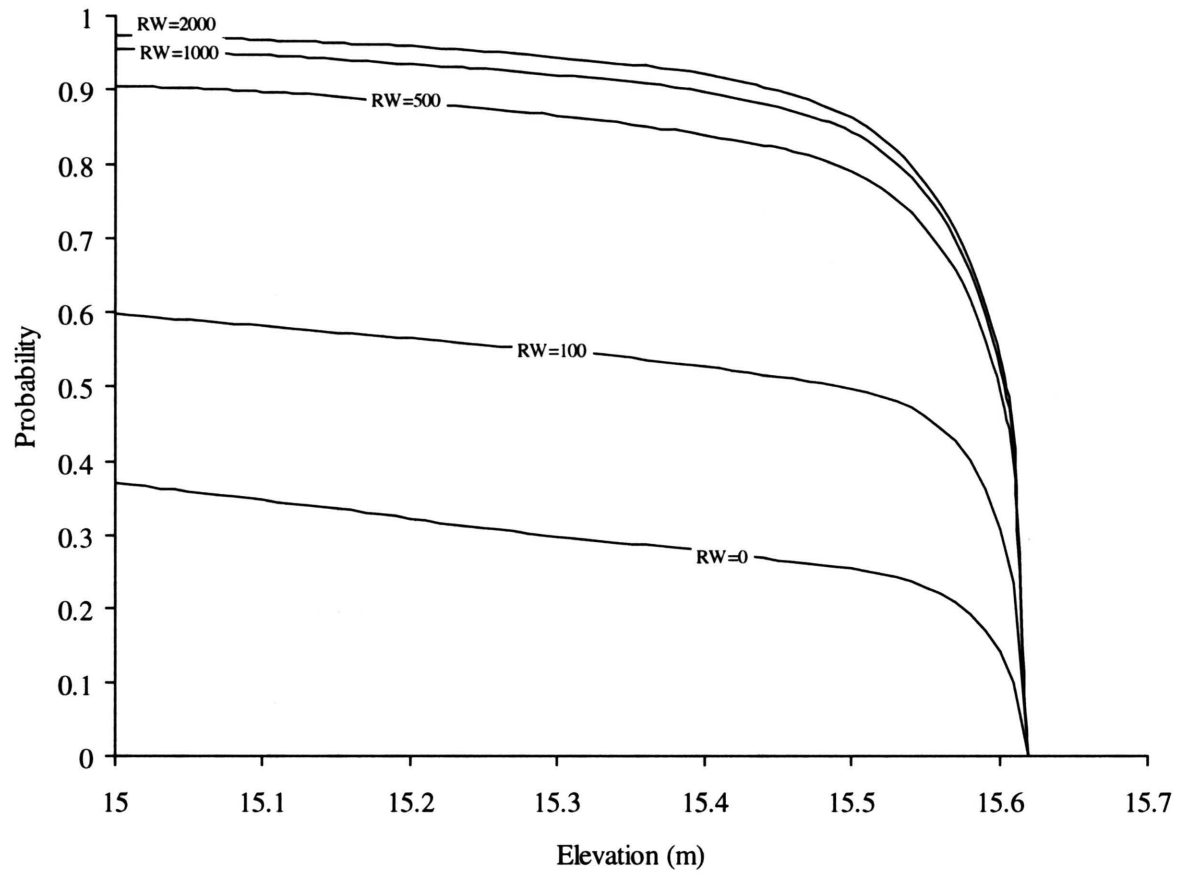


**Figure 50.** Cumulative probability plots for five stochastic simulations. Each line represents the probability that the water level will be above the elevation along the x-axis. Units of RW are  $\text{m}^3/\text{day}$ .

each RW rate is calculated by summing the number of median water levels (for the six-year period) that exceed the elevations along the x-axis of Figure 50. The total number of median water levels exceeding an elevation is then divided by the number of water balance runs for each stochastic simulation (8000). As expected, large RW application rates result in a high probability that the median water level will be relatively high. For example, with  $RW = 100 \text{ m}^3/\text{day}$ , the probability that the annual median water level is greater than land surface is 17 percent (Figure 50). For  $RW = 2000 \text{ m}^3/\text{day}$ , the probability that the annual median water level is greater than land surface is 84 percent.

## **Discussion**

### ***Potential for Wetland Restoration***

The stochastic model presented here is developed from a hydrologic standpoint. These results, therefore, cannot be used directly to determine if the ecosystem at North Lakes will be restored. A study by Hull (1997) relates ecological damage to water level elevations. In his study, the ecological status of 36 cypress domes in west-central Florida was evaluated using a variety of ecological indicators. Each wetland was assigned a value that pertains to the overall health of the wetland. To compare hydrology among wetlands, water levels were normalized to an elevation known as “normal pool”. Normal pool elevations were determined from biological indicators. Hull (1997) suggests that there is a 50 percent chance that wetlands with a median water level below a threshold elevation will experience significant environmental damage. That threshold elevation was determined statistically to be 0.55 m below normal pool.

Assuming that the study by Hull can be used in reverse to predict environmental restoration, there is a 50-percent chance that a wetland will be restored if the median water level (calculated over a six-year period) is raised above the threshold elevation. The normal pool elevation has not been determined for the North Lakes wetland; however, it is probably close to the elevation of the weir crest (15.62 m), which was designed specifically to restore the wetland (Florida Land Design and Engineering, 1987). At the North Lakes wetland, then, the threshold elevation is probably near 15.07 m ( $15.62 \text{ m} - 0.55 \text{ m}$ ), or approximately 0.5 m below the average elevation of the land surface. If the success of the rehydration project is defined as maintaining a median water level above the threshold elevation for six years, the probability of success

can be determined from the stochastic simulations. From the work of Hull (1997), success, therefore, does not mean that the wetland will be restored, but rather that the wetland has a 50 percent chance of being restored. The probability of success, when plotted against RW, provides a useful and graphic way to present results to decision-makers (Figure 51). From this graph, it appears that success will be easily achieved with the allocated rate of 5700 m<sup>3</sup>/day. It also appears that allocated rates between 600 and 2000 m<sup>3</sup>/day will produce nearly equally probable chances for success.

### ***Probability of Worst Case***

The idea of “worst case” is commonly used in decision making. To estimate the worst case, values for independent variables are selected in such a way that the “worst” likely outcome is produced. Under some circumstances, this approach may be warranted. The problem with the worst-case approach is that the probability that the predicted result will occur is very low.

To illustrate potential problems with basing decisions on worst-case predictions, the methods developed here are used to estimate the probability of a worst-case outcome. Using the water balance equation, a time series of water levels is generated using worst-case estimates of the stochastic parameters. Worst-case estimates for  $r$ ,  $et$ ,  $L$ ,  $dh$ , and starting water level are selected from their respective PDF's. Values for  $r$  and starting water level are selected from their CPDF's at a cumulative probability of 0.10. Values for  $et$ ,  $L$ , and  $dh$  are selected from their CPDF's at a cumulative probability of 0.90. The values are selected in this manner because low values of  $r$  and starting water level elevation result in a low median water level. High values for  $et$ ,  $L$ , and  $dh$  also result in a low median water level. The probability values of 0.10 and 0.90 are arbitrary.

The worst case model was run deterministically (one time) with an RW value of 5700 m<sup>3</sup>/day (as before, RW is applied only during the four summer months). The median, six-year water level simulated with the worst-case parameters is 14.87 m. This median water level, however, has a very low probability of occurrence (Figure 52). The worst-case median water level lies far outside the most probable median water levels. More importantly, the worst-case prediction suggests that there is little hope of restoring the wetland with the allocated rate of reclaimed water. The stochastic simulations indicate that there is a very

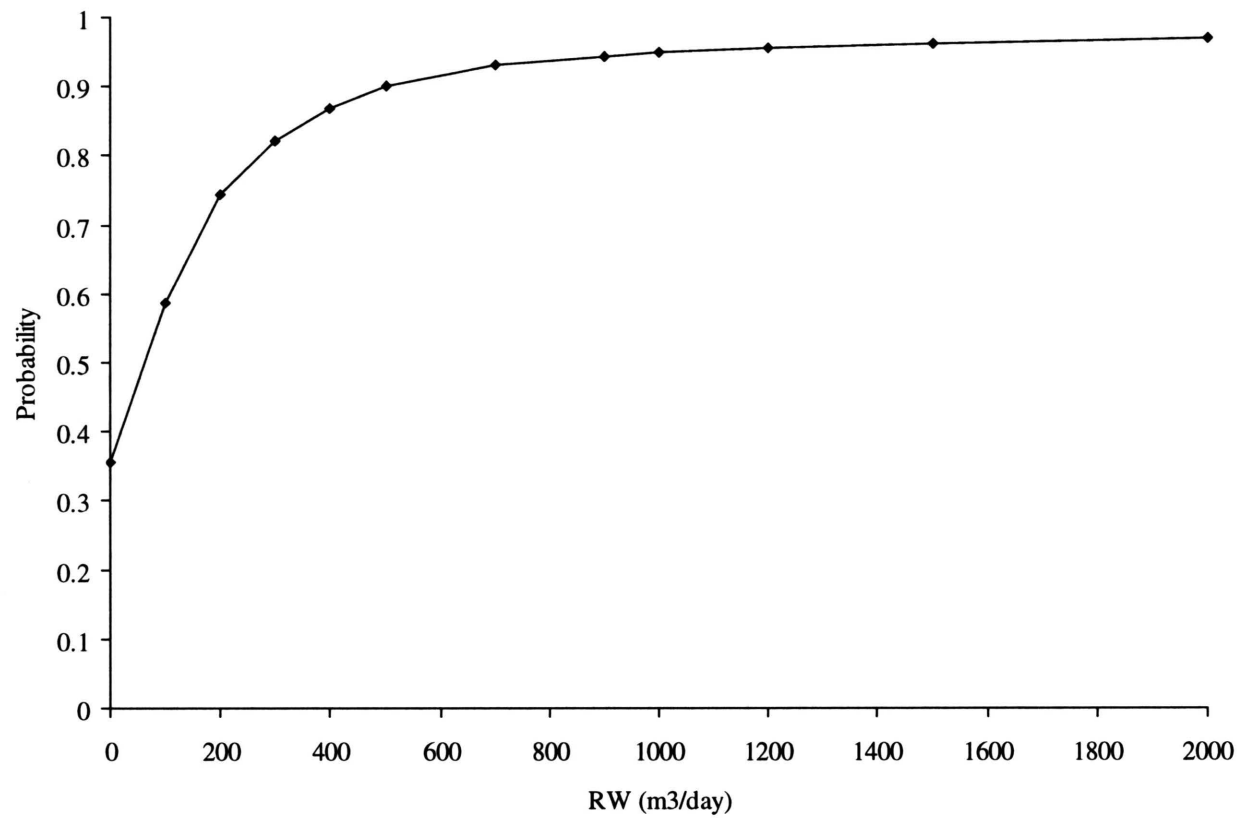


**Figure 51. Probability that the six-year, median water level will be above the threshold elevation (15.07 m) plotted against the reclaimed water application rates (RW).**

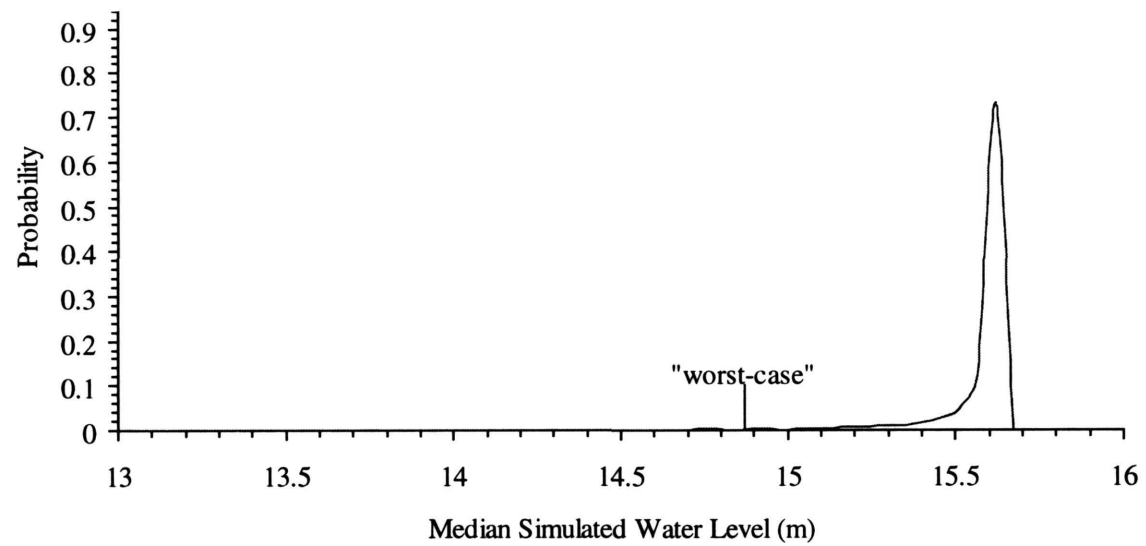


**Figure 52. Simulated PDF of the six-year, median water level. The worst-case median water level lies far outside the most probable median water levels.**



high probability for restoring acceptable water levels with the reclaimed water application rate of 5700 m<sup>3</sup>/day.

### ***Model Improvements***

The objective of this paper is primarily to illustrate the methods used to solve these types of problems rather than to answer specific questions about North Lakes. For this reason, there a number of simplifications have been made about the nature of the stochastic parameters. Model improvements could be made in the representation of the stochastic parameters with their respective PDF's. The stochastic estimates of rainfall are good because the RMS values, which describe the goodness of fit, are small (Table 8), and there is a long period of record. Statistical estimates for ET, however, could be improved. One level of improvement could be to vary the ET rate as a function of pan evaporation rather than rainfall.

The PDF for leakance could also be improved. In an attempt to better understand the distribution of leakance, a histogram for leakance was generated from data contained in a regional, numerical model of groundwater flow. For several reasons, the histogram of leakance from the model could not be used to help select a PDF of leakance for the North Lakes wetland. The first reason is that the discretization of the numerical flow model is too coarse as compared with the North Lakes site. The area of a cell in the flow model ( $1.6 \times 10^5 \text{ m}^2$ ) is much greater than the area of the North Lakes wetland ( $6.5 \times 10^4 \text{ m}^2$ ). For this reason, the regional flow model does not contain leakance variability at the wetland scale. Another reason why model-derived leakance values cannot be used to guide the selection of a PDF is that the semi-confining layer beneath the North Lakes wetland is absent. In terms of the spatial domain of the regional model, an absence in the semi-confining layer is anomalous. Finally, leakance values from the model cannot be used because numerical flow models are typically calibrated using a zone method. Rather than adjusting the leakance values for individual cells, calibration occurs by adjusting the leakance values for zones of cells. This calibration procedure results in a discontinuous distribution of leakance that does not represent the actual leakance distribution at site scales.

The statistical distribution of head difference between the surficial and Floridan aquifers is probably the weakest variable in the model. Values for dh act in a Markovian manner; that is, the value of dh for one

month is dependent on the value of  $dh$  from the previous month. In addition,  $dh$  is probably correlated with values of rainfall. This behavior has not been incorporated into the North Lakes simulations due to lack of field data. If more water level data were available, the  $dh$  parameter could be correlated with monthly or daily rainfall rates. This procedure could improve the model results by constraining the uncertainty in  $dh$ . Another approach would be to look at a time series of head difference data from nested wells with a continuous water-level recorder. While these data are not available at North Lakes, the Berger shallow and deep wells, which are located within 1 km of North Lakes, have continuous water-level measurements. The problem with using the Berger head difference data is that the leakance value at the Berger wells is different from the leakance value at North Lakes. This may pose problems for translating the water level fluctuations from Berger wells to the North Lakes site.

## **Conclusions**

Results from stochastic analysis suggest that, from a hydrologic perspective, the North Lakes wetland is an ideal site for restoration with reclaimed water. While Hillsborough County has allocated reclaimed water at a rate of approximately  $5700 \text{ m}^3/\text{day}$  during the four summer months, results from the model suggest that a much lower rate will suffice. According to Hull (1997), when the median annual water level in a wetland drops below the threshold elevation, there is a 50 percent chance that significant wetland damage will occur. Using this logic in reverse then, by restoring the water level in a wetland above the threshold elevation, there is a 50 percent chance of wetland restoration. According to the stochastic model, under normal conditions there is a 36 percent chance of the annual median water level exceeding the threshold elevation. By using 1/10 of the allocated rehydration rate ( $500 \text{ m}^3/\text{day}$ ), the probability of exceeding the threshold elevation increases to 89 percent. If  $2000 \text{ m}^3/\text{day}$  is applied to the wetland during the summer months, then the probability of increasing the annual median water level above the threshold elevation is nearly 100 percent.

The stochastic model developed here suggests that the results from worst-case scenarios, while conservative, may be highly improbable. Results from the water balance model, run with conservative, worst-case, input parameters, suggest that the wetland cannot be restored with reclaimed water. This

worst-case result conflicts with the results from the stochastic model, which suggest that the wetland can be successfully restored with allocated rates of reclaimed water.

## CHAPTER 5. CONCLUSIONS AND SIGNIFICANCE

Augmentation with reclaimed water can be a viable solution for wetland rehydration if feasibility criteria are met. Answering questions of feasibility requires many site-specific data as well as an understanding of the uncertainties in the data. Stochastic analysis provides a way to quantify uncertainties in predictions that result from uncertainties in model data. This dissertation has shown the types of data that are important for evaluating feasibility and ways to quantify the predictive errors that result from these data.

Chapter 2 presents the results from a detailed study at the North Lakes wetland. The results are significant because they quantify groundwater flow rates at a wetland in a covered-karst terrane. Flow patterns in covered-karst terranes are complicated by preferential pathways, which link surficial aquifers with deeper aquifers. These preferential pathways are commonly used to explain why surficial aquifers are drained near sites of significant groundwater withdrawal. Results from North Lakes, however, do not support the general model of groundwater flow in covered-karst terranes. Of the five sinkholes that were studied at the site, only two act as preferential pathways for flow into the Floridan aquifer. Sinkholes do not tend to channel groundwater flow at the site because the semi-confining layer beneath the surficial aquifer is thin or absent. In fact, data suggests that sinkholes restrict the downward flow of groundwater. One explanation for this observation is that low-permeability soils layers form in the bottom of sinkholes. Through further subsidence, the low-permeability materials sink down into the aquifer and plug the preferential pathway. It would be interesting to test this hypothesis in the future by extracting cores from these sinkholes. Results from carbon dating on the soil layers could provide useful information for subsidence rates, sinkhole evolution, and deactivation as a preferential pathway.

Chapter 2 also presents estimates of groundwater flow velocities. In the surficial aquifer, maximum flow velocities in the horizontal direction are about 1 m/day. In the vertical direction, downward flow velocities range between 0.1 and 0.2 m/day. Based on these velocities and the thickness of the surficial aquifer, groundwater does flow far in the surficial aquifer before flowing down into the Floridan aquifer. This

observation is significant for a number of reasons. First, few studies have quantified the downward flow of groundwater into deeper aquifers. Results from the North Lakes study provide estimates of groundwater flow velocities that may be useful for studies with similar hydrogeologic conditions. Second, the characterization of flow velocities under normal conditions helps predict the residence time of reclaimed water in the surficial aquifer. In covered-karst terranes, this is important because most of the adsorption of contaminants occurs in sands, silts, and clays, rather than in the underlying limestone. This statement is supported by the results of a geochemical study that was performed on sediment and limestone samples from North Lakes. The concentrations of metals are four to five times higher in the unconsolidated deposits than in the underlying limestone (Bek et. al, 1998). Based on these observations, regulations for reclaimed water projects should be based on chemical and viral concentrations at the base of the surficial aquifer, at the location in the aquifer where most adsorption will have already occurred.

Once groundwater enters the underlying carbonate aquifer, the dominant flow direction changes from vertical to horizontal. Quantifying horizontal flow rates and directions is important for rehydration feasibility studies, but is also important for many other groundwater investigations, such as wellhead protection and other contaminant transport-related problems. The delineation of groundwater flow paths in carbonate aquifers is often complicated by the presence of solution cavities, fractures, and fracture zones. The properties and locations of these features have eluded scientists for years. At local scales, fracture zones can be detected on aerial photographs as linear patterns in vegetation, soil tone, or sinkhole alignment. In Chapter 3, a method is developed for incorporating large-scale fracture zones into numerical models of groundwater flow and particle tracking. The method is easily applied to existing models of groundwater flow that treat the aquifer as an equivalent porous medium (EPM). When inserting highly permeable, vertical fracture zones into an EPM model, it is important to decrease the block transmissivity so that the bulk transmissivity is equal to the original EPM transmissivity.

Recognizing that the locations and properties of fracture zones are highly uncertain, the method in Chapter 3 includes stochastic analysis to characterize the uncertainties in groundwater travel times that result from uncertainties in fracture zone properties. To illustrate the approach, the method is applied to the North Lakes study area. To apply the model, assumptions were made about the vertical fracture zones that may

exist in the study area. For example, a 1:100 ratio was assumed for block to fracture transmissivity. This ratio is an estimate and is not directly supported by field observations. In addition, other statistical properties for fracture zones were described by data from a photolineament study 20 km north of the study area. Without better data for the fracture zones, results from the North Lakes application in Chapter 3 should be viewed with caution. The plots of possible travel paths, however, are particularly useful for illustrating the type of variability that might be expected.

To estimate the volume of reclaimed that is required to rehydrate a wetland, a stochastic method was developed to predict statistically reasonable water levels (Chapter 4). The method works with the water balance equation and statistical descriptions for variables that contain uncertainty. The approach for applying the method is similar to the approach used in Chapter 3. The model was applied to the North Lakes wetland, and assumptions were made about the statistics of the input variables. Results from the stochastic simulations were used to make inferences about the concept of “worst case” predictions of the effects of wetland restoration. In many studies, worst-case scenarios are used to reduce management options. In Chapter 4, the model was also used deterministically to make a worst-case prediction of water levels in the wetland. The worst-case prediction was based on low probability, but conservative, values for the input variables. The simulation included the application of reclaimed water. This worst-case scenario was then compared with results from the stochastic simulations. The comparison shows that results of the worst-case scenario are highly improbable.

In addition to answering questions with this dissertation, a few have been raised. One question that persists is should the North Lakes wetland be rehydrated with reclaimed water. Unfortunately, this question cannot be answered by this dissertation because there are many factors outside the field of physical hydrogeology to consider, such as public opinion, viral transport, and the biological response of a wetland ecosystem to augmentation with reclaimed water. From a hydrogeological perspective, there are still other questions to answer. One that is particularly interesting relates to the properties of fracture zones. Are fracture zones significant, and if so, can their properties be determined? Most of the questions raised by this dissertation are the result of insufficient data. By developing the methods for these types of studies, however, this dissertation has outlined those data that are required to answer questions of feasibility.

## REFERENCES

- American Society for Testing and Materials. 1990. ASTM Designation: D 422-63 (Reapproved 1990), Standard Test Method for Particle-Size Analysis of Soils.
- Anderson, M.P. 1979. Using models to simulate the movement of contaminants through groundwater flow systems. *Critical Reviews in Environmental Control*. 2:97-156.
- Anderson, M.P. and W.W. Woessner. 1992. *Applied Groundwater Modeling. Simulation of Flow and Advective Transport*. San Diego: Academic Press, Inc.
- Bear, J. 1993. Modeling flow and contaminant transport in fractured rocks. In *Flow and Contaminant Transport in Fractured Rock*, eds. Bear, J., Tsang, C.F. and G. de Marsily. Academic Press.
- Bek, R., Langevin, C.D., and J. Ryan. 1998. Geochemical baseline study of Upper Floridan Aquifer host rocks, SW Florida. Abstract presented at Southeastern GSA meeting.
- Cacas, M.C., Ledoux, E., de Marsily, G., and B. Tillie. 1989. In *Groundwater Contamination: Use of Models in Decision-Making*, eds. Jousma, G. et al. Kluwer Academic Publishers.
- Chiles, J.P., and G. de Marsily. 1993. In *Flow and Contaminant Transport in Fractured Rock*, eds. Bear, J., Tsang, C.F. and G. de Marsily. Academic Press.
- Dagan, G. 1986. Statistical theory of groundwater flow and transport: Pore to laboratory, laboratory to formation, and formation to regional scale. *Water Resources Research* 22(9):120S-134S.
- Dettinger, M.D. and J.L. Wilson. 1981. First order analysis of uncertainty in numerical models of groundwater flow. Part 1: Mathematical development. *Water Resources Research* 17(1):149-161.
- Domenico, P.A. and F.W. Schwartz. 1990. *Physical and Chemical Hydrogeology*. John Wiley & Sons, Inc.
- Edwards, D. and M. Hamson. 1989. *Guide to Mathematical Modeling*. Boca Raton: CRC Press.
- Fetter, C.W. 1993. *Contaminant Hydrogeology*. New York: Macmillan.
- Freeze, R.A. 1975. A stochastic conceptual analysis of one-dimensional ground-water flow in non-uniform homogeneous media. *Water Resources Research* 11(5):725-741.
- Freeze, R.A., Massmann, J., Smith, L., Sperling, T., and B. James. 1990. Hydrogeological decision analysis, 1: A framework. *Ground Water* 28(5):738-766.
- Florida Land Design and Engineering 1987. North Lakes Park wetland restoration study. A study prepared for the Hillsborough County Engineering Department. Tampa, Florida.
- Gelhar, L.W., Gutjahr, A.L., and R.L. Naff. 1979. Stochastic analysis of macrodispersion in a stratified aquifer. *Water Resources Research* 15(6):1387-1397.

- Gelhar, L.W. 1993. *Stochastic Subsurface Hydrology*. Englewood Cliffs:Prentice Hall.
- Geotrans, 1988a. FRACFLOW: Finite-element model of groundwater flow in double-porosity media.
- Geotrans, 1988b. Hydrologic investigation of the northern portion of the Southwest Florida Water Management District: Northern district model project, phase II final report. A report prepared for the Southwest Florida Water Management District.
- Hantush, M.S. 1960. Modification of the theory of leaky aquifers. *Journal of Geophysical Research* 65:3713-3725.
- Hull, C.W. 1997. Establishment of minimum levels in wetlands. A report prepared by the Southwest Florida Water Management District. Brooksville, Florida.
- Kraemer, S.R., and H.M. Haitjema. 1989. Regional modeling of fractured rock aquifers. In *Groundwater Contamination: Use of Models in Decision-Making*, eds. Jousma, G. et al. Kluwer Academic Publishers.
- Langevin, C.D., Thompson, D., Laroche, J., Albury, C., Shoemaker, W.B., and M.T. Stewart. 1998. Development of a conceptual hydrogeologic model from field and laboratory data. Phase II results. North Lakes Wetland Project, Hillsborough County, Florida. A report prepared for the Southwest Florida Water Management District. Geology Department. University of South Florida.
- Langevin, C.D., and M.T. Stewart, 1997. North Lakes Wetland Project: Phase I Final Report. A report prepared for the Southwest Florida Water Management District. Geology Department. University of South Florida.
- Laroche, J. in preparation. Distribution of hydraulic conductivity at the North Lakes wetland. Master's thesis in progress.
- Lattman, L.H., and R.P. Nickelson. 1958. Photographic fracture mapping in the Appalachian Plateau. *American Association of Petroleum Geologists Bulletin* 2:2238-2245.
- Lattman, L.H. and R.R. Parizek. 1964. Relationship between fracture traces and the occurrence of groundwater in carbonate rocks. *Journal of Hydrology* 2:73-91.
- Mabee, S.B., Hardcastle, K.C., and D.U. Wise. 1994. A method of collecting and analyzing lineaments for regional-scale fractured-bedrock aquifer studies. *Ground Water* 32(6):884-894.
- McDonald, M.G., and A.W. Harbaugh. 1988. A modular three-dimensional finite-difference ground-water flow model. Techniques of Water-Resources Investigations 06-A1, United States Geological Survey.
- Miller, J.A. 1986. Hydrogeologic framework of the Floridan Aquifer system in Florida and parts of Georgia, South Carolina, and Alabama. United States Geological Survey Professional Paper 1403-B.
- Moore, 1981. Geophysical signatures to photolinears at the Cross-Bar Wellfield, Pasco County, Florida. M.S. Thesis, Geology Department. University of South Florida.
- Neuman, S.P. 1982. Statistical characterization of aquifer heterogeneities: An overview. Geological Society of America Special Paper 189.



- Parizek, R.R. 1976. On the significance of fracture traces and lineaments in carbonate and other terrains. In *Karst Hydrology and Water Resources* (Proceedings of the U.S. Yugoslavian Symposium, Dubrovnik, June 207, 1975). Fort Collins: Water Resource Publications. Volume 1:47-108.
- Peck, A., Gorelick, S., de Marsily, G., Foster, S., and V. Kovalevsky. 1988. Consequences of spatial variability in aquifer properties and data limitations for groundwater modelling practice. IAHS Publication 175.
- Perry, 1995. Regional assessment of land use nitrogen loading of unconfined aquifers. Ph. D. Dissertation. Department of Civil Engineering. University of South Florida.
- Pollock, D.W. 1989. Documentation of computer programs to complete and display pathlines using results from the United States Geological Survey modular three-dimensional finite-difference groundwater model. United States Geological Survey Open File Report 89-381.
- Robinson, J.L. 1995. Hydrogeology and results of tracer tests at the Old Tampa Well Field in Hillsborough County, with implications for wellhead-protection strategies in west-central Florida. United States Geological Survey Water-Resources Investigations Report 93-4171.
- Robinson, P.C. and D.P. Hodgkins. 1986. Exact solutions for radio-nuclide transport in the presence of parameter uncertainty. Report AERE R 12125. Theoretical Physics Division, AERE, Harwell Laboratory, Oxfordshire, UK.
- SDI Environmental, 1994. An integrated surface and groundwater flow model. A report prepared for the West Coast Regional Water Supply Authority.
- Siddiqui, S.H., and R.R. Parizek. 1977. Hydrogeologic factors influencing well yields in folded and faulted carbonate rocks, central Pennsylvania. *Water Resources Research* 7:1295-1312
- Sitar, N., Cawfield, J.D., and A. Der Kiureghian. 1987. First-order reliability approach to stochastic analysis of subsurface flow and contaminant transport. *Water Resources Research* 23:794-804.
- Stewart, M.T. 1998. The Florida Water Wars: A geologic perspective. *Geotimes*. March 1998.
- Stewart, M.T., and J. Parker. 1990. Localization and season variation of recharge in a covered karst aquifer system, Florida, USA. In *Hydrogeology of Selected Karst Regions*. eds. Paloc, H. and W. Back. Hannover:Verlag Heinz Heise.
- Townley, L.R. 1984. Second order effects of uncertain transmissivities on prediction of piezometric heads. In *Proceedings of the 5<sup>th</sup> International Conference on Finite Elements in Water Resources*. Burlington: Springer-Verlag.
- Townley, L.R., and J.L. Wilson. 1985. Computationally efficient algorithms for parameter estimation and uncertainty propagation in numerical models of groundwater flow. *Water Resources Research* 21:1851-1860.
- Vukovic and Soro. 1992. *Determination of Hydraulic Conductivity of Porous Media from Grain-Size Composition*. Water Resources Publications.
- Wagner, B.J., and S.M. Gorelick. 1987. Optimal groundwater quality management under parameter uncertainty. *Water Resources Research* 23:1162-1174.
- Williams, S.R. 1985. Relationship of ground water chemistry to photolineaments in a karst aquifer. Unpublished Master's Thesis, Geology Department, University of South Florida.

Yevjevich, V. 1976. General overview of application of stochastic methods to water resources problems. In *Stochastic Approaches to Water Resources*. ed. and published by H.W. Shen.

Zheng, C. 1989. PATH3D. S.S. Papadopoulos and Associates. Rockville, MD.

## **VITA**

Christian Langevin received a Bachelor's Degree in Geology from the University of Wisconsin at Madison in 1991 and a Master's Degree in Geology from the University of South Florida in 1993. In 1993, he entered the Ph. D. program at the University of South Florida.

While in the Ph. D. program, Mr. Langevin taught "Introduction to Hydrogeology", consulted for the U.S. Geological Survey, and headed an extensive study of the North Lakes Wetland that was funded by the Southwest Florida Water Management District. His first paper was published in May of 1998 in the journal, Ground Water. In the spring of 1999, his second paper will be published in the journal, Ground Water.

During his final semester in the Ph. D. program, Mr. Langevin accepted an offer for full-time employment by the U.S. Geological Survey in Miami. His current work at the Survey includes the quantification of groundwater discharges to Biscayne Bay, Florida.